IJICTR International Journal of Information & Communication Technology Research

Volume 4- Number 3- June 2012 (65-98)

All Optical Logic Gates: A Tutorial

Fatemeh Davoodi
Faculty of Electrical & Computer Engineering,
K. N. Toosi University of Technology
Tehran, Iran
F.davoodi@ee.kntu.ac.ir

Nosrat Granpayeh
Faculty of Electrical & Computer Engineering,
K. N. Toosi University of Technology
Tehran, Iran
granpayeh@eetd.kntu.ac.ir

Received: October 24, 2012- Accepted: April 13, 2012

***Abstract*—- In this paper we describe the performances of different kinds of all-optical logic gates reported up to now. We introduce all-optical logic gates based on semiconductor optical amplifiers such as ultrahigh speed logic gates exploiting four-wave mixing, cross gain modulation, cross phase modulation, and cross polarization modulation. We demonstrate the performances of all-optical logic gates using delayed interferometers, such as all-optical gates based on Mach-Zehnder and nonlinear loop mirror interferometers. We describe the performances of semiconductor based microring resonator logic gates, such as all-optical logic gates based on nonlinear photonic crystal, couplers and waveguides, lasers and cavities. We illustrate optical gates based on electro-absorption modulator, nonlinear fibers, nanoslabs, and optical thyristor. We introduce molecular logic gates and logic gates based on thermal lens effects**

Keywords: Optical logic Gates, Photonic Crystals, molecular logic gates, Thermal Lens effect, MEMS

I. INTRODUCTION

Nowadays ultra compact all-optical integrated circuits become attractive in communication systems and high-speed signal processing. All-optical gates are the basic block of the optical devices and networks. These devices can perform many advanced functions such as all-optical computing, bit-error rate monitoring, all-optical packet address, payload separation, etc. All-optical processing is especially required in the systems and networks, which want to avoid opto-electronic conversions and need high speed data receptions and transmissions.

In this paper, a deep review of different kinds of all-optical logic gates exploiting different basics and phenomena are reviewed and described. The paper structure is as follows: in the section I all optical logic gates based on semiconductor optical amplifiers exploiting various working mechanism such as nonlinear effects of four wave mixing, cross gain modulation, cross phase modulation, cross polarization modulation, nonlinear interferometers, delayed interferometer, delayed interferometer, Mach-Zehnder interferometers, nonlinear loop mirror interferometers are presented. In section III and IV, optical logic gates microring resonators such as single, cascaded, nonlinear photonic crystals are described. In section V, all optical logic gates based on directional couplers, waveguides, lasers, cavities are illustrated. In section VI, and VII all-optical logic gates based on electro-absorption modulator and nonlinear effects in optical fibers are described, respectively. In section VIII-XI, optical polarization, vertical cavity laser and thyristor structure, molecular, polymer, thermal lens are respectively presented. The paper is concluded section XII.

II. ALL-OPTICAL LOGIC GATE BASED ON SEMICONDUCTOR OPTICAL AMPLIFIERS

Semiconductor optical amplifiers and their components are very interesting as the basis of the all-optical logic gates. Semiconductor optical amplifiers are characterized by a nonlinearity that is four orders of magnitude higher than that of high-nonlinear fibers.

SOAs have small footprint, and are easy to implement, able to be stable cascaded circuits at high speed communication. The devices have integration potential for mass production and commercial availability. There are several nonlinear effects based on SOAs. These devices have various working mechanisms, such as four-wave mixing (FWM) [1-21], cross-gain modulation (XGM) [22-33], cross-phase modulation (XPM) [34], cross-polarization modulation (CPM) [35-41], and nonlinear polarization rotation [42-48]. Some of the logic gates using single SOA [49-56] and some of them use SOAs in interferometric forms [57-130]. Usually the XGM method needs more than one SOA. The implementation of logic gates based on XGM is easy but their speed limits to slow gain recovery in active region of SOAs. In the FWM technique pattern dependent degeneration can be reduced due to the constant intensity nature of the signals in logic gates. FWM is limited by conversion efficiency and must lie within certain wavelength for efficient FWM effect. The CPM effect requires matching both the polarization and the wavelength of the input beams, which impose an exact technical procedure for practical applications. Of course it should be considered that in the CPM method only two input signals without an additional CW beam are needed, which enable us to get more compact designs. The XPM method limits the operating speed of such devices due to the intrinsic slow carrier lifetime of the SOAs. The operating speed can be increased by utilizing of a high-power CW beam, different interferometer structures, differential scheme, and using quantum-dot semiconductors

A. Ultrahigh-speed logic gates exploiting four-wave mixing SOAs

Here we introduce all optical logic gates based on FWM in SOAs [1-6, 8-13]. The information is encoded in polarization of the input signal. Even though these devices are simple but they can generate several logic functions by exact tuning the polarization in the output and input. In binary encoding, the logical "one" is distinguished with a linear polarization state and the logical "zero" with orthogonal one. The two data streams are injected to the SOA at the wavelengths λ_1 and λ_2 as the pump and the probe signals. The logic gates can be grasped by detecting the idler signal generated due to the FWM of λ_1 and λ_2 [1].

The FWM effect in the SOA acts only when the probe and the pulse components are in the same polarization. Therefore, when the polarizations of two signals are parallel, the resulting intensities and polarization states of the idler signals are as shown in Figure 1.

If the output is directly detected by an optical receiver, the polarization states can be ignored and results an XNOR gate. Anyway, if the idler is isolated in two polarization components by polarization splitter, AND and NOR logic gates are generated.

If the polarization states of the inputs are orthogonal, XOR operation is gained by direct detection and two logical functions $\overline{D1}\cdot D2$ and $D1\cdot\overline{D2}$ are obtained by utilizing polarization splitter.

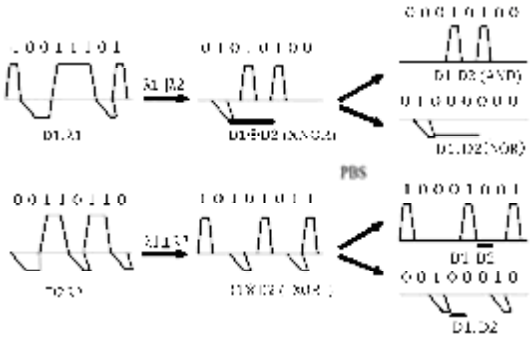

Figure 1. Schematic view of all-optical AND, XNOR, XOR, NOR, $\overline{D1}\cdot D2$ and $D1\cdot\overline{D2}$ logic operations [1].

An XOR logic gate based on FWM in SOA, with optical RZ-DPSK is reported in [2]. The proposed XOR gate can be in two-input or three-input mode, which offers better flexibility for cascading. This logic gate operates up to 20 Gb/s. The proposed all-optical XOR gate with its truth table is depicted in Figure 2. A reconfigurable logic gate based on SOA exploiting FWM and XGM effects is shown in Figure 3. It has two polarization-aligned input data signals, 'A' and 'B', and a probe co-propagating at the same wavelength of generated FWM term.

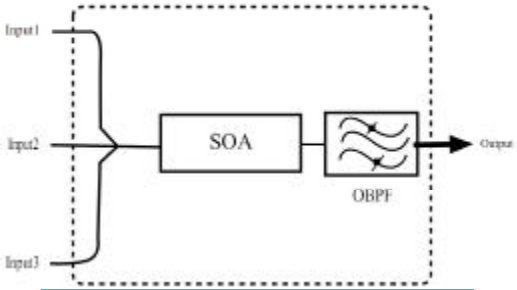

φ_1	φ_2	φ_3	$\varphi_1-\varphi_2-\varphi_3$	Boolean
0	0	0	0	0
0	0	π	-π	1
0	π	0	π	1
0	π	π	0	0
π	0	0	π	1
π	0	π	0	0
π	V	0	2π	0
π	π	π	π	1

Figure 2. All-optical XOR based on FWM in SOA [2].

The SOA-based devices are unable to process ultrafast signals due to the limited SOA gain recovery speed; here a method to overcome this limitation is proposed. Using a propagating continuous-wave (CW), reduces the SOA response time. The presence of the CW light increases the main saturation level of SOA, thus the dynamics of gain recovery reduces after the arrival of the input signals. In this way, the ability to process the signals in SOA-based gates is improved [3]. When both signals are present in the SOA, due to the FWM effect the idler component is generated, and the channel is saturated, so the probe signal experiences a very low gain. The idler component can be filtered optically and the output is in high state. If both the input data signals are absent the FWM effect does not take place and the SOA is not saturated. Therefore, the SOA now is amplifier and the probe beam is experienced by high amplification.

In the absence of the idler component at the FWM wavelength, the output is in the high level. In case that one input is present, the FWM effect does not occur, but the SOA is saturated (each one of the input power is sufficient to saturate the device), so the gain of probe is strongly reduced. Different states of this XNOR are demonstrated in Figure 3.

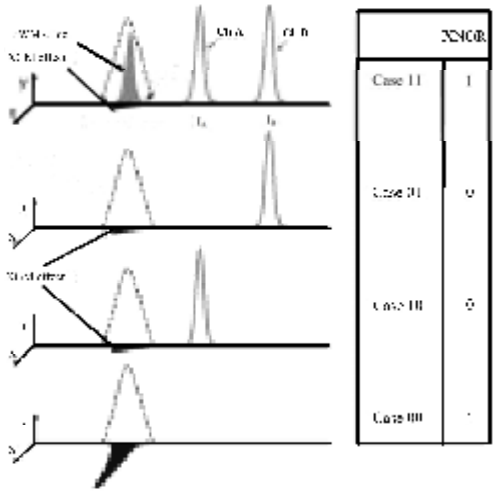

Figure 3. Different states of proposed XNOR gate [3].

By splitting the output in two part and utilizing two BPF, or using a tunable filter, AND, NOR, NOT logic functions can be obtained. If the probe signal is 'OFF', and the BPF is adjusted at λ_{FWM}, the structure represents a logic operation AND. Moreover in the case that the probe wavelength is not tuned at the FWM wavelength, and the BPF centered at the probe wavelength, the NOR function is generated. Finally the NOT operator can be obtained when only one input signal is inserted.

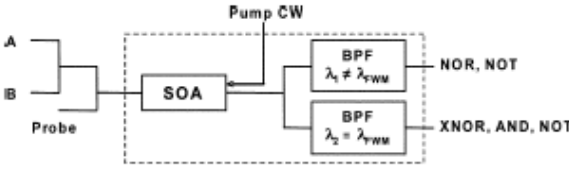

Figure 4. Scheme of reconfigurable logic gate [3].

All optical XNOR and AND gates simultaneously realized in the single SOA [4], and a complicated all-optical logic gate based on FWM for CSRZ-DPSK and format conversion from CSRZ-DPSK to RZ-DPSK by HNLF is reported in [5]. This XOR logic gate operates up to 40 Gbs^{-1}. The principle operation of the FWM gate is shown in Figure 5.

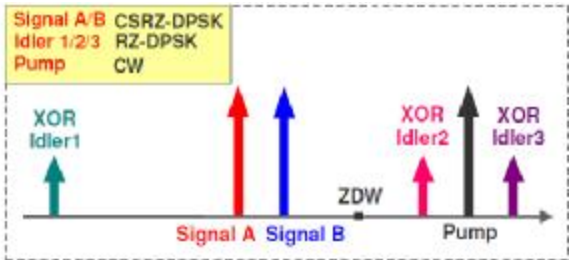

Figure 5. Operation principle for FWM based XOR logic gate [5].

A novel scheme for ultrafast 40 Gb/s multifunctional all-optical logic gate was proposed, which can perform not only as the simple logic gates of AND, OR, XNOR, XOR, and etc, but also can perform as the complex gates including half adder, half subtractor, decoder, and comparator based on FWM in SOAs with PolSK modulated signals [6].

An AND/OR 40 Gb/s all-optical logic gate is recently proposed to process NRZ-OOk, RZ-OOk, and CSRZ-OOK format signals. AND and OR logic gates are achieved through a single logic unit, which is compact and cost-effective for processing application [9].

Other kinds of all-optical AND and OR logic gates based on cavity-enhanced FWM combined with optical injection locking phenomenon integrated in SRLs at speed of 2.5 Gb/s have been experimentally demonstrated [7].

B. All-optical logic operation using cross gain modulation in SOA

The XGM method needs more than one SOA. The speed is limited to the slow gain recovery in active region of SOA but the method is easy to implement.

This 10 Gb/s NAND gate works due to the XGM effect of SOA. The carrier density will affect the other inputs, so it is possible to influence a signal at one wavelength the input gain for another wavelength. When a high power signal passes through the SOA, it causes carrier depletion in active region of amplifier. Therefore a deep gain saturation is taken place, causing an intensity reduction of incoming probe signal which leads no pulse existence in the output [22].

The schematic diagram of the NAND gate is shown in Figure 6. In the NAND gate $\left(\overline{A}+A\overline{B}\right)$, $\overline{A}$ is obtained by using clock signal as probe beam and signal 'A' as the pump beam.

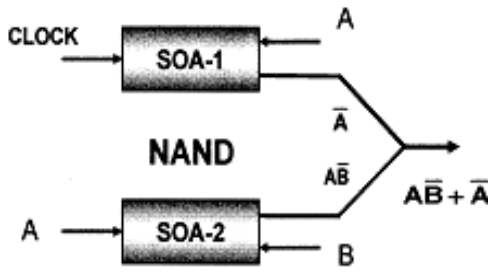

Figure 6. The implementation of NAND logic operation [22].

In the $A\overline{B}$, signal 'A' works as probe beam and signal 'B' works as pump signal in the SOA-2. The NAND logic function is the sum of the two signals $A\overline{B}$ and $\overline{A}$.

An interesting optical gate based on XGM was proposed in [29] that uses reflected input beam for the production of cross gain modulation. It does not use an extra continuous wave (CW) source. This structure shows no reduction in the performance in addition to surpassing integrability and simpler form.

This logic gate is similar to the nonlinear optical gate which uses auto-correlated XGM in folded tandem-SOA but without extra CW. The performance factors can be increasing the mirror reflectance.

The novel idea of this logic gate, according to [29], is shown in Figure 7a, compared to the CW assisted gate depicted in Figure 7b.

In both schemes, there are two SOAs connected with a 3-dB coupler with outer edge receiving the input power (the input port of the SOA1) and CW (the input port of the SOA2) in CW assisted gate and reflected input instead of CW in folded type. In the second type, the pattern of the CW signal propagating through the SOA2 has been inverted by XGM effect. After entering the SOA1 again the input power modulates it by utilizing the XPM effect. This process in the presence results in "0" of the input signals and "1" in the absence of the inputs. In the reflected input acts as a CW signal.

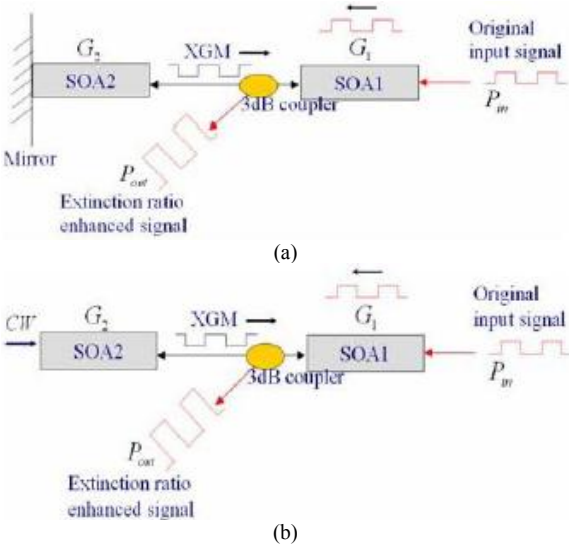

Figure 7. The structure of the optical logic gate based on auto-correlated XGM effect in folded tandom-SOA (a), compared to the CW assisted gate (b) [29].

This is a three input AND-NOR gate, the performance of which demonstrated in Figure 8. The probe signal at wavelength λ_s, is shown $x = x_0$ in logic operation. The P_{pump} is the sum of P_{pump1} and P_{pump2} with wavelengths λ_{p1} and λ_{p2}, respectively and in logic operation as shown by $y = x_1 + x_2$. The logic operation is obtained at output wavelength λ_s. As long as one of the two pump inputs exits, $y = 1$ and the SOA is deeply saturated, so the output signal will be 'zero'. When two pump signals are absent, SOA works normally and the probe signal appears in the output. The combination of probe and pulse signal generates high output only when pump signals are absent and the probe beam exists. Thus we can obtain $x \cdot \overline{y}$ and in presence of three inputs $x = x_0$ and $y = x_1 + x_2$, the Boolean $x_0 \cdot \left(\overline{x_1 + x_2}\right)$ logic gate can be achieved [23].

The switching speed has been enhanced by adding the third SOA in the dual ultrafast nonlinear interferometer XOR gate (DUX) to benefit from the turbo-switch effect. A CW laser at wavelength of 1552 nm has been employed as the probe beam, and the 3 ps 1557nm control pulses A and B have been used. The differential delay of PM is 5.75 ps. The control pulse energies needed for switching are as low as 54 and 62 fJ.

C. *Proposal for boolean logic gates exploiting XPM*

An arbitrary two-input logic gates (AND, NAND, OR, XOR, XNOR, NOR) based on single SOA and optical filters are proposed [34]. Two input data with Pico second pulses and a probe signal are fed simultaneously into the SOA. The spectrum of the probe signal will be extended due to XPM effect, and different logic functions are obtained, such as AND, OR, XOR, and NOR by tuning the optical filters and using different frequency components. Finally, the logic XNOR and NAND are achieved by combining the two logic operators. A simple digital schematic view of these logic gates their truth table are illustrated in Figure 9 [34].

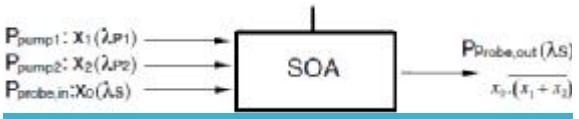

$y = x_1 + x_2$	$x = x_0$	Probe output	Notes
0	0	0	Probe output power is low with low probe power and low pump inputs
0	1	1	Probe output is high with high probe power and low pump inputs
1	0	0	Probe output is low due to SOA gain saturation in the presence of a high input pump power and a low input probe
1	**1**	**0**	Probe output is low due to SOA gain saturation in the presence of a high pump power and a high input probe power

Figure 8. Principle of the AND-NOR operation based on XGM [23].

Two data signals 'A' and 'B', and the probe signal are injected to the SOA. Due to cross phase modulation (XPM), the probe signal has some frequency shifts. Data 'A' and 'B' have equal peak power with RZ format. The frequency shift of the probe signal depends on the peak power of the inputs. The logic function is obtained by tuning the optical bandpass filter (OBF) at different wavelengths. Figure 10 depicts that the output peak power depends on and the wavelength and the filter detuning. P_{11} and P_{10} represent the states when both or one of the input pulses are present, respectively.

If both of the input signals are present, the probe signal receives much stronger blue shift at the wavelength compared to the case that only one input pulse is present. By adjusting the OBF to select the stronger shift and reject the weaker one, the AND logic gate is created. In similar way, if the OBF is tuned to select the weaker wavelength shift and reject the stronger one, an XOR gate is generated. As shown in Figure 10, if the OBF is tuned at middle region of the weaker and the stronger blue-shift the probe pulse can be generated when both of the inputs exist or either of the inputs is present. In this manner we can obtain an OR logic function.

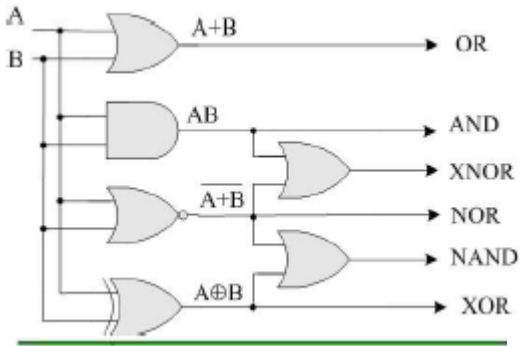

Input data		Output logics					
A	B	XNOR	AND	NOR	XOR	NAND	OR
RZ	RZ	DRZ	RZ	DRZ	RZ	DRZ	RZ
0	0	1	0	1	0	1	0
0	1	0	0	0	1	1	1
1	0	0	0	0	1	1	1
1	1	1	1	0	0	0	1

Figure 9. The digital logic schematic view and the truth table of the digital logic gates [34].

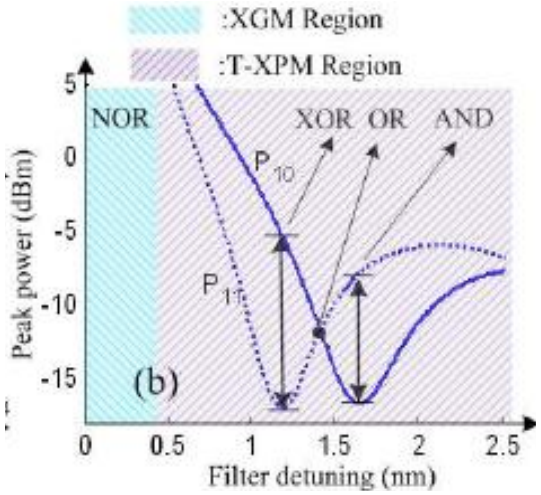

Figure 10. The output peak power variations as a function of filter's detuning [34].

If the OBF has small detuning from the probe signal, the XGM is dominant to invert the output pulses. Thus the small detuning filter is useful to speed up the amplitude recovery. In this way, the NOR gate in dark RZ (DRZ) is achieved. As shown in Figure 11 with proper power proportion, the XNOR/ NAND is obtained by mixing AND/ XOR and NOR.

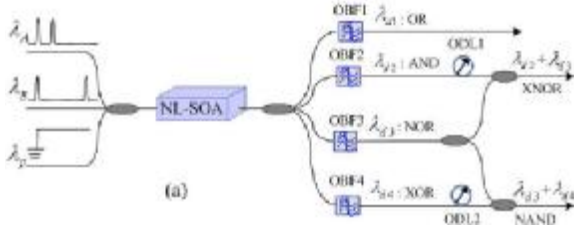

Figure 11. Schematic diagram of the arbitrary logic gates [34].

According to the optimization of these logic gates, the probe wavelength must be near 1552 nm and 1554 nm. The wavelength of data signals is at 1563 nm. The data signals have pulse width of 2.5 ps and the peak power of 10 mV.

D. All-optical AND gate utilizing cross polarization modulation effect

An all-optical 10 Gb/s AND gate exploiting cross polarization modulation (CPM) in the SOA is shown in Figure 12. This device needs no additional continuous-wave beam to carry the logic information out of the gate and the output is gained at wavelength of one of the input data. The input logic signal A at wavelength λ1 and B at wavelength λ2 is injected into the SOA, concurrently. The intensity of the input data modulates the carrier density in active region and induces different phase shift on TM and TE modes. Thus the polarization states of one beam at the output of the SOA will be modulated by the intensity of another input of the SOA. This is so called cross polarization modulation. Afore-mentioned output is obtained at one of the input wavelengths. Here the filter is tuned at wavelength λ_1. So if input 'A' is in 'OFF' state, the output will be in low level. But in case the input A is in 'ON' state, the presence or absence of the input B influences its polarization and results in different states [42].

The polarization change of signal 'A' is converted to intensity information after polarizer. The polarizer is tuned orthogonally to the state when signal A is 'ON' and signal 'B' is 'OFF'. Thus, only when input A is in the ON-state and B is in the OFF-state the polarization of input signal A will be rotated by the intensity of signal 'B' due to CPM, and the output will be in high level after the polarizer.

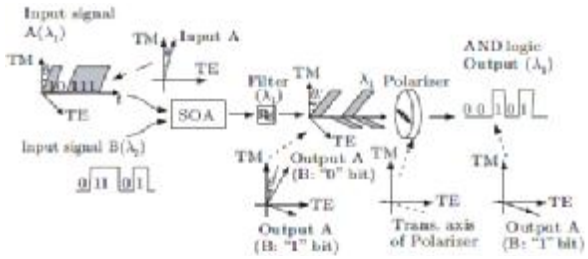

Figure 12. Proposed AND logic function [42].

The simulation results show that the higher output power can be obtained when the input power of both signals increase. Higher power of signal 'B' will strengthen the CPM effect on signal 'A', so higher output power is gained. Higher input 'A' weakens the XGM effect in SOA and increases its output. Thus higher power of both inputs improves the logic operation.

E. All-optical logic gates exploiting nonlinear interferometers

Here we introduce different schemes of all-optical logic gates based on interferometric structures, such as turbo switches [61, 62], delay lines [63-65], Mach-Zehnder interferometer [66-4, 7-38], nonlinear optical loop mirror [39-41], ultrafast nonlinear interferometers [42-44], and Michelson interferometer.

A scheme to speed up the optical switches is using two nonlinear ultrafast interferometers based on SOA,

which was enhanced by merging the turbo switch configuration. In this technique a turbo-switch configuration is adopted instead of a single SOA [62]. The turbo-switch consists of a pair of SOAs separated by a wide band-pass filter (BPF), to prevent the pump pulses from entering the second SOA, as shown in Figure 13. Measurements have shown that the overall response time of a turbo-switch is about four-folded faster than a single SOA [61].

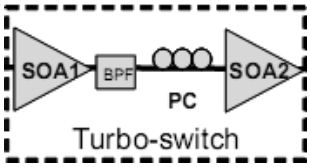

Figure 13. A turbo-switch configuration. PC is the polarization controller [61].

A and B input probe pulses are launched into a polarization-maintaining fiber (PMF) with the same intensities on the fast and slow fiber axes. As a result, the TE pulse lags the TM pulse by Δt, this delay depends on the PMF length [62].

As shown in Figure 14, a control pulse is injected between two probe pulses, in which it induces π-radian phase shift experienced by TE mode alone. The probe pulses are introduced to another PM fiber by a delay line of -2Δt. The fast and slow axes of the fiber are orthogonal to the former PM fiber, so reversal of the delay between TE and TM pulses result TE mode leads the TM pulse by Δt. The control pulse B is introduced between TM and TE probe pulses before entering SOA2. The imposed π-radian phase shift adopts TM mode. The third PM fiber with delay of Δt resynchronizes the TE and TM modes at the end of fiber. If two control pulses are present and identical, the nonlinear phase shift between two TE and TM mode is zero. (π and –π), like the result when both control pulses are absent. In the cases either one of 'A' or 'B' is present, the induced phase shift will be ±π. π-radian phase difference between TM and TE pulses gives polarization rotation of π/2 when they recombine at the polarizer, which is crossed with the unrotated probe. A pulse is generated after polarizer even if one of the control signals is presented. Thus the operation of device satisfies XOR logic function.

F. All-optical logic gate using SOA and delayed interferometer

Several kinds of logic gates were demonstrated based on SOA-delayed interferometer. An inverter function at speed of 100 Gb/s [63], an OR function at 20 Gb/s [64], an OR logic gate at 80 Gb/s [65] operates based on SOA-DI.

Their operations are similar, so we consider one of them. In the all-optical OR operator based on SOA-DI at 80 Gb/s, the DI is based on polarization maintaining loop mirror. This technique has advantages over SOA Much Zehnder interferometer (MZI) gates. The SOA-DI gates require one SOA and operate at low power consumption. The SOA-MZI devices due to their differential schemes can operate in higher speed in comparison with DI type. This all-optical logic gate is based on gain saturation and phase modulation signals in the SOA. The schematic view is shown in Figure 15.

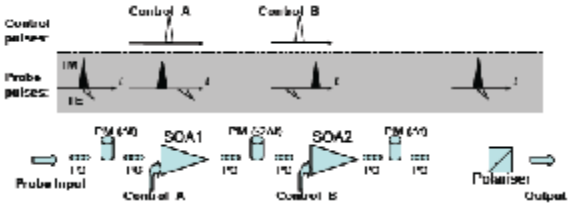

Figure 14. Configuration of XOR logic function, where PMs are polarization-maintaining fibers and PCs are the polarization-controlling [62].

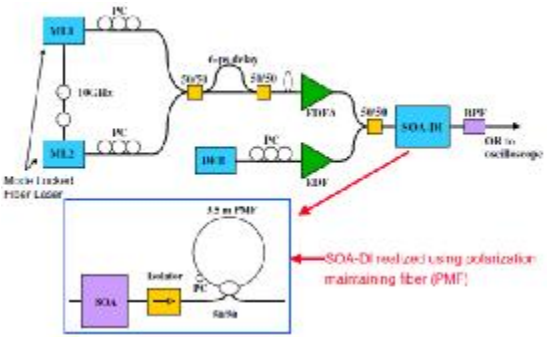

Figure 15. Experimental setup for the OR function, ML: mode locked fiber laser, PC: polarization controller, DFB: distributed feedback laser, BPF: band pass filter, DCF: dispersion compressing fiber, PMF: polarization maintaining fiber [65].

Two input signals A and B in company with CW signal are injected into the SOA. Two inputs impose a time variant phase shifts to the CW which operates as the probe signal via XPM effect. The CW signal is injected into a polarization maintaining loop mirror. The CW is polarized along fast and slow axis of the PMF before injection into the polarization maintaining loop (PML). The CW signal splits into clockwise (CW) and counter clockwise (CCW) components. The polarization controller is adjusted to make 90° rotation. So, the CW and the CCW components are polarized along two axis of the fiber. So, the fiber birefringence along two fast and slow axes imposes the differential phase delay of $k_0 \Delta n L$, where k_0 is the wave vector, Δn is the refractive index difference between two slow and fast axes, L is the PML fiber length. According to this differential phase shift the CW and the CCW components interfere at the coupler and create required logic operation. In the absence of signal 'A' or 'B', there is no output pulse after the DI. If 'A' or 'B' or both of them are present, the SOA gain saturates and imposes a time dependent phase shift on the CW signal. The Signal enters the PC and the coupler split it in two CW and CCW components in the loop mirror. The clockwise and the counter clockwise signals travel along the fast axis and the slow axes, respectively. Since the two components arrive at different times due to the birefringence of the fiber. The different time dependent phase of the two components and the output pulse of the coupler are shown in Figure 16.

The phase gate can be easily tuned by the variation of the fiber length. For appropriate operation each of 'A' and 'B' should saturates the SOA. In the presence

of both of the inputs, the phase shift introduced to CW due to the gain saturation are the same as when either 'A' or 'B' is present. This gate works in the third communication window, and its speed is limited by gain recovery time. The Q-factor is a function of gain recovery time and the alpha-factor.

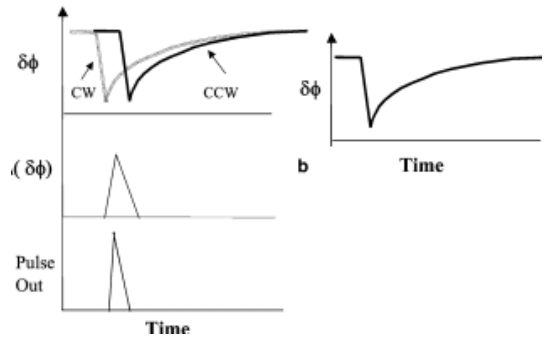

Figure 16. $\delta\Phi$ represents the time dependent phase shift induced by inputs, $\Delta(\delta\Phi)$ represents the phase difference between the CW and CCW components at the coupler, and the pulse output represents the power output (bottom) [65].

G. All-optical logic gate based on Mach-Zehnder interferometer

The schematic view of the first all-optical XNOR logic gate which is demonstrated base on Mach-Zehnder Interferometer (MZI) with simple structure operated at 10 Gb/s is shown in Figure 17. It operates in cross-phase modulation (XPM) mode. Because of the counter propagation scheme, there is no need to frequency selective filter after MZI output. Two input data are combined and coupled into the lower arm of the MZI. The clock signal is split and launched into the MZI arms. When the signal with high power is launched into the IN port, it modulates the carrier density and as a result the refractive index of the SOA in lower arm of MZI, prepares a phase-modulating signal. At the output of the MZI, two split of probe pulses interfere constructively or destructively, depends upon the phase shift created in the SOA of the lower arm of MZI. Figure 17(b) shows the whole operation this optical logic gate . The logic gate output is "one" whereas the two pump inputs are the same. Thus there is no difference in phase of the two arms of the MZI, and the output is "zero" when two input signals are different [71].

The optimum CW input power signals is about 2 dBm, and the wavelengths of the clock and the input CW signals are 1553.8 nm and 1545 nm, respectively. This gate operation speed can increase up to 40 Gbs^{-1}. The XNOR structure is based on the wavelength conversion by XPM.

The XOR logic operation is indispensable to critical networking function, such as switching, signal regeneration, etc. Several analyses are reported for the schematic diagram is shown in Figure 18. One of them can operate up to 20 Gbs^{-1} [72], and the second is demonstrated at 10 Gbs^{-1} and 40 Gbs^{-1} [73] and another form is reported in [74-79].

This optical XOR gate is consisted of symmetric MZI and one SOA located in each arm. A clock pulse enters the port1 and splits in two equal parts through the coupler C1 as the probe beam. The probe and the pulse beams counter propagate through both arm of the MZI (CMZI). If pump signals A and B are the same, the MZI are balanced and there is no signal at port3. When two pump signals are different, due to the XPM effect in the SOA two different phase shifts occur. Thus induced probe signal switches out from port3.

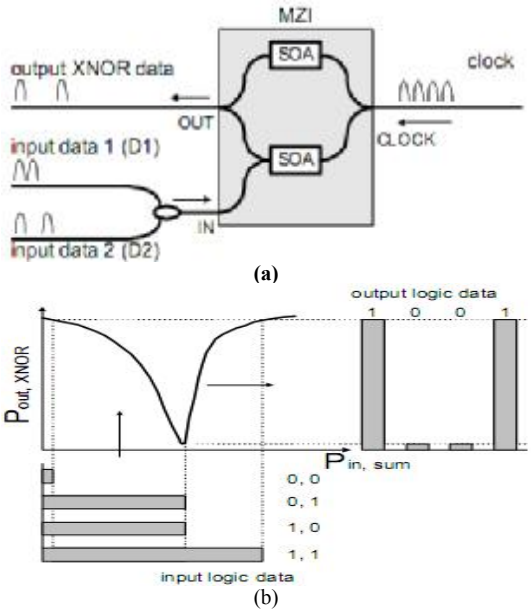

Figure 17. (a) Schematic diagram and (b) illustration of the principle of operation of XNOR logic gate [71].

Because of CMZI formation of this XOR function, BPF is not necessary after MZI and the device can be compact. Both SOAs are polarization independent and the polarization-dependent effect is negligible. The schematic diagram is shown in Figure 18(b) operates like previous in Figure 18(a). To achieve ideal interfering in MZI, phase difference must be $k\pi$, where k is an odd integer number. To have satisfactory operation the phase shift is unnecessary to be $k\pi$. Appropriate switching can be achieved by less power energy, even if $\Delta\varphi$ is less than π. Because of the carrier life time, the speed of gate is limited so this logic gate can operate up to 40 Gb/s [73].

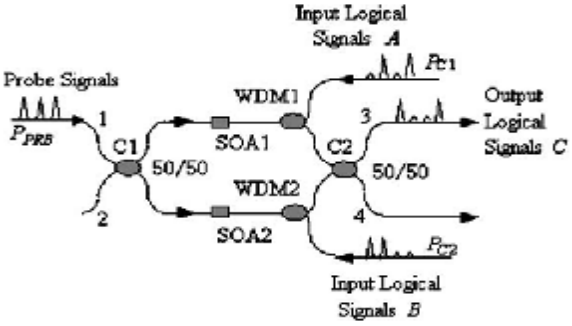

Figure 18. Configuration of 10 Gb/s all-optical XOR gate [72].

The schematic view shown in Figure 20 is an all-optical 10 Gb/s NAND gate SOA based symmetrical MZI demonstrated for the first time. The input signal B combined with clock pulses through the coupler C2

and WDM2 enters the lower arm of MZI. Signal A as the second input signal enter to upper arm of MZI via WDM1. A clock pulse as a probe signal enters through port5 [82].

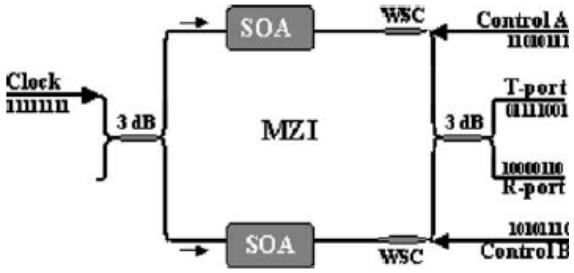

Figure 19. . Configuration of a 40 Gb/s all-optical XOR gate [73].

The probe signal is split in two equal parts by C1 and is transmitted in two arms of MZI. The input signals 'A' and 'B' and the clock pulse have the same amplitude. The scheme is filter free, because the input signals and the probe pulse propagate concurrently.

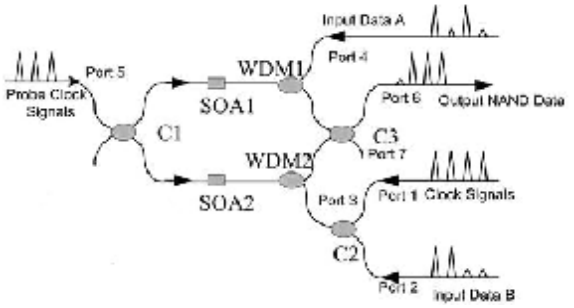

Figure 20. Schematic diagram of an all-optical NAND gate based on SOA-MZI [82].

The combination of signal B and clock pulse modulates the carrier density and hence the refractive index of SOA2. Signal 'A' modulates the refractive index of SOA. Two parts of the probe pulse interfere via coupler C3. As a result the refractive index of SOAs is modulated by the input data signals due to the XPM effect. The phase shift experienced by the probe pulses, determines the output signal of the MZI. If data A and B are in high level, the date signal from port3 and port4 are identical and two probe pulses interfere destructively at the output of the MZI. In the other cases the controls signal at port3 and port4 are different which generate a pulse at wavelength of the probe signal at the output. The schematic shown in Figure 21 demonstrates a multiple logic gates with XOR, OR, NOR, XNOR, and NAND functions [86].

The design of structure of Figure 21 is optimized by tuning optical gain and phase shifts to obtain the output pulses with maximum Extinction ratio (ER). The XOR diagram was previously introduced. P_{in} is the optical power level of the CW probe signal entering the two parallel MZI structures. For NOR and OR function, first A and B signals are combined and launched to upper arm of SOA-MZI. For NOR gate the phase shifter which is placed in the upper arm of the MZI should be tuned to zero. Thus the probe parts interfere constructively when two input data are zero. In OR gate operation, if two inputs are zero, they interfere destructively and the output will be zero. Because of phase shift due to XPM in the presence of one of the inputs or both of them, the output is '1', so we can obtain OR logic operator.

Another form of NAND logic function is introduced here, which is the sum of XOR and NOR gates. Thus XOR, NOR, and NAND gates can be concurrently operated. The wavelength of the probe input signal is 1549.79 nm and the pump input signals in the upper and the lower MZI are 1551.47 nm and 1553.79 nm, respectively. The probe and the pump (P_{AH}=P_{BH}) and (P_{AL}=P_{BL})) input power levels are 0.2 mw, 0.15 mw, and 0.001 mw.

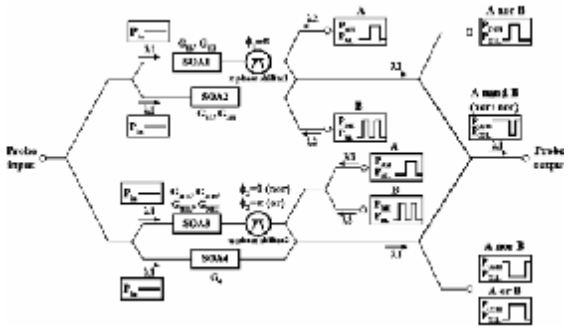

Figure 21. . Conceptual multiple logic gates based on SOA-MZI [86].

The first type 42.6 Gb/s of XOR logic based on SOAs are reported in [90]. In the paper, two types of SOA-MZI based and dual ultrafast nonlinear interferometer (UNI) arrangement are compared. As declared formerly the high speed operation is limited by the carrier life time in SOA. In order to solve the limitations imposed by carrier life time, a differential scheme for XOR operation is considered that has potential of working over 100 Gb/s [91].

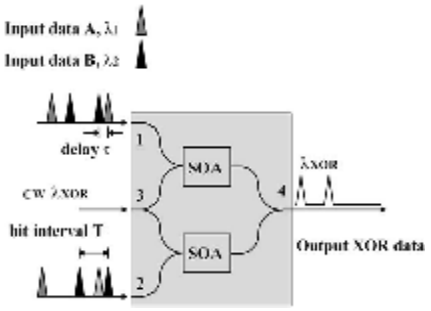

Figure 22. Schematic diagram of an SOA-MZI as the XOR gate operation with differential phase scheme [91].

An XOR gate with differential phase modulation based on SOA-MZI is shown in Figure 22. Two inputs at wavelengths λ_1 and λ_2 are combined before coupling into ports 1 and 2 of the MZI. In the port1, data 'A' is T ps ahead of signal 'B' and in $port_2$ data 'B' is T ps ahead of signal 'A'. The combined input data modulate the SOA gain, and as a result the phase of co-propagating CW probe signal. At the output of the MZI two split probe signal interfere constructively or destructively. If two input data are identical the probe signal interfere destructively, and the output will be in low level. When two input data are different, for example, data 'A' is "1" and data 'B' is "0", the phase shift on the lower arm is induced first and open the switching window, T ps later the phase shift in upper arm is induced so the switching window is closed. The duration of phase difference is controlled by T ps

delay and not by gain recovery time. As a result this gate has higher speed for differential operation. The wavelengths of the inputs A and B are 1545 nm and 1550 nm, respectively. For 10 Gb/s operating, delay time, T, should be 35 ps. In higher speed the delay time becomes shorter.

This conceptual AND logic gate works based on cross phase modulation of two inputs in SOA based MZI. The incoming signals modulate the gain and the phase of SOAs placed in each arm of the MZI. The interferometric optical signal carries the logic AND information. The schematic view of the proposed AND logic function are introduced in Figure 23. The signal 'B' with wavelength λ_2 is coupled into middle port and split into equal parts. By exactly tuning injection currents and the phase shifter located in each arm, the MZI will be balanced at the beginning [92].

The input signal 'A' and the delayed version of it enter the upper and lower arms of MZI structure. The presence of A and A-delayed influences B signal in the upper and lower arms of MZI, respectively, due to the XPM in SOAs. The signal 'A', if it is present, induces a phase shift on signal 'B', and two part of signal 'B' interfere at the output of MZI instructively. In fact, 'A' and A-delayed signals (if 'A' is '1') modulate the carrier density and the gain of SOA in both arms of MZI, and as a result the refractive index of SOAs. Thereby this happening specifies the phase of signal 'B' at the output. As a matter of fact, signal 'A' opens a window for passing signal 'B', and after T ps A-delayed closes it. Thus, if 'B' and 'A' are '1', the output will be '1', but if A= '0' there is no phase gate and the output is '0' for the both states of B='0' or B= '1'. In the case A= '1' and B= '0' the window is open but there is no signal to pass through it, therefore the output is in low level. Since the relative delay between signals 'A' and 'B' leads to switch phase gate for signal 'B', the phase change of 'B' depends on the delay time. To achieve the best signal to noise ratio during the AND operation, the optimum delay time is 2.25 ps. Q factor decreases with increasing the carrier life time. Input data 'B' and signal 'A' are at λ_2=1550 nm and λ_1=1555 nm, respectively. In this way the logic function AND is realized. Operation at higher data rate is feasible using SOAs with shorter phase recovery time. The real reason for limited speed of all optical logic gates based on SOAs and spatially SOA-MZI is the carriers' long life time in bulk SOAs, which decreases the output quality factor below the acceptable range. Using quantum-well and quantum-dot SOAs can improve the optical switching operation. An AND logic gate based on QW-SOA is investigated in [106]. It can operate up to 1 Tb/s using 800 fJ optical pulses with duration of 200 fs while having contrast ratio larger than 11 dB.

An ultrafast XOR logic gate based QD-SOA is designed similar to the former one based on SOA-MZI. Optical amplifiers having nano-sized semiconductor particles, called quantum-dots, show attractive features such as an ultra wide operating wavelength range, suppressed waveform distortion in the high power output, and capability of noise reduction. The ultrafast gain response and the fast gain regeneration are the key properties that make QD-SOAs suitable for regeneration, amplification and also application in logic gate operating due to the XPM and XGM effects [111].

In the paper, an ultrafast all-optical signal processor based on QD SOA-MZI is presented theoretically. For Q factor of 6, the bit rate is up to (100-200) Gb/s depending on the value of the bias current I ~ (30-50) mA. Speed of this logic gate is limited by relaxation time of electron transition between wetting layer (WL), the exited state (ES) and the ground state (GS) in QD conduction band.

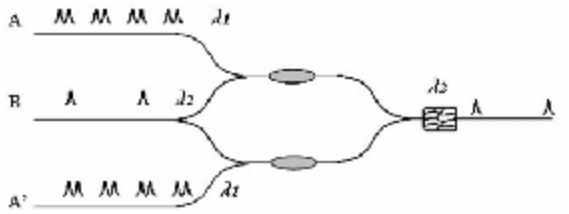

Figure 23. Proposed AND logic gate in differential scheme [92].

An AO-XOR gate based on integrated SOA-MZI composed of symmetrical MZI and two QD-SOAs located in each arm is depicted in Figure 24 [111].

Two data signals 'A' and 'B' with the same wavelength are injected in each arm of the MZI separately. A clock pulse as the probe enters in the MZI. The detuning $\Delta\omega$ of signals 'A', 'B' and probe pulse must be less than homogeneous bordering of QDs spectrum.

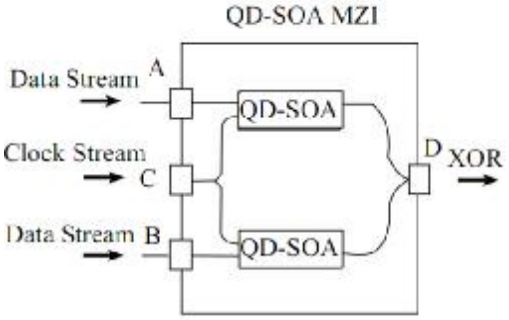

Figure 24. an all optical XOR based on QD SOA-MZI [111].

The simulation has been for L= 1500 μm, W = 10 nm, $\lambda_B = 1560\,nm$, $\lambda_A = 1550\,nm$, and $\lambda_p = 15300\,nm$.

Recently a Tb/s optical gate based on QD-MZI-SOA using XGM effect is theoretically analyzed, which has capability of operation up to 2.5 Tb/s with appropriate quality factor [114]

In order to reduce the switching power consumption, different ring resonator structures have been used in the arms of MZI instead of SOAs [116].

Control of light in all-optical devices is proposed by the use of III-V semiconductors due to their stronger and faster nonlinearity compared to the silicon to achieve the high-density integration with CMOS fabrication technology. Thus, control of light in Si-based devices has received increasing interests. The all-optical MZI-XOR gate based on Si slot waveguides is demonstrated in Figure 25. Si strip waveguides are used as the input and output waveguides. In the arms of the MZI two nonlinear

elements (NLEs) are located to achieve nonlinear phase shift due to the XPM effect.

The NLEs are implemented with slot waveguides, consisting of two parallel Si strip waveguides. The gap between them is filled with low index nonlinear material that consists of silicon nanocrystals (SiC) embedded in silica (SiO_2). Its Kerr nonlinearity coefficient is two orders of magnitude higher than that of Si. The nonlinear properties of Si-nc/SiO_2 material and the effective refractive index can be tuned based on Si-nc density and size. If two inputs are identical, the control signal interferes destructively at the output because of π-shifter is placed in upper arm of the MZI, which can be easily implemented by changing the optical length of one of both arms. If only one of the inputs is present the nonlinear phase shift that depends on its power, makes them to interfere constructively at the output [116].

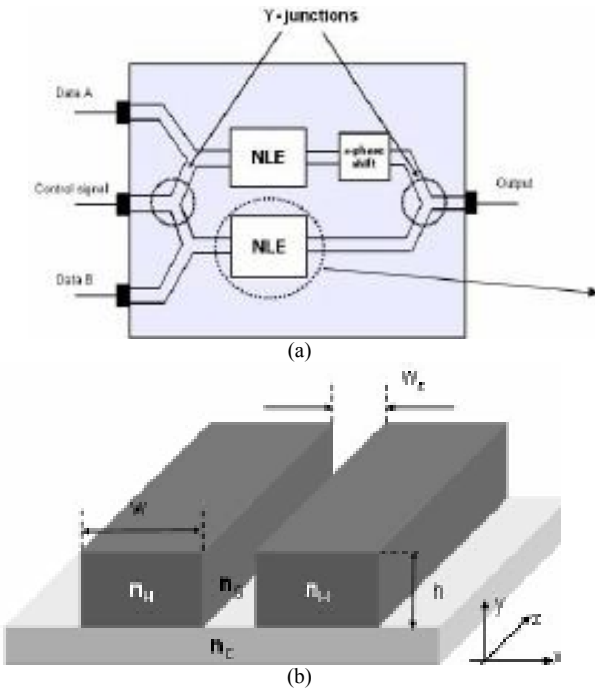

Figure 25. Schematic view of the proposed MZI XOR logic gate (a). The nonlinear elements in the arms of MZI are slot waveguides (b) [116].

All designs have been performed at communication wavelength of 1550 nm and for TE polarization. According to the simulation and calculation results for $n_2 = 10^{-16}$ m^2/W the required power is 2.5 W. Moreover, the device length and the required input power could be reduced by use of resonant structures such as resonators are illustrated in Figure 26.

Figure 26. (a) Ring resonator side coupled for reduction of device length and required input power of the nonlinear elements of MZI-XOR logic gate of Figure 25, (b) mirror formed into the slot waveguide, (c) top view of the coupled resonator waveguide [116].

For ring resonator radius of 10 μm, the intensity inside the ring will be 20 times higher than that of the input waveguide. The incident frequency of the data signal can be red-detuned from resonance to avoid saturation that prevents the effective nonlinear phase shift to reach the value of π. However, the required power for the same value of n_2 reduces to less than 0.13 W.

H. Ultrafast all optical XOR based on non-linear loop mirror interferometer

1) Ultrafast all-optical Boolean XOR gate with semiconductor optical amplifier Sagnac interferometer

In this section we explain two types of devices based on Sagnac interferometric structure. In the first one, the SOA as the nonlinear medium placed asymmetrically with respect to the center, as depicted in Figure 27. To perform 10 Gb/s XOR logic function two control signals 'A' and 'B' enters into loop through two couplers, which can be wavelength or polarization selective. A clock stream is injected to the loop via 3dB coupler splitting into equal parts of clockwise (CW) and the counter-clockwise (CCW) [117, 118].

The data pulses should arrive at the SOA just before their corresponding co-propagating clock components and their energy must be 10 times higher than that of clock pulse. Any of the data pulses modulates the carrier density and the refractive index of the SOA. This causes a phase shift due to the XPM on clock pulse arriving at the SOA exactly after the data signal. In the case that two data signals are identical, the signals 'A' and 'B' have effect on the CW and CCW clock components, respectively.

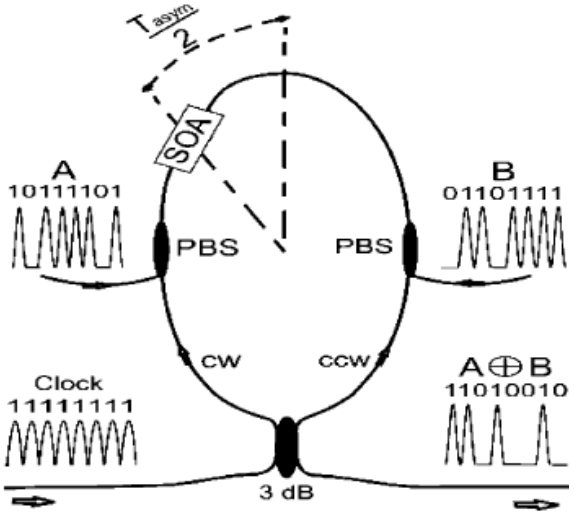

Figure 27. Configuration of asymmetrical XOR gate based on Sagnac interferometric structure [117].

If two data pulses are different, for example 'A' is '1' and 'B' is '0', the CW pulse experiences a saturated gain in SOA. The CCW counterpart arrives in the SOA after a relative delay due to the asymmetry in partial recovery gain. The difference in gain and phase of two parts of clock pulse causes constructive interference when arriving the coupler and producing a signal at the output. It means that when either data is

'1', it is depicted on that exits the gate, so XOR operation is achieved. The time difference in the arrival of the complementary clock pulses at the SOA is defined as asymmetry time, T_{asym}. This parameter determines the width of gate's switching window. In order to achieve optimum operation, T_{asym} can partially be adjusted by using an optical delay line in the loop. The delay must be more than half of the period of the clock, T_{per}. An additional requirement for clock pulse to be fully transmitted is its width, T_{FWHM}, which should be less than switching window, and also the width of the switching window cannot be shorter than the data pulse width. Moreover, the asymmetry must be less than the SOA gain recovery time that is expressed by carrier lifetime parameter, T_{car} [117].

The frequency of the data pulses is located at the peak of the SOA gain spectrum at 1550 nm. The SOA carrier lifetime is the most crucial and imposes stricter limitation on the performance of the gate. For this reason, it is necessary to utilize either the complex gain recovery enhancement techniques or to use the technology of quantum dot to reduce the carrier life time. The first method has been utilized below.

The second device based on Sagnac interferometer is shown in Figure 28. The operation of this scheme with 80 Gb/s is simulated correctly with high performance. This scheme is proved to exceed the speed limitation imposed by carrier life time of the SOA [118].

There are four ports A, B, C, and D. Two data trains enter the loop mirror via A and B. The clock pulses as probe signal are injected into the loop through 50/50 coupler, which split in two CW and CCW parts, and recombined there. At port D, the XOR logic results of data A and B, at probe wavelength are obtained.

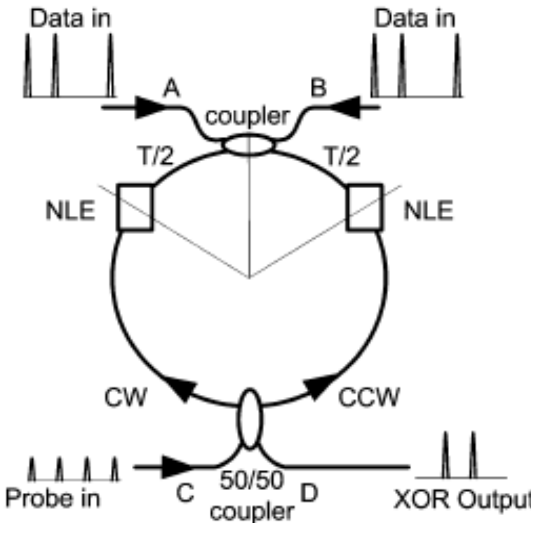

Figure 28. . Schematic diagram of symmetric XOR based on Sagnac interferometer [118].

It is obvious that signals A and B affect the right and left nonlinear elements, respectively. If data signals 'A' and 'B' are different, the differential phase shift between CW and CCW is not zero, so two data signals interfere constructively at port D and the output will be '1'. In the case that two inputs are identical, the structure is balanced and the differential phase shift is zero, hence the output becomes '0'. So the all-optical XOR function is realized.

In this section, all-optical logic gates using ring resonator as NLE and the proposed logic gates based on semiconductor micro-racetrack resonators [132-143], and logic operation based on photonic crystal will be described subsequently [144-160].

The two first logic gates operate as AND/NAND. They have the same configurations, but one of them is based on GaAs [132, 133] and the other is based on compact silicon [134]. The logic gate based on GaAs operates up to 30 Gb/s. It uses two photon absorption effect (TPA). The silicon logic gate is based on the free-carrier dispersion effect in silicon and TPA effect and can operate at 310 Mb/s with extinction ratio of 10 dB. The operations of the two gates are similar, but their difference is in experimental results.

III. PHOTONIC AND/NAND LOGIC GATE USING SEMICONDUCTOR MICRORESONATORS

A. All-optical AND/NAND logic operation using a microring resonator

The all-optical AND/NAND logic gate using a microring resonator exploiting TPA effect is operating up to 30 Gb/s [132].

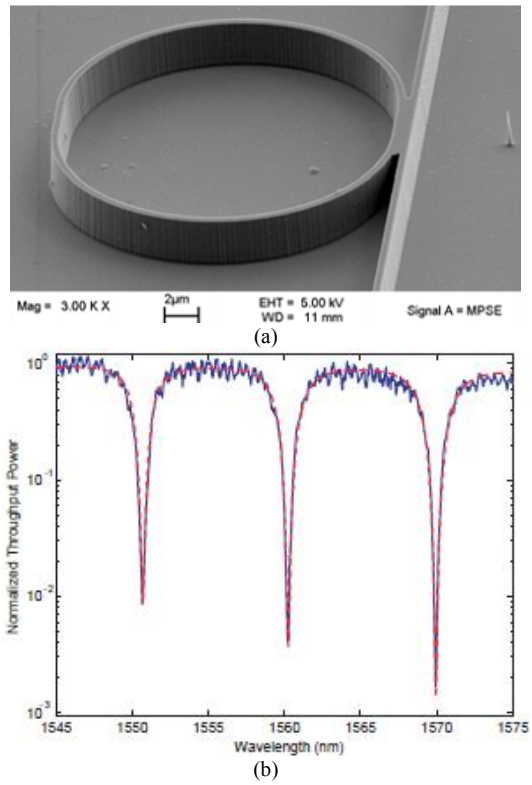

Figure 29. (a) Scanning Electron Microscope (SEM) image of the InP racetrack resonator, (b) Measured (line) and fitted (dash) spectral response at port of the resonator [132].

The nonlinearity used in the all-optical gate is the variation of the refractive index due to the two- photon absorption (TPA) effect. When pump beam has energy more than half of the band gap energy of the resonator material, the photons are absorbed, TPA and hence free carriers are generated.

The amount of carriers is proportional to the squared of intensity, which is quadratically proportional to the field increment inside the resonator. The phase change needed for switching resonator is reduced by FE^2. So, the optical power required for switching resonator is proportional to the square of field enhancement power of six of the field enhancement (FE). The free carriers decrease the refractive index and cause a blue shift in its resonance wavelength. If probe beam is tuned initially at resonance frequency, the output will be in low level or '0'.

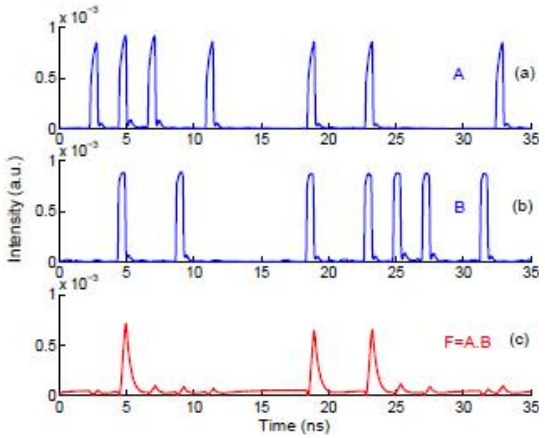

Figure 30. The performance of the AND logic gate. (a)' A' and (b) 'B' are two input data and (c)'F=A.B' is the output signal tuned to next higher resonance [132].

'A' and 'B' are input data, when either A or B is one, the amount of phase shift obtained by resonator is not enough to switch out of resonance. If both of the inputs are in high level, the nonlinear transmission of resonator enhances the switching and brings the probe out of resonance to high level. This returns to the function AND of logic gate. If the probe beam is initially out of resonance, the device can be operated as a NAND logic gate. This device is demonstrated and tested with InP and GaAs core. The demonstrated all-optical logic operation in [133] is the first optical logic function using compact silicon resonator and is fabricated on silicon on insulator substrate.

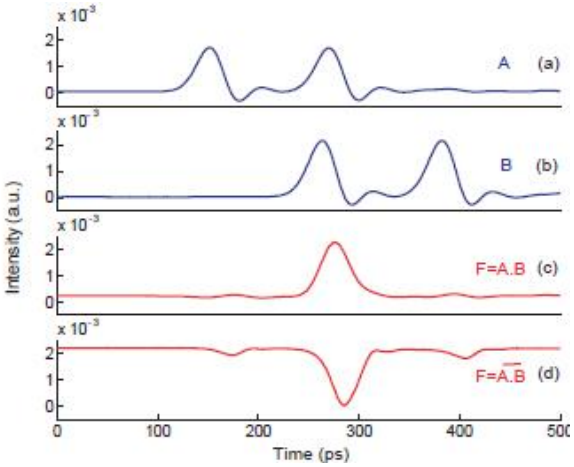

Figure 31. The logic operation: (a) A and (b) B are inputs; (c) output 'F' is tuned at probe resonance wavelength; and (d) output 'F' when the probe was initially blue tuned out of resonance [132].

The InP device shown in Figure 29, consists of a racetrack resonator that has a 10 µm radius and a 3 µm straight coupling section. In the InP device the probe beam tuned at resonance wavelength at 1560 nm, and was 10 mw as the input of the device. The pump pulse energy is 18 PJ as the input of the operator.

The diagrams in Figure 30 are the plot of time traces of the inputs and the output data patterns illustrating AND gate operation, and Figure 31 (a) and (b), are the plot of time traces for the inputs 'A' and 'B'. Figure 31 (c) shows the plot of the output probe, 'F', when the probe beam was initially tuned to resonance. It confirms that the output is in high level, only when both 'A' and 'B' are '1', demonstrating AND logic gate. If the probe beam was initially 0.4 nm blue tuned to resonance wavelength. When both A and B are '1', the generated carriers shift the resonance wavelength to bring the probe beam in resonance in nonlinear regime and make low transmission, this is the NAND logic gate. The switching window is 35 ps. It is limited by carrier life time and detection system.

B. Cascaded integrated photonic AND logic gates based on GaAs ring resonators

Figure 32 shows two cascaded AND logic gate is demonstrated using two symmetric GaAs ring resonator to perform more complex logic operation. The cascaded AND logic gate has 3 input and 1 output. 'A' and 'B' are the data pulse and 'D' is a continuous wave to be used to switch ON and OFF manually. Two ring resonators work as two cascaded AND logic gate [135].

The band gap energy is planned to be 800 nm, so 1550 nm pump pulse can be partially absorbed through TPA inside the ring resonator and free carriers are generated. This additional carrier decreases the refractive index of the resonator and makes a blue shift in the resonance wavelengths. According to some estimation the intensity required to spectral shift of 0.2 nm in ring is 12 GW/cm^2.

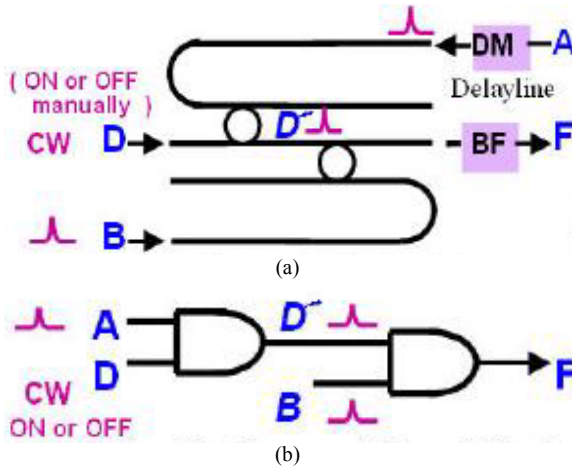

Figure 32. . (a). Double-ring device, (b) Cascaded two AND device [135].

Figure 33 shows the performance of the AND gate. 'A' and 'B' are tuned at 1558.6 nm and 'D' at 1548.18 'nm'. In Figure 33(b) when the CW probe beam D is 'ON' and pump pulse A is 'ON', the pulses of A and 'D' change the refractive index of the ring and blue shift switching D' out of first ring, so first ring works as an AND gate.

In Figure 33(c) when 'D' reaches the second ring, it will be switched out of ring at right time if B is 'ON' and the second beam works as another AND gate If 'D' is 'OFF' there is no output at port F even if 'A' and 'B' are in high level. The pump pulse wavelength is at 1558.6 nm with 18 and 16 pJ per pulse at input [135].

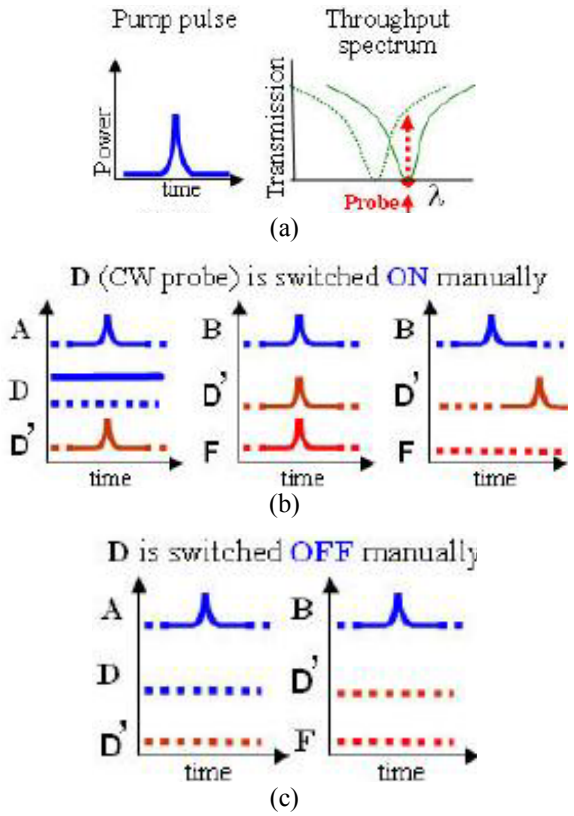

Figure 33. All-optical AND gate: (a) pump input and left shift of probe signal, (b) D input is ON, (c) D is OFF [135].

IV. All-Optical Logic Gates Based on Nonlinear Photonic Crystal Micro Ring Resonators

Nowadays ultra-compact all-optical integrated circuits become the most attractive appliance for real time information communication. Photonic crystals (PCs) are one of the best candidates because the size of photonic crystal logic gates can be reduced to the order of the wavelength. In this device nonlinear properties of Kerr effect in Si nanocrystal and its derivations are utilized. Si nanocrystals show high nonlinearity in the third window of communication. Strong nonlinearity and compatibility with Si technology make it more interesting than the other semiconductor crystals.

Dependency of this material to intensity is due to the Kerr effect and two-photon absorption. Two nonlinear parameters, which describe the two effects, are related to the real (n_2) and imaginary (β) parts of the third order nonlinear susceptibility ($\chi 3$). Because the real part of nonlinearity is one order of the magnitude higher than its imaginary part, TPA is negligible compared to the nonlinear Kerr effect at this wavelength [151].

The intensity-dependent all-optical logic gates based on MZI photonic crystal (PC) devices [148, 150, 156, 160] and resonator-based type [144-147, 149, 151-155, 157-159] are described here. The resonator-based are smaller and required lower switching power for operation. In the photonic crystal medium if the height of the glass rods in air is high enough in comparison with the propagating wavelength, and the structure is excited by localized source, the structure behaves as two dimensions instead of three dimensions. There are different types of PC-microring resonators (MRR) with different radius, which have different resonant frequency, quality factors, and mode type [144].

All-optical switches and logic gates can be implemented with different designs. One shape is consisted of two parallel waveguide and a PC-MRR between them as in $part_1$ and $part_2$, port4. This structure in this posture cannot be cascaded with the same structure due to the inseparable ports, but by a brief change can build cascadable one. With T-shaped structures, there is potential to cascade two more switch and logic gates as the NOR gate in $part_2$.

V. Controllable Photonic Crystal Logic Gates

The two most common devices used in processing systems are memory elements like flip-flaps and latches. The controllable logic gate consists of a photonic crystal ring resonator, placed between two parallel waveguides, as demonstrated in Figure 34. This ring resonator is built by replacing Si rods with GaAs with the same radius. GaAs rods has the same refractive index as the background in linear regime in the absence of high power clock pulse, but in the presence of high power input clock signal, the high power electromagnetic field intensities, created by the resonant phenomenon in the ring, change its refractive index. So the resonant wavelength increases due to the nonlinear Kerr effect at 1550 nm. This wavelength variation depends on the Kerr coefficient and the quality factor (Q) of the resonator which represents the lightwave confinement in the resonator.

Figure 34. All-optical PC controllable gate [151].

TABLE I. Data Transmission in the Presence and Absence of the Clock Signal [151].

X		Clk		Y	
Power W/μm	Logic level	Power W/μm	Logic level	Power W/μm	Logic level
33	1	330		47.855	1
0	0	330		14.72	0
33	1	0		1.87	0
0	0	0		0	0

Input data with 33 W/μm power are injected from port A. If the clock pulse is low level, the device will be placed in "cross" state and the data pulses exit from port C. However, in case a that the clock pulses with

330 W/µm power flow into port D, the resonant frequency of the ring will be changed and the input data exit from port D. In the design of this logic gate, a coupler is added beside port B for adjusting the logic level of the device. This coupler couples 20% of the flowing power in the waveguide terminated to port D. Data transmission in the absence and presence of clk signal is summarized in Table 1.

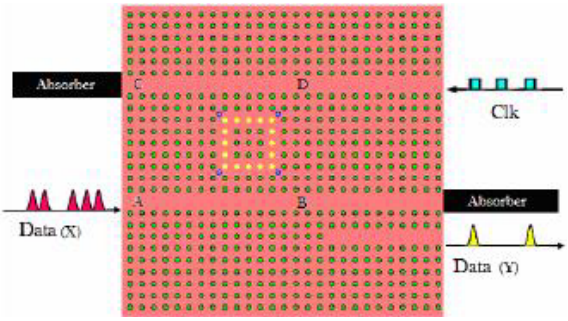

This optical logic gate defines 0 to 16 W/µm as the logical '0' and 30 to 50 W/µm as the logical '1'. Obviously this device can operate as instrument for applying clock signal in optical sequential devices.

A. All-optical NOR gate based on nonlinear microring resonator

Now a T-shaped all-optical switch based on photonic crystal microring resonators are described. By cascading two of these switches a NOR gate is created. The T-shaped switch is shown in Figure 35. This switch has two input ports, A and C, for the data and the pump signals, respectively. When there is no pump signal, ring resonator cannot resonate because the data wavelength is higher than its resonant wavelength in the linear regime, so we can receive input A at output B and there is no signal at port C. The efficiency of the transmission is approximately 81%. In the presence of pump signal due to nonlinear Kerr effect, a blue shift in resonant wavelength of microring is induced, now the frequency of the input data and the ring resonant frequency are equal. So, the lightwave will be confined in the ring and there is no energy at port B [154].

In the logic NOR gate structure there are three input ports as 'A', 'D', and 'C' as shown in Figure 36. Signal 'A' acts as a probe signal that carriers NOR result operation between 'C' and 'D' to output 'B'.

In the proposed NOR logic gate two switch act separately, if one or both of the pump signals are present, the resonant wavelength in the rings is blue shifted in nonlinear regime, so the power of data signal, 'A', is confined in one or both of the resonators and therefore the output will be OFF. In the case that both inputs are absent, none of the rings resonates, and hence the output 'B' is ON.

Different states of the NOR gate is demonstrated in Figure 37. The NOR gate works at wavelength of 1550 nm, and its switching time is about 3 ps (333 Gb/s).

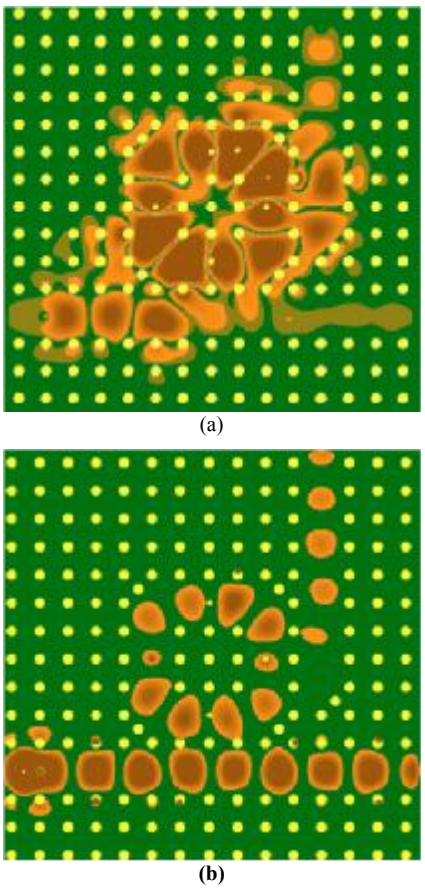

Figure 35. All-optical T-shaped switch (a) no pump signal (ON) and (b) with high intensity pump signal (OFF) [154].

Another proposed NOR logic gate consisting of two Kerr nonlinear ring resonators, located above a common waveguide to impose logic function to the probe signal transmitting through, it is depicted in Figure 38. Three linear ring resonators are placed below the common waveguide for filtering and preventing disruptive interaction of two linear ring resonators. There is a parallel waveguide to each of the rings as controller in nonlinear regime and as the receiver for the filters.

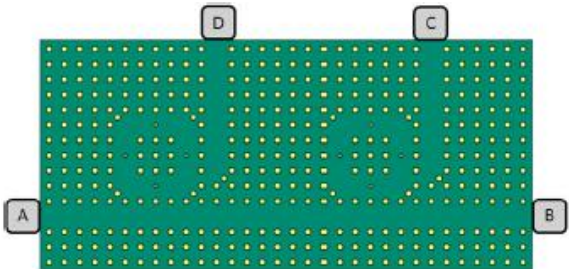

Figure 36. The NOR gate structure [154].

A weak CW probe beam, P, is injected to the middle waveguide. When one of the input signals A or B or both of them are present, the high Q factor of resonator causes considerable variation of the nonlinear refractive index of the inner resonator rods and imposes blue shift at resonant wavelength. So the weak probe signal drops in its related ring resonator and gives logic '0' in the output. In the case that both of the input signals are absent, the probe beam will be guided through the common waveguide and the output would become logic 1. When signal A is ON and

signal B is OFF, the probe is confined in the first ring and just 6% of it transmits to output port. The same procedure happens, when signal A is OFF and B is ON. Also when both of the input signals are present 3.3% of the probe can be received in the output (Figure 39).

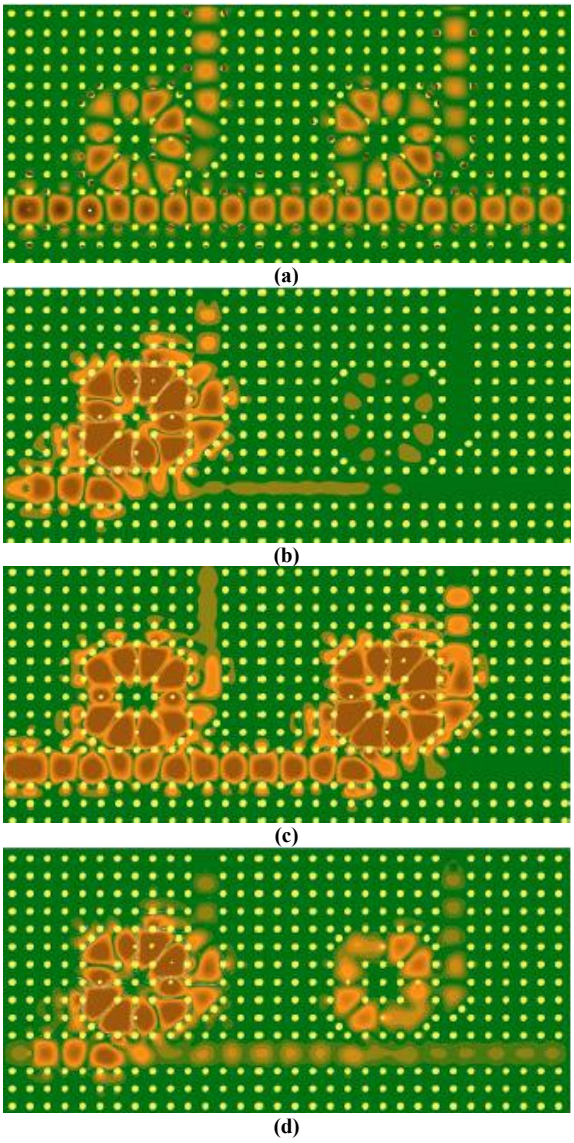

Figure 37. . Four states of the proposed NOR gate [154].

Figure 38. Schematic diagram of the conceptual NOR gate. The materials of different rods are introduced in the figure. The rods are embedded in BSC glass background [157].

By this method, the response time of the logic NOR gate is less than 7.2 ps, so it can operate as a logic gate with bit rate of 138.9 Gb/s.

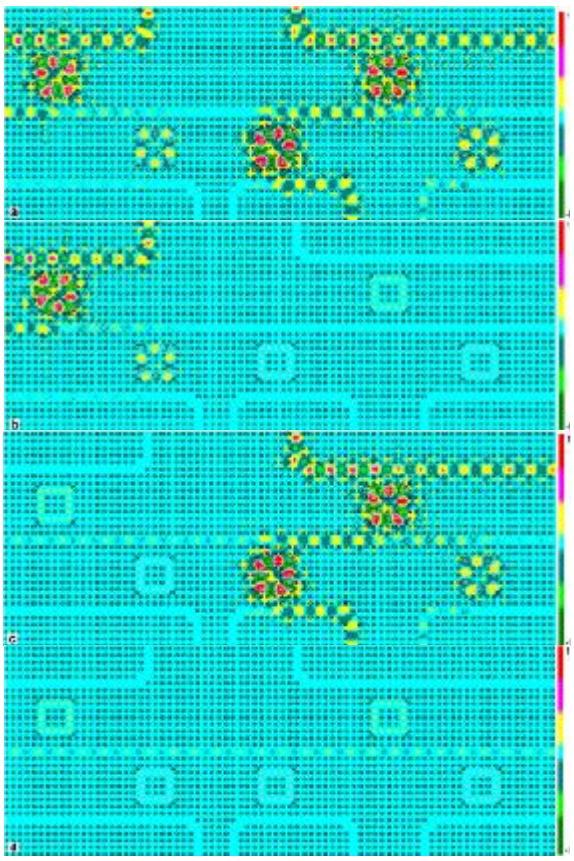

Figure 39. Electric field distribution when (a) signals A and B are on, (b) signal A is on and signal B is off, (c) signal B is on and signal A is off, (d) signal A and B are off [157].

VI. All Optical Logic Gate Based on Couplers and Waveguides

A. All optical logic gates based on directional coupler

A simple fundamental device for optical logic gates is the optically controlled directional coupler, as shown in Figure 40. This device can be constructed in variety of nonlinear materials [161].

Figure 40. . An optical directional coupler switch [161].

Optical control signal launched at port C allows input signals A and B pass directly through coupler. In the absence of the control signal, the switch is in cross state so the input signals are exchanged before arriving at output ports. By cascading these, as shown in switches like Figure 41, arbitrary optical gates can be formed.

Various types of all optical logic functions including AND, OR, XOR, NOR, XNOR, and NAND exploiting cascaded nonlinear fibre couplers structure are reported in [162]. Figure 42 shows the schematic of several cascaded nonlinear couplers.

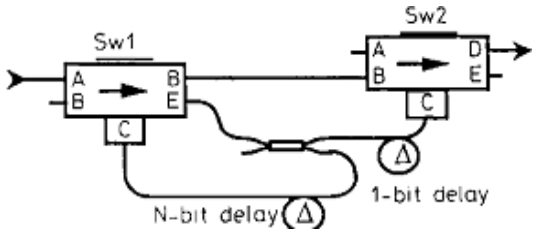

Figure 41. Cascading two directional Coupler switches [161].

Optical logic gates based on directional couplers utilize different nonlinear effects such as self-phase-modulation (SPM) [163], localized optical nonlinearity [164], pulse position modulation (PPM) [165], coupler assisted distributed feedback (DFB) waveguide [166], Coupler with triple core [167] and multi-mode interference (MMI) devices [168].

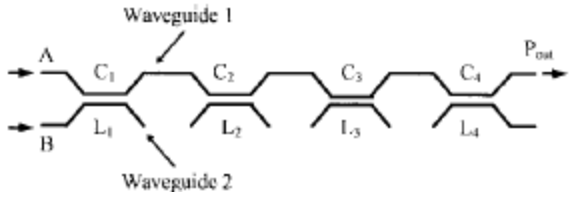

Figure 42. . Schematic view of a cascaded nonlinear coupler device [162].

B. All optical logic gates based on waveguides

All optical gates based on waveguides employ different nonlinear effects for nonlinear switching such as nonlinear polarization rotation in birefrigent waveguides [169, 170], Kerr nonlinear effect [171], two photon absorption in silicon waveguides [172, 173], stimulated Raman scattering, free carrier absorption, and cross phase modulation in silicon-on-insulator waveguides [174], and complicated optical gates such as half-adders and half-subtracer based on sum-frequency and difference-frequency generation in a periodically poled Lithium Niobate waveguides [175-187].

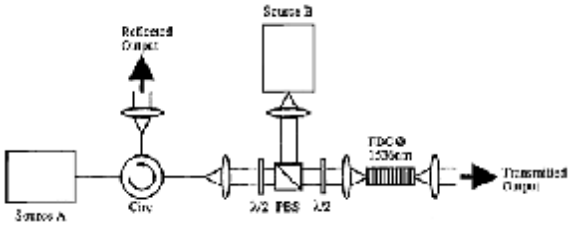

Figure 43. Experimental setup of an FBG based AND logic gate [188].

Bragg grating is consisting of a periodic modulation of the refractive index of a medium. The bragg grating devices are bistable, and have two low reflectivity and low transmission states. The high transmission state in resonant profile is called gap soliton [188]. The experimental setting of an all-optical AND gate based on fiber Bragg grating (FBG) are shown in Figure 43.

If one of the inputs is present, it is reflected by the grating and if both of them are present due to the gap soliton formation, both input pulses are transmitted. Different kinds of all-optical logic gates based on Bragg gratings are demonstrated in various configurations [188-196].

VII. Optical Logic Gates Based on Lasers and Cavities

Nonlinear Fabry-Perot (FP) etalons and laser cavities are the candidates for optical logic gates and processors.

Bistability is defined as existence of two different states for the same input value, even though it is not requisite for such logic gates. If a resonant cavity is filled with a nonlinear material, the absorption or the index of refraction varies with the intensity of light. If the absorption is a function of light intensity, its value decreases with increasing intensity. If the refractive index of medium depends on intensity, the etalon in or out of resonance will be tuned with light at fixed wavelength [197].

Nonlinear material by exploiting resonant cavities loop mirrors and lasers are designed and generated up to now [198-214] and different kinds of logic gate based on the material with absorption effect, called saturable absorber [215-219].

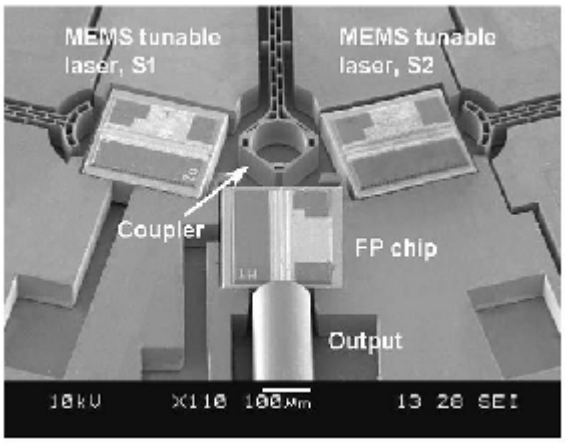

Figure 44. . Scanning electron micrograph of integrated MEMS logic NOR gate [209].

In this chapter, one example of the both kinds will be described. This explanation is about the first attempt to realize a single chip solution to the optical logic gates using MEMS technology and may motivate growth of other all-optical gates using MEMS optical devices. The all-optical logic gate is based on MEMS and tunable lasers. The MEMS structures including the adjustable coupler, movable mirror, comb-drive actuator, FP lasers, and a curved mirror, are fabricated on an SOI wafer by using deep-reactive-ion-etching (DRIE) process with structure layer of 100 µm thick as shown in Figure 44. This logic gate is demonstrated at 100 Mb/s but has potential to work up to 10 Gb/s. The schematic view is shown in Figure 45(a). It consist of two MEMS, external cavity tunable lasers (ECTL), a FP chip and a band-pass filter.

The data NOR function is illustrated in Figure 44. The data 'A' and 'B' radiate from two MEMS external cavity tunable lasers (ECTLs) (S_1 and S_2), and coupled to mode locked FP laser. Therefore the FP laser locked by means of the signals (A and B) through

nonlinearities, and a BPF is tuned on λ_0, defines the transfer window and select the preferred wavelength, consequently obtain NOR function at λ_0. The injection locking laser just depends on input power rather than the accurate phase matching and polarization control [209].

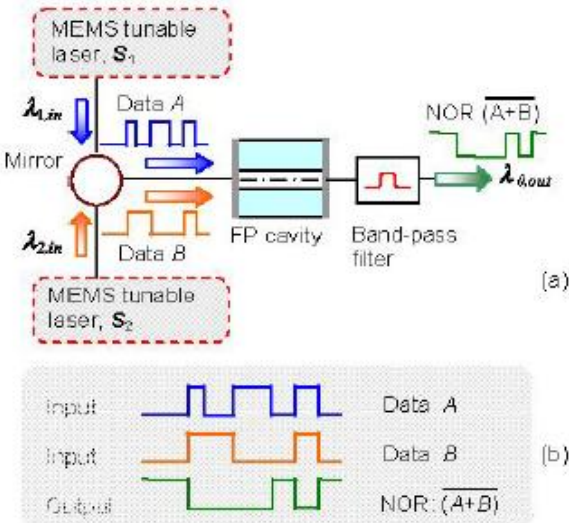

Figure 45. (a) Schematic view of the MEMS all-optical NOR logic gate, and (b) principle logic function [209].

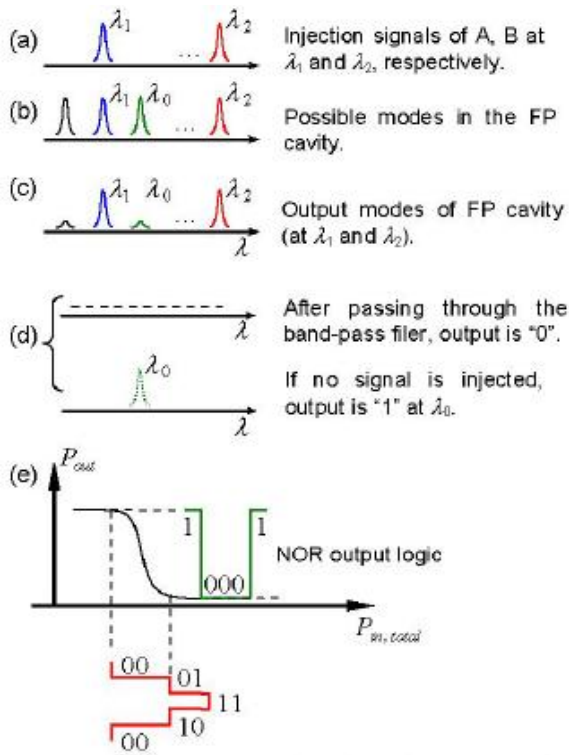

Figure 46. (a-d). The logic NOR logic function based on MEMS ECTL injection locking-mode FP. (e) relation of input and output power in this NOR gate [209].

FP has a multi mode laser output, shown in Figure 46(b). As shown in Figure 46(c), in the presence of 'A', 'B' or both of them, the output of FP can be locked on that wavelength, therefore the mode of λ_0 is suppressed to low power level. So only when both of 'A' and 'B' are zero the final output turns to high level at λ_0. Therefore the logic NOT function is realized. As long as the FP chip remains locked, the output is insensitive to variation of the input power.

There is a lockable wavelength range for injected beam. If the input falls into lockable range, the input is amplified strongly and other modes suppressed to very low level. When the input power wavelength is beyond the locking range, the output power is at low level even if input power is high level. In Figure 47(a) the bandwidth of FP is shown, it is about 30 nm, and λ_0 is 1553.34 nm.

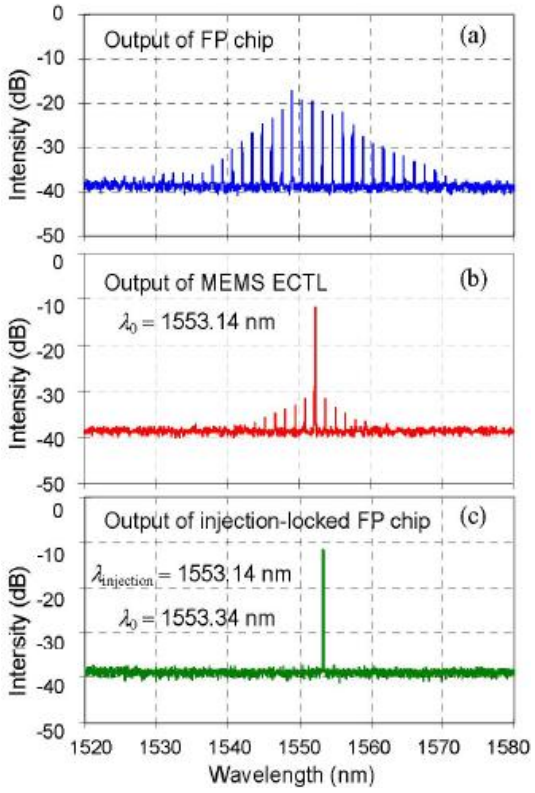

Figure 47. . Output of the FP chip in different states. (a) Original multimode output of the FP chip, (b) output of MEMS ECTL, and (c) single mode of the injection-locked FP chip [209].

After injection of inputs, the output wavelength is equal to the output wavelength of the MEMS ECTL that injected to FP chip, and become pure single-mode at 1553.14 nm. It is obvious that there is a red shift of $\Delta\lambda$ = 0.2 nm after the FP. The reason is the optical injection to the FP; it modulates the carriers and refractive index, leading to FP mode shift.

For any wavelength in locked range, the increase of input power causes the decrease of output power at λ_0, when λ_{in} is close to λ_0. For instance, an injection power at 1559.44 nm from -15 to 0 dBm produces -20.8 dBm decrease in FP output power.

It is obvious that for proper NOR logic gate operation, the injection power of input should be low and high enough and a middle level power injection may result in another type of logic operation. Smaller detune from target wavelength, low power injection requires for locking is shown in Figure 48. When injection power is higher than -30.7 dBm, the FP can be locked, and it is fully released from locking if input power is below -46 dBm.

A comparison between measured output signal and the Boolean NOR between signals A and B, approves the logic NOR function.

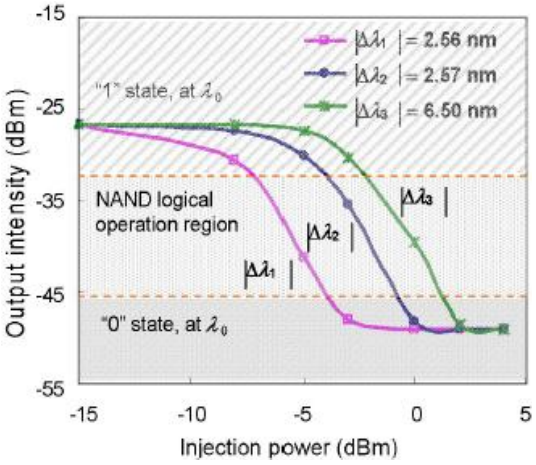

Figure 48. Output power of logic NOR gate. External injection power varies antithetical of different injection wavelength [209].

VIII. High Speed All-Optical AND Gate Using Nonlinear Transmission of Electro-Absorption Modulator

Electro-absorption modulator (EAM) is an optical device based on cross absorption modulation and uses saturation of absorption property. In this method, contrary to XGM method in SOAs, the output signal is not inverted.

If the input signal is '1' due to the generation of free carriers the amount of absorption decreases, the intensity of electrical field decreases and as a result the absorption decreases. So, the probe signal is confront with low absorption and its power remains constant. In the case that input power level is '0', the absorption property remains firm and the output power decreases.

Here we introduce a bit-wise logical AND gate operating based on EAM effect, shown in Figure 49. This 10 Gb/s logic gate is pumped with two counter-propagating data streams and has extinction ratio of more than 10 dB [220]. According to [219] with the proper timing between two counter-propagating pulse streams, the case that one of the inputs is detected as the output has better performance compared to the case of using the CW probe only. The transmission window time can be reduced down to 10 ps due to attenuation of the input power. So the operating speed can be increased up to 100 Gb/s.

Figure 49 is the experimental setup of this AND gate. The pump pulses were generated by mode locked laser. After amplification in an erbium doped fiber amplifier (EDFA), they were split by 3-dB coupler into two counter-propagating streams and the relative delay between two inputs was adjusted with variable optical adjust line.

The output pulses from one of the EAM arms was split off by 20-80 coupler to reach the output of the AND logic gate. The extinction ratio of the gate at 5 pJ in each input was 10 dB. The extinction ratio increases as the input power is decreased. This optical logic gate is suitable for cascading because the gate input and output powers have the same wavelength that is crucial for cascading and integrating the optical devices.

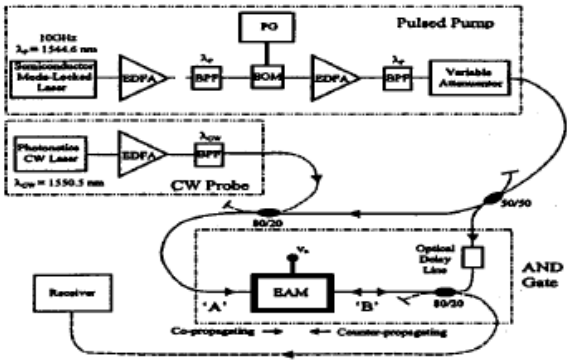

Figure 49. Experimental setup for optical logical AND gate based on EAM in a counter-propagating configuration [220].

IX. All-Optical Logic Gate Based on Highly-Nonlinear Fibers

The all-optical logic gate based on nonlinearities of optical fiber has potential of operating at terabits per second, due to the immediate fiber nonlinearity. In demonstration of all optical fiber logic gates, different properties are used, such as birefringence and polarizations rotation [228, 229], interferometric structure such as nonlinear loop mirror and Mach-Zehnder [230-237], Kerr nonlinearity [238, 239], XPM effect [240], multilevel modulation and self phase modulation (SPM) [241], FWM effect [242], and XGM effect [246]. A quantum control-NOT gate is reported in [244].

Because of the low nonlinearity of the conventional optical fibers, long segments from several kilometers to several meters are required, to fulfill an optical logic gate. Hence the optical fibers with high nonlinear index are built, to allow the use of small 10 m segments of the fiber [239]. But it is still very large compared to the semiconductor optical amplifiers to be fabricated in compact size. We review some kinds of this logic gates in this section.

A. All-optical XOR gate based on highly-nonlinear fiber

This scheme is about 10 Gb/s XOR logic gate based on Kerr effect in single highly-nonlinear fiber (HNLF). In Figure 50 a conceptual diagram of this device and its construction technique is shown. Due to the Kerr nonlinear effect two input wavelengths λ_1 and λ_2 vary the birefringence of the HNLF, so rotation of the polarization of the third light at wavelength of λ_3 occurs. The amount of induced birefringence is proportional to ON/OFF states of two inputs. Output λ_3 becomes distinct after a polarizer represents the XOR of two inputs. The logic device is made up of 2 km HNLF with nonlinear coefficient of 9.1 $W^{-1}Km^{-1}$ [238].

At input polarization states of λ_1 and λ_2 are orthogonal and both of them are aligned with 45° shift toward third CW at λ_3. The polarizer placed at end of fiber is orthogonal to original polarization state of λ_3.

When both λ_1 and λ_2 are OFF, there is no output at λ_3 after the polarizer. If one of the inputs is in high level, the refractive index in the direction corresponding to that input polarization (λ_1 or λ_2) will be changed. In this condition, the polarization of lightwave λ_3 will be rotated and resulting an output after polarizer.

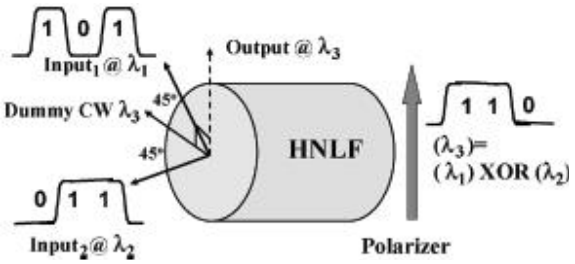

Figure 50. Concept of all-optical XOR gate based on Kerr nonlinear effect in a single highly nonlinear fiber [238].

In the case that both of λ_1 and λ_2 are present the birefringence induced by λ_1 and λ_2 are eliminated, so there is no output after polarizer. Therefore the output after polarizer at λ_3 is XOR of the two inputs λ_1 and λ_2. In experimental setup wavelengths of λ_1 and λ_2 are 1548 nm and 1550 nm, respectively, and wavelength of is 1554 nm. Wave light and combined first and the output of which is coupled with into HNLF. In this 2 km fiber the nonlinear coefficient is 9.1 1/w.km and fiber loss is 0.45 1/dB.km. The input power of λ_3 at input into HNLF is 3 dBm and the optical power of λ_1 and λ_2 at input of logic gate are 0.11 W. The output power is continuously change from -40 dBm up -15 dBm. When two inputs are equal output is -40 dBm and when only one of them is present the output is -15 dBm. By using HNLF with higher nonlinearity or using HNL (holy fiber) both of output power and ER will be improved and required power can be decreased.

B. 160 Gbs-1 Photonic logic gate based on cross-phase modulation in the fibers

This part is about a fiber based all-optical logic gate exploiting cross-phase modulation (XPM). Using this technique, can obtain five logic operations (XOR, OR, NOR, NAND and NOT) [239].

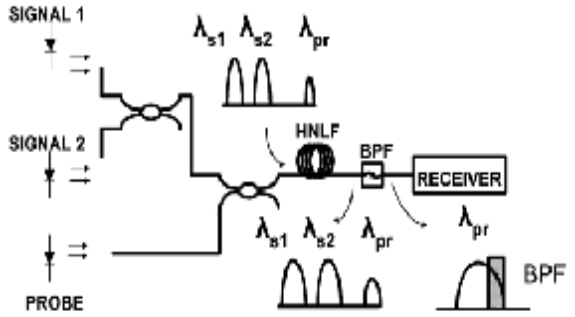

Figure 51. Scheme of reconfigurable all-optical gate. The Spectrum of probe is broadened through XPM. BPF selects the slice that provides the preferred logical Function [239].

Because of instantaneous response of fiber nonlinearity, this kind of logic gates have potential to work at Tb/s and with new highly nonlinear fiber can use fiber segment <10 m to make them. The conceptual scheme of the logic gate is shown in Figure 51. When two or more optical fields propagate concurrently inside the fiber, they interact with each other through fiber nonlinearity (Figure 52).

When only one of the pump signals is present a BPF can be utilized to select weaker spectral broadening caused by one Gaussian in order to obtain XOR logic operation.

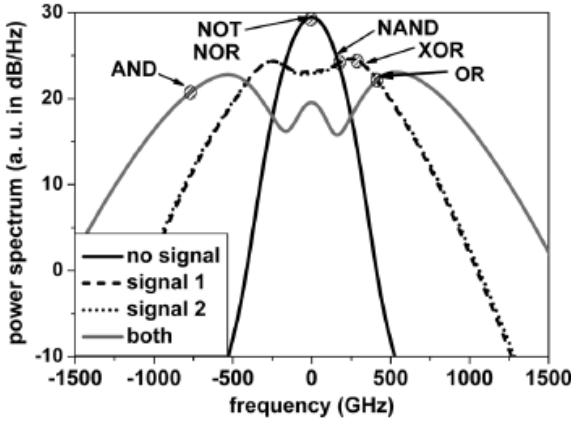

Figure 52. Spectral broadening the probe beam due to XPM. The circles show wavelength where the BPF should be tuned for operation of each logic gate [239].

A number of other logic gate such as AND, NAND, OR, NOT, and NOR obtained by properly tuning the optical filter. The spectral position of three waves which determines the value parameters δ_1 and δ_2, the value of initial delay between the two signals, the peak power, and width of signal pulses are critical operation parameters. When two high power pump input with peaks P_{s1}, P_{s2} and a weak probe beam with peak P_r are coupled into high-nonlinear fiber simultaneously, the probe beam will be experienced a time dependent nonlinear phase shift through XPM. In order to avoiding FWM between two strong signal and modulation instability noise, both signals should have wavelength shorter than the zero-dispersion wavelength.

Three input Gaussian pulses are placed at 1535 nm, 1550 nm and 1580 nm. A typical 125 m long highly-nonlinear fiber with nonlinear parameter γ=34 1/w.km, fiber losses $\alpha = 0.9$ dB.km^{-1} and zero-dispersion wavelength λ_0 =1560 nm, is considered. The pulse width T_0 is chosen to be equal to 1ps to be short enough for 160 Gbs^{-1}. Peak power for pump pulses is 400 mW, and for probe pulse is 30 mW. In order to achieve symmetrical broadening of probe spectrum, the signal at 1553 nm must be placed 2 ps prior to probe while the 1550 nm one has 0.28 ps delay toward the probe pulse.

To sum up in terms of nonlinear media for optical processing, the optical fiber have demonstrated benefits of ultra-high speed due to femtosecond response of Kerr nonlinear effect in silica, but the fiber based configuration is so large in size as it usually as to incorporate on cascading several stages.

C. A reconfigurable AND/OR logic gate exploiting multilevel modulation and self-phase modulation

Two fiber-based optical logic gates are reported need subtle control. However, the schemes require exact polarization control on the input signals. Here

we demonstrate a 10 Gbs^{-1} reconfigurable logic AND/OR logic gate optical multilevel modulation in an EAM and SPM, that is polarization independent [245].

As depicted in Figure 53, two data streams, data 'A' and data 'B', with equal power are launched into a power addition module, which can generates three level output signals. After converting this three level to another wavelength by wavelength converter (WC), it are fed into a section of polarization maintaining fiber in which SPM broadens the different intensity levels to different spectral widths. The zero level has narrowest broadening, the highest level (level-2) has broadest spectrum. When the spectral OBPF is placed where that covered by both level-1 and level-2 but not covered level zero, OR logic function is obtained. When the OBPF is tuned at spectral region that only covered the level-2, the all-optical AND logic gate is generated. The AND and OR logic can be obtained by two fixed OBPF or a tunable OBPF. This logic gate works at third communication window.

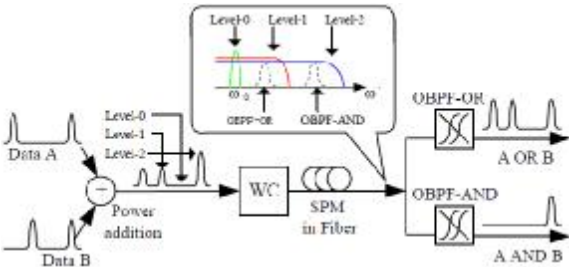

Figure 53. Proposed AND/OR logic gate [245].

X. Optical Polarization Based Logic Functions with Nonlinear Nanoslab

Here we introduce a XOR/XNOR logic gate, based on non phase matched noncolinear second harmonic generation from a symmetric crystalline Gallium Nitride nanoslab. The functionality can be obtained by using a crystalline medium belonging to symmetry class as hexagonal like GaN. The group-III Nitride semiconductors have a massive impact on photonics due their transparency over large frequencies from deep UV to far IR [254].

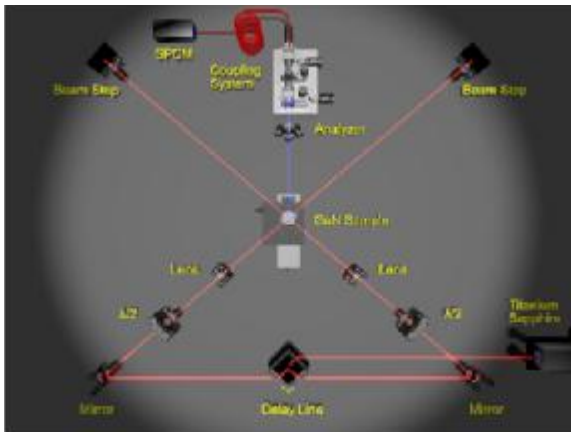

Figure 54. Non-collinear SHG experimental setup [254].

The polarization of the generated beam is a function of both pump beams. Only some of all possible polarization combinations are generated and that the interaction of optical signals behaves as a polarization based XOR/XNOR. Figure 54 shows the experimental setup of this polarization based logic gate.

If two pump signals are parallel polarized or normal polarized, the generated SH is parallel polarized, while if one of them is parallel polarized and the other is normal polarized, the SH polarization is normal polarized.

By setting the logical "0" to $\hat{p}$ polarization and the logical "1" to $\hat{s}$ polarization the nonlinear interaction behaves as XOR, when two equal bits arrive at the input of gate, the output will be '0' or $\hat{p}$ polarized. As two different bits arrive at input, the output bit will be '1' or $\hat{s}$ polarized. By inverting the bit polarizations, by setting the logical '0' to $\hat{S}$ polarization and the logical '1' to $\hat{p}$ polarization the nonlinear interaction behaves as XNOR.

XI. Optical Gates Based on Vertical Cavity Laser and Optical Thyristor Structure

Logic operation OR has been realized by connecting parallel connecting of discrete optical thyristor and AND logic gate has been realized by connecting serial connecting optical thyristor [255, 256]. An optical logic AND/OR logic gate, that has been demonstrated monolithically integration of a vertical cavity laser with optical thyristor [257] is explained briefly here.

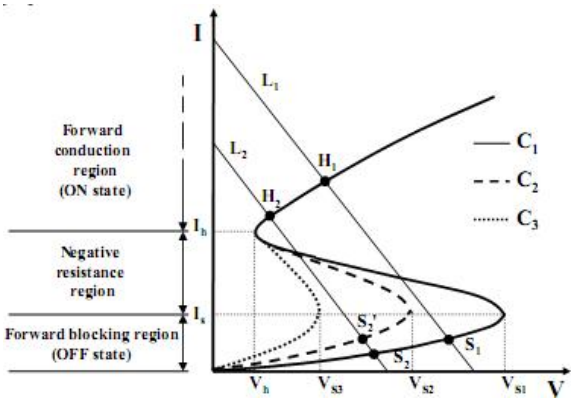

Figure 55. Typical s-shaped I-V curve of an optical thyristor [257].

XII. All-Optical Molecular Logic Gates

An optical thyristor is a bistable device with an s-shaped current-voltage curve (Figure 55). In forward bias, the thyristor has three distinct states: (1) high impedance region (off-state), (2) negative resistance region, (3) low impedance region (on-state). In on state, the optical thyristor emits as laser [257]. By increasing the input optical power, I-V curve varies from c_1 to c_3. If the driving voltage is upper than the switching voltage the thyristor will be in on-state. Due to shine light on thyristor and generation of carriers in the gate layers, the switching voltage is reduced. c_1 Is the original I-Curve, c_3 is the I-V curve when two inputs are injected into thyristor, and c_2 is I-V curve

when only one is injected into thyristor. When driving voltage is between v_{S2} and v_{S3} the device only turns on at c_3 condition, thus providing AND logic operation. If deriving voltage is between v_{S1} and v_{S2}, it turns on at c_2 and c_3 conditions, thus providing OR logic function.

All-optical molecular device is one of the candidates in ultrafast communication and computing systems. Molecular devices offer number of advantages of small size and nanometric dimensions, weight, high speed, low propagation delay, and power dissipation [259]. Organic molecules are promising candidates. They can be easily produced and are cheap to make and their properties can be tuned through the chemical modifications [260]. Here we introduce some kind of all-optical organic molecular devices, such a half-adder [259] and bR based a NOR/NAND logic gate, a multi function logic gate [263-266], a microtubule based XOR gate [267], and some chemical polymer based all optical logic gates [268-270], different all-optical diodes, switches, and integrated logic gate based on LB films [271-276], and different complicated molecular based logic gates and switches were demonstrated [277-296].

A. Half adder logic circuit with Azulene and Rhodamine

Half-adder is basic component in digital computers. For building a half-adder, a XOR and an AND operation should work in parallel [259].

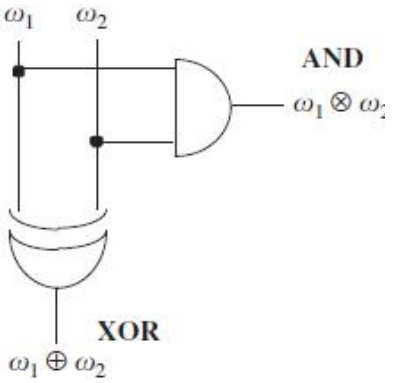

Figure 56. Schematic of half-adder circuit [259].

The half-adder is shown in Figure 56 and the truth table for this operation is given in Table 1. The XOR operation produces sum of two inputs, so-called 'sum out" and AND produces an output called "carry out". An all optical molecular half-adder is represented in Figure 56. A molecular half-adder can be implemented on molecules that have one photon absorption and two photon absorption. This kind of molecule has $s_2 \rightarrow s_0$ fluorescence and also is probed $s_1 \rightarrow s_0$ fluorescence. Molecular fluorescence from s_2 state seems to oppose kasha's rule. According to kasha's rule photon emission occurs from the lowest exited electronic state s_1, .Azulene and its derivates and Rhodamine are exception to this rule. Both of the XOR operation produces sum of two inputs, so-called 'sum out" and AND produces an output called "carry out".

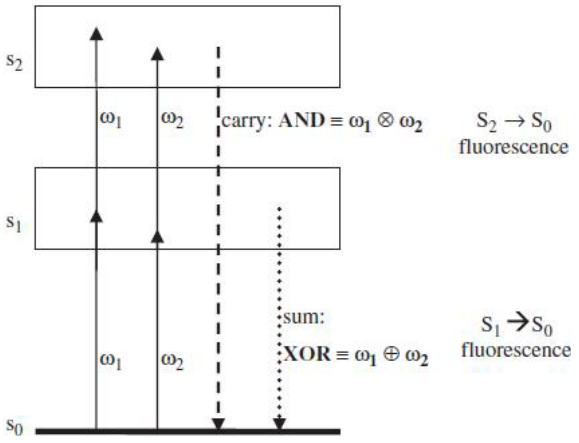

Figure 57. Scheme of all-optical molecular half-adder [259].

TABLE II. TRUTH TABLE FOR HALF-ADDER [259].

ω_1	ω_2	Midway sum	Carry 1
0	0	0	**0**
1	0	1	**0**
0	1	1	**0**
1	**1**	**0**	**1**

The output is probe as $s_2 \rightarrow s_0$ only when both and inputs ω_1 and ω_2 are present (AND logic operation), the sum output is probed as for presence of one of ω_1 or ω_2 photon excitation (XOR operation). The degenerate case of logic function is also possible when $\omega_1 = \omega_2$.

An all optical molecular half-adder is represented in Figure 57. A molecular half-adder can be implemented on molecules that have one photon absorption and two photon absorption. This kind of molecule has $s_2 \rightarrow s_0$ fluorescence and also is probed $s_1 \rightarrow s_0$ fluorescence. Molecular fluorescence from s_2 state seems to oppose kasha's rule. According to kasha's rule photon emission occurs from the lowest exited electronic state s_1, .Azulene and its derivates and Rhodamine are exception to this rule. Both of radiation are detectable, because emission from s_2 state is blue shifted in comparison to the emission from s_1 state.

B. All-optical logic gates with bacteriohodospin

All-optical logic gates with bR protein molecules have been demonstrated based on different protocols, NOT, NAND/NOR logic gate based on nonlinear absorption [260], an AND gate using sequential photo excitation [261], all-optical AND and OR based on degenerate four wave mixing geometry [262], and all-optical logic gates based on complementary suppression-modulated transmission [263] and for complicated structures, we can refer to [264-267]. We suffice to explain some of them and to direct others in this review paper. The photochromic protein bacteriohodospin places in the purple membrane fragments of Halobacterium halobium, is a proper material for bio-molecular photonic applications. It exhibits high efficiency. Response in the visible range,

low production cost, capability to form thin films in polymers and gels, and etc [261]. The bR absorbs green-yellow light and through the several transformations generates a number of intermediate states. The bR main photocycle is shown in Figure 58.

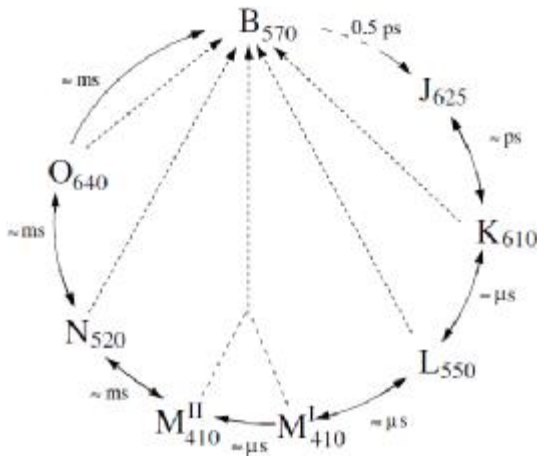

Figure 58. Photocycle of bR molecule [261].

After excitation with green-yellow light at 570 nm, the molecules in the initial B state get transformed into intermediate states like Figure 5. An important point is the ability of all the intermediate states to switch back to the initial B state by illuminating at corresponding absorption peak wavelength. The absorption peak wavelength each state is shown in Figure 58 in nm.

This all-optical gate has been demonstrated based on all-optical switching of a CW probe at 640 nm beam by the pump pulse beam at 570 nm due to nonlinear exited states absorption. The transmitted intensity of probe input is initially high due to low linear absorption in absence of pump pulse (switch on state). In presence of pump pulse due to enhancement of O state population the absorption of the probe pulse increases (switch off state). There is 6 ms delay between the peak of the input and the minimum in the output due to time taken to populate the O state.

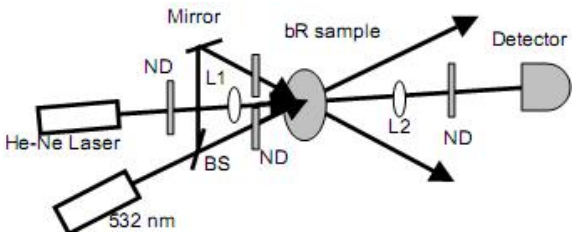

Figure 59. Experimental setup for demonstrated all-optical logic gate [265].

This switching configuration conform an all-optical NOT gate. For NOR logic gates, consider two pump pulses at 570 nm, the output is low if either one or both of inputs are present and high in case none of them is present.

In all-optical NAND logic gate if we consider a threshold level, the output is high when either one or none of inputs are present and low when both input pump pulses are present.

Most of previous proposals [260-264] are based on B and M or based on B and O two-state model. bR photocycle is complex process, but in some situations the intermediate states cannot be neglected. The absorption of O state at 633 nm is larger than that of B and M states so it largely varies the absorption properties [265]. Based on optical switching and pump-probe method and adjustment of intensities compared with threshold intensity 11 kinds of binary all-optical gates using the bR film are designed in ref. [265]. The experimental setup of the all-optical logic gate is presented in Figure 59.

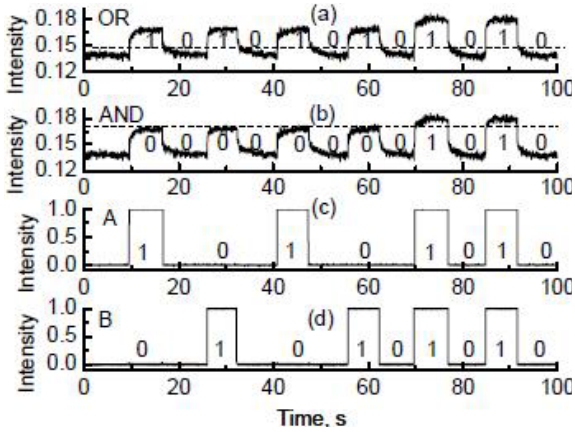

Figure 60. . All-optical logic gate: (a) optical OR logic, (b) optical AND logic, (c) and (d) is two inputs [265].

Two inputs at 532 nm acts as two inputs 'A' and 'B', and probe beam at 633 nm caries the logic operation between them to output. When the intensities of two green inputs are below 0.56 mW/mm^2, there is no change in transmitted probe beam. By considering threshold below or above this level, this intensity can be supposed as "0" or "1". When pump intensity is high 0.56 mW/mm^2 and probe intensity is less than 3.1 mW/mm^2, the probe beam intensity increases in presence of one or both of pump beam, this switching behave like OR logic gate Figure 60(a). AND logic gate can be obtained by setting the threshold level as dashed line Figure 60(b).

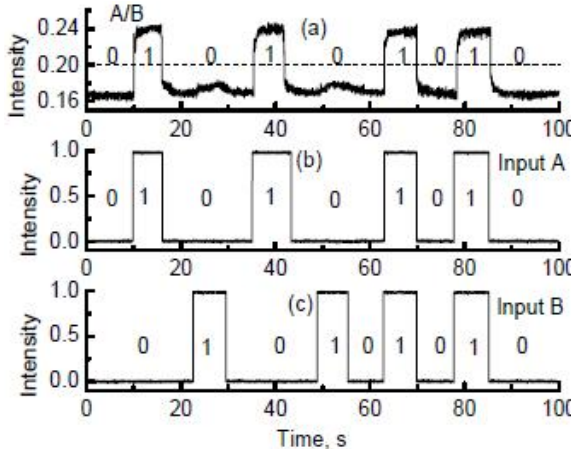

Figure 61. . All-optical logic gate: (a)A/B logic operation, (b) and (c) two optical inputs [265].

When one pump beam is less than $0.56 mW/mm^2$ and the other is higher than 0.56 mW/mm^2, the intensity of probe increases only when high intensity pump beam is present , this shows configuration A/B logic function (Figure 61).

In the case that both pumps are 0.56 mW/mm^2 and probe is less than 3.1 mW/mm^2, when pump beam is on, transmitted probe beam intensity is decreased due to the increased absorption of Br state so in the presence of one of the pump inputs or both of them, the output probe intensity is reduced and in the absence of pump beams, is high. This switching characteristics, as shown in Figure 62, can be used for demonstration of NOR logic gate [265].

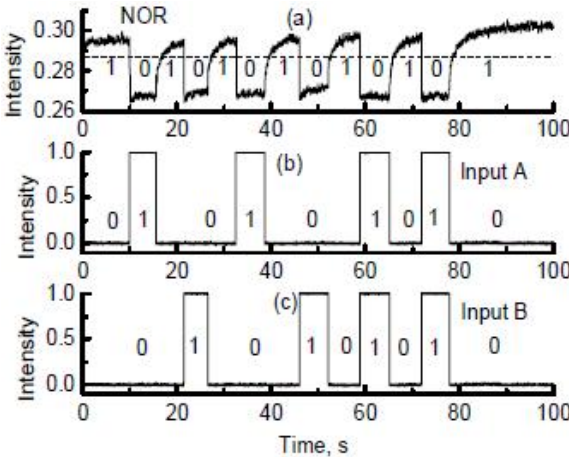

Figure 62. All-optical logic gate: (a) optical NOR gate operation, (b) and (c) are the normalized input [265].

In this manner by setting the pump and probe intensities NOT, NA/NB, $\overline{(A \otimes B)}$, flip-flop, and etc logic function can be demonstrated .

Here we investigate the properties of the cytoskeletal protein tubulin (microtubules-MTs), which can be used in storing and processing information in biomolecular circuits (Figure 63) [267].

C. Microtubules based XOR gate

The simulation is based on tubulin atomic structure and amino acid. It has a permanent electric dipole moment which changes the conformation of tubulin. This property can be used for binary switching.

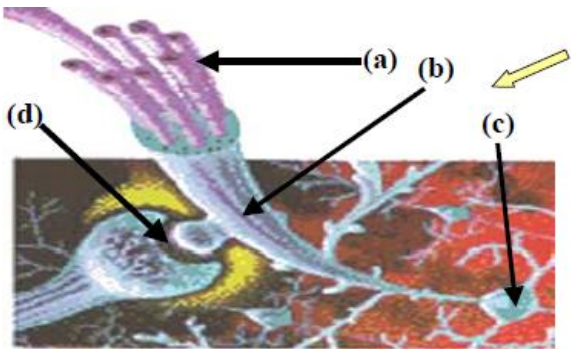

Figure 63. (a) Microtubule, (b) Neural axon, (c) soma of neuron [267].

MT has two solitons traveling, two counter-propagating MAPs to transmit to MT b. The solitons arrive at MT b cancel each other. In this case if the MAPs are arranged such each can transmit a soliton, but if they both transmit, the solitons cancel each other (Figs. 63 and 64) [267].

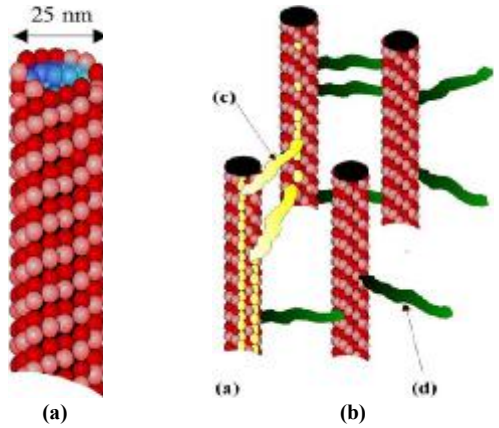

Figure 64. . (a) A typical neuronal microtubule, (b) MT based XOR gate, (a) Input MT, (b) Output MT (c) A MAP transmitting a soliton, (d) A quiet MAP [267].

D. Polymer based photonic logic gate

First all optical molecular logic systems are based on one coupling operation of two molecular switches that is to say photo-acid [268].

Photo-acid transducers optical input to ionic output (Sw1), and three states switch that respond to ionic inputs and provides optical outputs (Sw2). The two switches communicate with each other by chemical signals and are connected serially, that output of Sw1 is as input of Sw2. this system can perform AND, OR, and XNOR logic functions.

The proton inputs for RU^{+2} switch can be photo-generated by dosing the amount of light absorbed by $ME-H^+$ Photo-acid. Two input wavelengths are at 400 nm. The input string '00' is dark condition which no H^+ transfers. The inputs string '10' and '01' transfer on proton from $ME-H^+$ to RU^{+2} so the complex $RU-H^{+3}$ is generated. The input string '11' caused two protons are transferred to $ME-H^+$ and the complex $RU-H_2^{+4}$ is gained.

Different logic functions with corresponding threshold values can be obtained. If threshold A is applied and luminescence intensity is obtained at 626 nm, the XNOR gate is obtained, if threshold B at 732 nm is used, the function's behavior is like an OR whereas the logic behavior is like an AND gate with adoption of threshold 'C'. By taking advantage of getting different channel for outputs the three fundamentals logic operations can be integrated (Figure 65).

Other kinds of logic functions are presented based on thin film so called polymer Langmuir-Blodget films which are based on acrylamide polymer and its copolymers [269].

By applying LB technique, monolayers with different functions in molecular dimensions with mimic photo energy conversion cab are assembled [270].

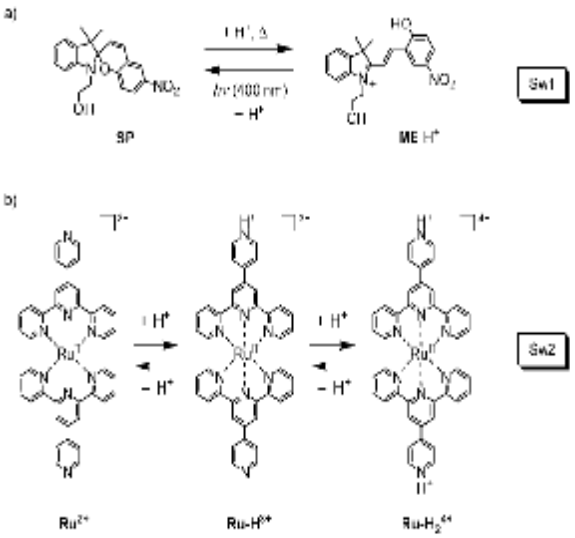

Figure 65. Structure of two molecular switches, (a) Sw1:the acid and light controlled balance, (b) Sw2: the acid based driven interconversion between the three protonation states [268].

To fabricate photonic nanodevices, different photoactive chromophores such redox species, aromatic hydrocarbons, photonic nonlinear groups, and metal nanoparticles into polymer nanosheet are used. Here optical logic gates based on photo induced electron transfer are introduced. Bottom-up approaches such as self-assembled monolayer, layer by layer, and LB method are based on molecular interactions. By using super molecular chemistry and polymer materials, the ultrathin films have been extended to surface-based photonic devices. The dimensions are in nanometer ranges which are much smaller than the visible wave range. The special arrangement of molecules enables the control of electron transfer direction.

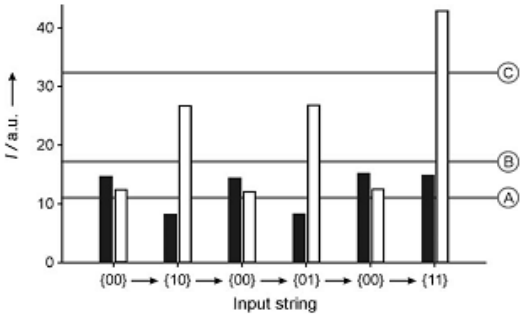

Figure 66. Response of device to different input strings, cycling shaded and white bars represent the luminescence at 626 nm (out1) and 732 nm (out2) [268].

The first photodiode based on LB films were reported in [271].by changing the deposition of the molecules, the direction of photocurrent can be controlled to anodic and cathodic kind, and this operation can switch and control the photocurrent direction [272-274]. The polymer photodiodes have been applied in generating logic operations [275, 276].

The AND and XOR logic gate are shown in Figure 12 are fabricated by connecting two polymer nanosheet photodiodes in series. Phenanthrene and anthracene were used as sensitizers and can be exited at 300 nm and 380 nm.

Two excitation wavelengths 300 nm and 380 nm used as inputs and photocurrent from assembly is as an output. When the structure in Figure 66 is irradiated with strings '01' or '10', the only irradiated diode generates photocurrent and the other is in steady state. If two diodes are connected in series like Figure 66(a), the total photocurrent is low and in presence of both wavelengths, both diodes generate photocurrent and also transfer the charges to the electrode, there for enhancing the total electron flow.

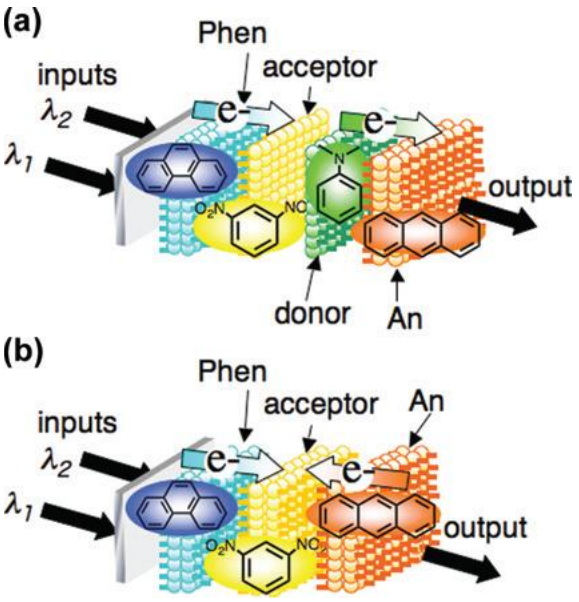

Figure 67. Photofunctional polymer nanosheet assembly for optical logic (a) AND logic gate (b) XOR logic gate [269].

The basic operation of XOR gate is like the AND gate but the only difference between them is the two photodiodes are connected so that the photocurrent directions are opposite so when both diodes are exited simultaneously, a small current is observed, because of the opposite directions of photocurrents Figure 66(b). The directions of photocurrents are dependent on which chromophore is exited and by changing the irradiation wavelength; the output direction can be controlled.

XIII. Optical Logic Gate Using the Thermal Lens Effect

A sensitive method of demonstrating all-optical logic gates is using well known phenomenon so called thermal lens effect (TL). In this technique, when molecules of a material are illuminated with laser beam, some of energy is absorbed by them, and the molecules in ground state are excited to higher energy level. The excess energy is dissipated by the molecules. This non-radiative decay process causes the heating of the sample, which generated a refractive index gradient [297].

The total amount of heating depends on how strongly the sample absorbs laser power. The refractive most material decrease with increasing temperature, thus cause the refractive index lowest at the centre of beam path. Therefore the laser path is shorter at beam centre. So the heated sample operates

as a lens that diverges or blooms the injected laser beam [296].

It is obvious there are two kind of boundary, a minimum level so called threshold intensity and a maximum state that is saturation intensity. The formation of thermal lens is shown in Figure 68. In threshold laser intensity, the refractive index of the sample becomes so large that the laser beam is diverged like a bottle with dark centre surrounded by a bright region. So we can demonstrate all-optical logic gates by tuning the injecting beams intensities as compared with threshold and saturation intensities [297].

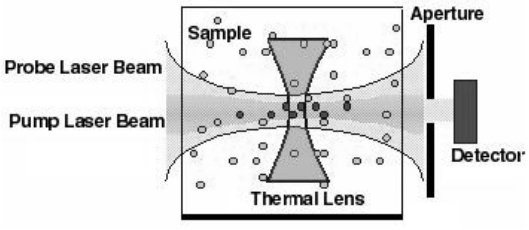

Figure 68. Thermal lens formation in a sample [296].

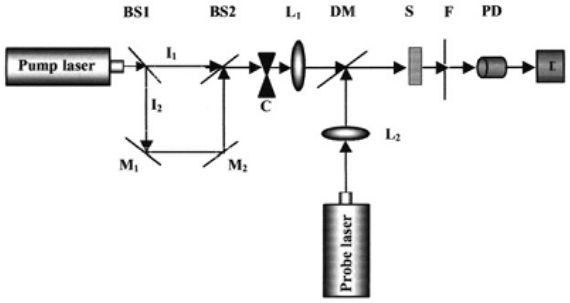

Figure 69. Schematic diagram of experimental setup logic gate. BS1 and BS2 - Beam Splitter, C - Coupler, L1, L2 - Lens, DM - Dichroic Mirror, S - Sample, F - Filter, PD - Photodiode, D – Detector [297].

The conceptual schematic diagram of this optical logic gate is shown in Figure 69. Laser radiation at 532 nm wavelength is used as pump inputs, and a low power (1mw) intensity laser at 632.8 nm wavelength is used as probe beam. The sample is form of disc (thickness 3 mm and 1 cm diameter). And a filter is placed after sample to select induced probe beam, is tuned at 632.8 nm wavelength. Optical media used for this study are chemically stabilized Rhodamine 6G doped PMMA, due its transparency and resistance to laser damage.

TABLE III. TRUTH TABLE OF NAND GATE OF FIGURE 68 [297].

I_1 (Input)	I_2 (Input)	Photodiode output
0	0	1
0	1	1
1	1	1
1	1	0

For realizing NAND logic gate, if I_1 and I2 are absent, sample works in normal form and photo-thermal phenomena don't occurs, so the probe beam can pass through the sample and PD can detect it. Output is in high level which gives the first condition in Table III. If either both of pump beam are below the threshold intensity, when one them is high output is high and photo diode can detect it. If both of input beams are present thermal blooming is so strong that the output of photo detector is low which is taken as zero. Figure 70 is shown output-input relation of TL experiment that satisfies NAND logic operation.

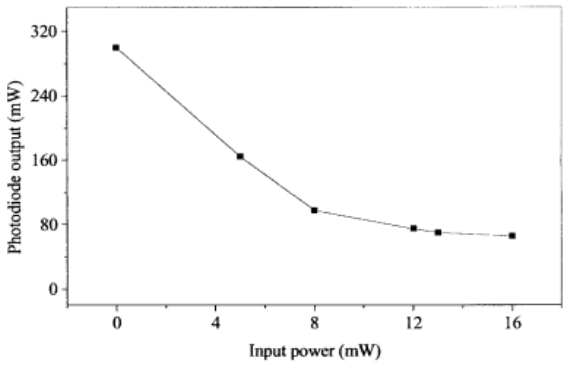

Figure 70. Relationship between output of photo detector and input power [297].

In order to realize AND logic function, we just need two pump inputs and output can realize at beam wavelength. It is obvious that when both pump beams are absent output is zero. If either I_1 or I_2 is below saturation and over threshold intensity (Figure 71), when one of them is presented thermal lens signal is low which can be considered as zero. In case both of them are present, we can have the last condition of Table IV.

TABLE IV. TRUTH TABLE OF AND GATE OF FIGURE 68 [297].

I_1 (Input)	I_2 (Input)	Photodiode output
0	0	0
0	1	0
1	0	0
1	1	1

TABLE V. TRUTH TABLE OF OR GATE OF FIGURE 68 [297].

I_1 (Input)	I_2 (Input)	Photodiode output
0	0	0
0	1	1
1	0	1
1	1	1

By tuning the input beams power, can implement OR logic gate. If we adjust the input beams greater than I_s the output is high when one of inputs or both of them are present, that can satisfies Table V.

The absorbed power must not be so large to introduce photo degeneration of the dye and aberration of thermal lens. In contrast to other optical logic gates this method is sensitive as well as it does not required any nonlinear optical materials.

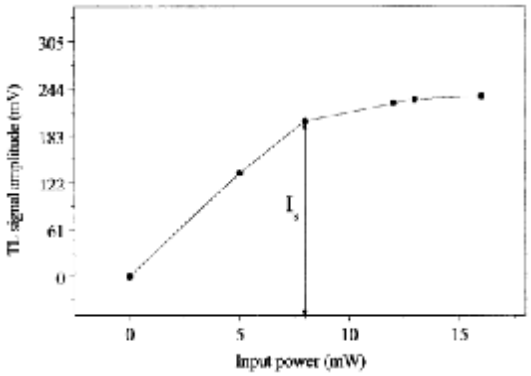

Figure 71. Output-input characteristics for AND gate [297].

XIV. Conclusion

In this paper, we have instructively reviewed all types of all-optical logic gates. The optical logic gates those exploiting different optical basics that can be used in optical computations, systems and networks to avoid opto-electronic conversions. They can speed up the information communication and computing in the future optical computers, communication systems and networks. We have described the performances of all kinds of all optical logic gates. We have explained briefly the advantages of optical gates. We have illustrated all-optical logic gates based on SOAs and nonlinear phenomena of FWM, XGM, XPM, and CPM effects. We have depicted all-optical logic gates utilizing interferometers, such as delayed interferometer, Mach-Zehnder and nonlinear loop mirror interferometers. We have introduced two types of semiconductor microring resonator logic gates. We have described the performances of all optical logic gates based on nonlinear photonic crystal microring resonators, couplers, waveguides, lasers, cavities, electro-absorption modulator, nonlinear fibers, nanoslabs, optical thyristor, and thermal lens. We have also explained the molecular logic gates.

XV. Acknowledgment

The authors would like to thank the Iran Research Institute for ICT (formerly, the Iran Telecommunication research canter (ITRC)) for financial support of this paper.

References

[1] Li, Z.; Li, G. Ultrahigh-Speed Reconfigurable Logic Gates Based on Four-Wave Mixing in a Semiconductor Optical Amplifier. IEEE Photon Technol. Lett. 2006, 18, 1341-1343.

[2] Deng, N.; Chen, K.; Chan, C. K.; Chen, L. K. An all-optical XOR logic gate for high–speed RZ-DPSK signals by FWM in semiconductor optical amplifier. Sel. Top. Quantum Electron. 2006, 12, 702-707.

[3] Berrettini, G.; Malacarne, A. A.; Bogoni, A.; Poti, L. Ultrafast integrable and reconfigurable XNOR, and NOT photonic logic gate. Photon. Technol. Lett. 2006, 18, 917-919.

[4] Li, L. P.; Xiu, X. D.; Liang, Z. X.; Xi, Z. G. All-optical XNOR and AND gates simultaneously realized in single semiconductor optical amplifier with improved dynamics. Chin. Phys. 2007, 16, 3719-3727.

[5] Wang, J.; sun, Q.; sun, J. All-optical 40 Gb/s CSRZ-DPSK logic XOR gate and format conversion using four wave mixing. Opt. Express. 2009, 17, 12555-12563.

[6] Li, Z.; Li, G.; Reconfigurable all-Optical logic gates based on FWM in semiconductor optical amplifier. Presented at Conf. on lasers and Electro-Optics, paper, Long Beach, California, May 21, 2006.

[7] Li, P.; Huang, D. X.; Zhang, X. L. SOA-based ultrafast multi functional all optical logic gates with PolSK modulated signals. Quantum Electron. 2009, 45, 1542-1550.

[8] Li, B.; Lu, D.; Memon, M. I.; Mezosi, G.; Wang, Z.; Sorel, M.; Yu, S. All-optical digital logic AND and XOR gates using four-wave-mixing in monolithically integrated semiconductor ring lasers. Electron. Lett. 2009, 45, 1-2.

[9] Kennedy, B. F.; Bondarczuk, K.; Barry, L. P. Experimental analysis of Four-Wave Mixing in a semiconductor Optical amplifier using frequency resolved optical gating. 2007, 4, 263-266.

[10] Wu, B.; Fu, S.; Wu, J.; Shum, P.; Ngo, N. Q.; Xu, K.; Hong, X.; Lin, J. Simultaneous implementation of all-optical OR and AND logic gates for NRZ/RZ/CSRZ ON–OFF-keying signals. Opt. Commun. 2010, 283, 349-354.

[11] Nesset, D.; Tatham, M.C.; Westbrook, L.D.; Cotter, D. Degenerate wavelength operation of an ultrafast all-optical AND gate using four wave mixing in a semiconductor laser amplifier Electron. Lett. 1994, 30, 1938-1940.

[12] Nesset, D.; Tatham, M.C.; Cotter, D. All-optical AND gate operating on 10Gbit/ssignals at the same wavelength using four-wave mixing in a semiconductor laseramplifier. Electron. Lett. 1995, 31, 896-897.

[13] Chan, K.; Chau, C. K.; Chen, L. K.; Tong, F. 20-Gbit/s all-optical XOR gate by four-wave mixing in semiconductor optical amplifier with RZ-DPSK modulated inputs. Photon. Technol. Lett. 2004, 16, 897-899.

[14] Kumar, S.; Willner, A. E. All optical XNOR gate using simultaneous four wave mixing and cross gain modulation in an SOA. Presented at the 17th IEEE Annual Meeting on Lasers and Electro-Optics, California, USA, Nov. 7-11, 2004.

[15] Chan, K.; Chan, C. K.; Chen, L.K.; Tong, F. Demonstration of 20-Gb/s all-optical XOR gate by four-wave mixing in semiconductor optical amplifier with RZ-DPSK modulated inputs. IEEE Photon. Technol. Lett. 2004, 16, 897-899.

[16] Deng, N.; Chan, C. K.; Chan, L. K. Demonstration of an all-optical three input exclusive OR logic gate for high-speed optical DPSK signals. Presented at 31st European Conf. on Opt. Commun., Shatin, China, Sep. 25-29, 2005.

[17] Li, Z.; Li, G. Ultra-high speed reconfigurable logic gates based on four-wave mixing in a semiconductor optical amplifier. Photon. Technol. Lett. 2006, 18, 1341-1343.

[18] Wang, J.; Sun, J.; Zhang, X.; Huang, D. All-Optical 40 Gbit/s Multicasting XOR Logic Gate for NRZ-DPSK Signals. Presented at Optical Fiber Communication and Optoelectronic Exposition and Conference, Wuhan, China, 2008, Oct. 30- Nov. 2, 2009.

[19] Li, P. L.; Zhang, D. X.; Chen, H. M. Ultra-high speed multifunctional all optical logic gates based on FWM in SOAs with PolSK modulated signals. Presented at Conf. on National Fiber Optic Engineers, San Diego, California, February 24-28, 2008.

[20] Lai, D. M. F.; Kwok, C. H.; Wong, K. K. Y. All-optical picoseconds logic gates based on a fiber optical parametric amplifier. Opt. Express. 2008, 16, 18362-18370.

[21] McAulay, A. D. Optical computation using semiconductor optical amplifier in cross gain modulation. Presented at Conf. on the lasers and Electro-Optics, Bethlehem, PA, USA, 2002, 1, 328-329.

[22] Kim, S. H.; Kim, J. H.; Choi, J. W.; Byun, Y. T.; Jhon, Y. M.; Lee, S.; Wool, D. H. All-optical NAND gate using cross gain modulation in semiconductor optical amplifiers. Electron. Lett. 2005, 41, 1027-1028.

[23] Sharaiha, A.; Topomondzo, J.; Morel, P. All-optical logic AND–NOR gate with three inputs based on cross-gain modulation in a semiconductor optical amplifier. Opt. Commun. 2006, 265, 322-325.

[24] Kim, S. H.; Kim, J. H.; Son, C. W.; Kim, G.; Byun, Y. T.; Jhon, Y. M.; Lee, S.; Woo, D. H.; Kim, S. H. Implementation of all-optical logic AND using XGM based on semiconductor optical amplifiers. Presented at 5th Int. Conf. on Optical

Internet and Next Generation Network, Seuol, Korea, July 9-13, 2006.

[25] Kim,S. H.; Kim, J. H.; Son, W.; Kim, G.; Byun, Y. T.; Jhon, Y. M.; Lee, S.; Wool, D. H.; Kim, S. H. Design and simulation of all-optical AND gate using XGM in semiconductor optical amplifier without Input Additional Beam. Presented at Int. Conf. on Numerical Simulation of Semiconductor Optoelectronic, Seuol, Korea, Sep. 11-14, 2006.

[26] Sun, C. W.; Kim, S. H.; Jhon, Y. M.; Byun, Y. T.; Lee, S; Woo, D. H.; Kim, S. H.; T. Yoon, H. Simulation and realization of simultaneous operation of all-optical NOR, AND, XNOR gate using semiconductor optical amplifier. Presented at 5th Int. Conf. on Optical Internet and Next Generation Network, Seuol, Korea, July 9-13, 2006.

[27] Son, C. W.; Kim, S. H.; Jhon, Y. M.; Byun, Y. T.; Lee, S.; Woo, D. H.; Kim, S. H.; Yoon, T. H. Design of all-optical multi-functional logic gate in single format by using semiconductor optical amplifier. Presented at 6th Int. Conf. on Numerical simulation of optoelectronic Devices, Seuol, Korea, Sept. 11-14, 2006.

[28] Berrettini, G.; Malacarne, A.; Ghelfi, P.; Bogoni, A.; Poti, L. Reconfigurable all-optical logic gate based on a single SOA with improved dynamics. Presented at IEEE Conf. on Opt. Fiber, Anaheim, California, March 5-10, 2006.

[29] Jung, Y. J.; Park, N. Y. Non-linear optical gate based on auto-correlated cross gain modulation effect in folded Tandem-SOA. Presented at 5th Int Conf. on Optical Internet and Next Generation Networks, Jeju, July 9-13, 2006.

[30] Sharaiha, A.; Hamie, A.; Guegan, M.; Bihan, J. L.; Hamze, A. All optical logic OR gate based on cross gain modulation in semiconductors optical amplifiers. Presented at Int Conf. on Quantum Electronics, Munich, June 17-22, 2007.

[31] Choi, K S.; Jhon,,Y. M.; Woo, D. H.; Lee, S.; Kim, S. H.; Park, J. All-Optical OR and NOR Logic Gates in Single Format by Using Semiconductor Optical Amplifiers. Presented at Pacific Rim Conf. on Lasers and Electro-Optics, Seoul, Aug. 26-31, 2007.

[32] Choi, K. S.; Jhon, Y. M.; Lee, S.; Park, J. All-optical five fundamental logic generated by using semiconductor optical amplifiers. Presented at Int. Conf. on Numerical Simulation of Optoelectronic Devices, Nottingham, Sept. 1-4, 2008.

[33] Ghelfi, P.; Lazzeri, E.; Scatfardi, M.; Poti, L.; Bogoni, A. All-optical full adder exploiting cascade of semiconductor optical amplifier-based modular blocks. Presented at Conf. on Optical Fiber Commun., San Diego, California, Feb. 24-28, 2008.

[34] Dong, J.; Zhang, X.; Huang, D. A proposal for two-input arbitrary Boolean logic gates using single semiconductor optical amplifier by picosecond pulse injection. J. Opt. Soc. Am. B. 2009, 17, 7725-7730.

[35] Erasme, D.; Soto, H.; Ortiz, Y.; Guekos, G. Cross polarization modulation in semiconductor optical amplifiers. Photon. Technol. Lett. 1999, 11, 970-972.

[36] Erasme, D.; Soto, H.; Guekos, G. All-optical switching and XOR-gating using cross-polarization modulation in a Semiconductor Optical Amplifier. Presented at European Conf. on Lasers and Elecro-Optics, Nice , France, Sept. 10-15, 2000.

[37] Soto, H.; Erasme, D.; Guekos, G. 5-Gb/s XOR optical gate based on cross-polarization modulation in semiconductor optical ampliflers. Photonics Technol. Lett. 2001, 13, 335-337.

[38] Kim, J. H.; Jhon, Y. M.; Byun, Y. T.; Lee, S.; Woo, D. H.; Kim, S. H. All-optical XOR gate using semiconductor optical amplifiers without additional input beam. Photon. Technol. Lett. 2002, 14, 1436-1438.

[39] Soto, H.; Díaz, C. A.; Topomondzo, J.; Erasme, D.; Schares, L.; Guekos, G. All-Optical AND Gate Implementation Using Cross-Polarization Modulation in a Semiconductor Optical Amplifier. Photon. Technol. Lett. 2002, 14, 498-500.

[40] Byun, Y. T.; Kim, J. H.; Jhon, Y. M.; Lee, S.; Woo, D. H.; Kim, S. H. High-speed all-optical NOR gate using semiconductor optical amplifier. Presented at European Conf. on Lasers and Elecro-Optics, Munich, Germany, June 22-27, 2003.

[41] Han, L.; Teng, X.; Hu, L.; Hua, N.; Zhang, H. All Optical NOR and OR Gates Using Cross Polarization Modulation in a Single SOA. Presented at 18th IEEE Annual Meeting on Lasers and Electro-Optics, Sydney, Australia, Oct. 22-28, 2005.

[42] Yan, H. L.; He, W.; Huan, J.; Li, G. Y.; Yi, Z. H. All-Optical AND Logic Gate without Additional Input Beam by Utilizing Cross Polarization Modulation Effect. Chin. Phys. Lett. 2008, 25, 3901-3904.

[43] Dorren, H. J. S.; Ju, H.; Yang, X.; Tangdiongga, E.; Zhang, S.; Li, Z.; Hill, M. T.; Mishara, A.; Liu, Y.; Geldenhuys, R.; Lenstra, D.; Khoe, G. D. All-optical logic based on ultra-fast nonlinearities in a semiconductor optical amplifier. Selected Topics in Quantum Electron. 2004, 10, 1079-1092.

[44] Zhang, J.; Wu, J.; Feng, C.; Xu, K.; Lin, J. 40 Gbit/s all-optical logic NOR gate based on nonlinear polarisation rotation in SOA and blue-shifted sideband filtering. Electron. Lett. 2006, 42, 1243-1244.

[45] Zhang, J.; Wu, J.; Feng, C.; Xu, K.; Lin, J. All-Optical Logic OR Gate Exploiting Nonlinear Polarization Rotation in an SOA and Red-Shifted Sideband Filtering. Photon. Technol. Lett. 2007, 19, 33-35.

[46] Li, Z.; Liu, Y.; Zhang, S.; Ju, H.; de Waardet, H.; Khoe, G.D.; Lenstra, D. All optical logic gates based on SOA and assisted optical filter. Electron. Lett. 2005, 41, 1397-1399.

[47] Gopalakrishnapillai, B. S.; Lee, K. L.; Nirmalathas, A.; Lim, C. Polarization and bit length independent all-optical logic gate based on active correlator for bit serial label processing. Presented at Conf. on Optical Fiber Commnun., Anaheim, CA., Murch 5-10, 2006.

[48] J. Dong, X. Zhang, J. Xu,.D. Huang, “40 Gb/s all-optical logic NOR and OR gates using a semiconductor optical amplifier: Experimental demonstration and theoretical analysis. Opt. Commun. 2008, 281, 1710-1715.

[49] Lattes, A.; HAUS, H. A.; Leonberger, F. J.; Ippen, E. P. An Ultrafast All-Optical Gate. Quantum Electron. 1983, 19, 1718-1723.

[50] Hamié, A.; Sharaiha, A.; Guégan, M.; Pucel, B. All-optical Logic NOR Gate Using Two-Cascaded Semiconductor Optical Amplifiers. Photn. Technol. Lett. 2002, 14, 1439-1441.

[51] Choi, K. S.; Jhon, Y. M.; Woo, D. H.; Lee, S.; Kim, S. H.; Park, J. All-Optical OR and NOR Logic Gates in Single Format by Using Semiconductor Optical Amplifiers. Presented at Pacific Rim Conf. on Lasers and Electro-Optics, Seoul, Aug. 23-31, 2007.

[52] Minh, H. L.; Ghassemlooy, Z.; Ng, W. P.; Chiang, M. F. Simulations of all-optical multiple-input AND gate based on four wave mixing in a single semiconductor optical amplifier, Presented at Telecommun. and Malaysia Int. Conf. on Commun., Penang, May 14-17, 2007.

[53] Dong, J.; Zhang, X.; Huang, D. A proposal for two-input arbitrary Boolean logic gates using single semiconductor optical amplifier by picosecond pulse injection. J. Opt. Soc. Am. B, 2009, 17, 7725-7730.

[54] Nishida, T.; Shinada, S.; Wada, N.; Yamaji, T.; Ueno, Y. Ultrafast distortion-free semiconductor-based all-optical gate that contains optical-spectrum’s phase-and-amplitude synthesizer, Presented at 22nd IEEE Annual Meeting Photon. Society, Belek-Antalya, Oct. 4-8, 2009.

[55] Porzi, C.; Scaffardi, M.; Poti, L.; Bogoni, A. All-Optical XOR Gate by Means of a Single Semiconductor Optical Amplifier without Assist Probe Light, Presented at 22nd Annual meeting Conf. of the IEEE Photon., Belek, Antalya, Oct. 4-8, 2009.

[56] Porzi, C.; Scaffardi, M.; Poti, L.; Bogoni, Optical digital signal processing in a single SOA without assist probe light. Selected Topics in Quantum Electron. 2010, 16, 5-11.

[57] Patel, N. S.; Hall, K. L.; Rauschenbach, K. A. 40 Gbit/sec cascadable all-optical logic with an ultrafast nonlinear interferometer. Opt. Lett. 1996, 21, 1466–1468.

[58] Stubkjaer, K. E. Semiconductor Optical Amplifier-Based All-Optical Gates for High-Speed Optical Processing. Select. Topics Quantum electron. 2000, 6, 1428-1435.

[59] Ueno, Y.; Nakamura, S.; Tajima, K. Nonlinear phase shifts induced by semiconductor optical amplifiers with control pulses at repetition frequencies in the 40-160 GHz range for use in ultrahigh-speed all-optical signal processing. J. Opt. Soc. Am. B. 2002, 19, 2573-2589.

[60] Kalyvas, M.; Yiannopoulos, K.; Houbavlis, T.; Avramopoulos, H. Control signal generation from flag pulses to drive all optical gates. Photon. Technol. Lett. 2004, 16, 1122-1124.

[61] Yang, X.; Manning, R. J.; Mishra, A. K.; Webb, R. P.; Ellis, A. D.; Cotter, D. Application of Semiconductor Optical Amplifiers in High-Speed All-Optical NRZ to RZ Format Conversion. Presented at the 9th Int. Conf. on Transparent Opt. Networks, Rome, Italy, July 1-5, 2007.

[62] Yang, X.; Manning, R. J.; Webb, R. P. All-optical 85Gb/s XOR Using Dual Ultrafast Nonlinear Interferometers and Turbo-switch Configuration. Presented at European Conference on Optical Commun. Cannes, France, Sept. 24-28, 2006.

[63] Leuthold, J.; Joyner, C.; Mikkelsen, B.; Rayban, G.; Pleumeekers, J.; Miller, B.; Dreyer, K.; Burrus, C. 100 Gbit/s all-optical wavelength conversion with integrated SOA delayed-interference configuration. Electron. Lett. 2000, 36, 1129-1130.

[64] Dong, H.; Wang, Q.; Zhu, G.; Jaques, J.; Piccirilli, A. B.; Dutta, N. K. Demonstration of all-optical logic OR gate using semiconductor optical amplifier-delayed interferometer. Opt. Commun. 2004, 242, 479-486.

[65] Wang, Q.; Dong, H.; Zhu, G.; Sun, Jaques, H.; Piccirilli, A. B.; Dutta, N. K. All-optical OR gate using SOA and Delayed interferometer. Opt. Commun. 2006, 260, 81-86.

[66] Yang, X.; Manning, R. J.; Webb, R. P.; Giller, R.; Gunning, F.; Cotter, D. High-speed All-optical Signal Processing using Semiconductor Optical Amplifiers. Presented at Int. Conf. on Transparent Optical Networks, Nottingham, June 18-22, 2006.

[67] Xu, J.; Zhang, X.; Dong, J.; Liu, D.; Huang, D. Ultrafast all-optical AND gate based on cascaded SOAs with assistance of optical filters. Electron. Lett. 2007, 43, 585-586.

[68] Xu, J.; Zhang, X.; Dong, J.; Liu, D.; Huang, D. Simultaneous All-Optical AND and NOR Gates for NRZ Differential Phase-Shift-Keying Signals. IEEE Photon. Technol. Lett. 2008, 20, 596-598.

[69] Poustie, A. J.; Blow, K. J.; Kelly, A. E.; Manning, R. J. All-optical binary half-adder. J. Opt. Commun. 1998, 156, 22–26.

[70] Hill, M. T.; de Waardt, H.; Khoe, G. D.; Dorren, H. J. S. Fast optical flip-flop by use of Mach–Zehnder interferometers. Microwave and Opt. Technol. Lett. 2001, 31, 411–415.

[71] Lee, S.; Park, J.; Lee, K.; Eom, D.; Lee, S.; Kim, J. H. All-Optical Exclusive NOR Logic Gate Using Mach-Zehnder Interferometer. Appl. Phys. 2002, 14, 1155-1157.

[72] Hesimann, F. Numerical analysis of all-optical logic XOR gate based on active MZ interferometer. Presented at Conf. on Lasers and Electro-Optics, Long Beach, California, May 19-24, 2002.

[73] Kim, J. H. ; Jhon,Y. M.; Byun, Y. T.; Lee, S.; Woo, D. H.; Kim, S. H. All-Optical XOR Gate Using Semiconductor Optical Amplifiers Without Additional Input Beam. Photon. Technol. Lett. 2002, 14, 1436-1438.

[74] Yabu, T.; Geshiro, M.; Kitamura, T.; Nishida, K. Sawa, S. All-optical logic gates containing a two-mode nonlinear waveguide. Quantum Electron. 2002, 38, 37-46.

[75] Zhang, M.; Zhao, Y. P.; Wang, L.; Wang, J.; Ye, P. Design and analysis of all-optical XOR gate using SOA-based Mach-Zehnder interferometer. Opt. Commun. 2003, 223, 301-308.

[76] Webb, R. P.; Manning, R. J.; Maxwell, G. D.; Poustie, A. J. 40 Gbit/s all-optical XOR gate based on hybrid-integrated Mach-Zehnder interferometer. Electron. Lett. 2003, 39, 79-81.

[77] Kim, J. H.; Son, C. W.; Kim,Y. II; Byun, Y. T.; Jhon, Y. M.; Lee, S.; Woo, D. H.; S. Kim, H. All-Optical Signal Processing Using Semiconductor Optical Amplifier Based Logic Gates. Presented at 3rd Int. Conf. on Numerical Simulation of Semiconductor Optoelectronic, Tokyo, Japan, Oct. 14-16, 2003.

[78] Houbavlis, T.; Zoiro, K.E.; Kanellos, G.; Tsekrekos, C. Performance analysis of ultrafast all-optical Boolean XOR gate using semiconductor optical amplifier-based Mach–Zehnder Interferometer. Opt. Commun. 2004, 232, 179-199.

[79] Randel, S.; Melo, A.M.; Petermann, K.; Marembert, V.; Schubert,.C. Novel Scheme for Ultrafast All-Optical XOR Operation. IEEE J. Lightwave Technol. 2004, 22, 2808-2815.

[80] Wang, Q.; Zhu, G.; Chen, H.; Jaques, J.; Leuthold, J.; Piccirilli, Al B.; Dutta, N. K. Study of All-Optical XOR Using Mach–Zehnder Interferometer and Differential Scheme. Quantum Electron. 2004, 40, 703-710.

[81] Dorren, H. J. S.; Yang, X.; Mishra, A. K.; Li, Z.; Ju, H.; Ju, H.; Khoe, G. D.; Simoyama, T.; Ishikawa, H.; Kawashima, H.; Hasama,T. All-Optical Logic Based on Ultrafast Gain and Index Dynamics in a Semiconductor Optical Amplifier. Selected Topics in Quantum Electron. 2004, 10, 1079-1092.

[82] Kim, S. H.; Kim, J.H.; Yu , B.G.; Byun, Y.T.; Jeon, Y.M.; Lee, S.; Woo, D.H.; Kim, S.H. All-optical NAND gate using cross-gain modulation in semiconductor optical amplifiers. Electron. Lett. 2005, 41, 1027-1028.

[83] Pousie, A. Semiconductor devices for all-optical signal processing. Presented at 31st European Conf. on Opt. Commun., Glasgow, UK, Sept. 25-29, 2005.

[84] Xu, J.; Zhang, X.; Liu, D.; Huang, D. 40 Gb/s All-optical NOR gate based on semiconductor optical amplifier and fiber delay interferometer. Presented at Int. Conf. on Optoelectronics, Wuhan, China, Nov. 1-4, 2006.

[85] Ye, X.; Ye, P.; Zhang, M.; All-optical NAND gate using integrated SOA-based Mach–Zehnder interferometer. Opt. Fib. Technol. 2006, 12, 312-316.

[86] Kim, J. Y.; Han, S. K.; Lee, S. All-optical multiple logic gates using parallel SOA-MZI structures. Presented at 18th . 2006, 24, 3392.

[87] Sun, H.; Wang, Q.; Dong, H.; Chen, Z.; Dutta, N. K. All-optical logic XOR gate at 80 Gb/s using SOA-MZI-DI. Quantum Electron. 2006, 42, 747-751.

[88] Martinez, J. M.; Herrera, J.; Ramos, F.; Marti, J. All-optical correlation employing single logic XOR gate with feedback. Electron. Lett. 2006, 42, 1170-1171.

[89] Son, C.W.; Kim, S.H.; Byun, Y.T.; Jhon, Y. M.; Lee, S.; Woo, D.H.; Kim, S.H.; Yoon, T. H. Realisation of all-optical multi-functional logic gates using semiconductor optical amplifiers. Electron. Lett. 2006, 42, 1057-1058.

[90] Yang, X.; Mishra, A. K.; Manning, R. J.; Webb, R. P. Maxwell, G.; Poustie, A.; Harmon, R. Comparison of All-Optical XOR Gates at 42.6Gbit/s. Presented at 33rd European Conf. on Optical Commun., Berlin, Germany, Sept. 16-20, 2007.

[91] Wang, L.; Zhang, M.; Zhao, Y.; Ye, P. Performance analysis of the all optical XOR gate using SOA-MZI with differential modulation scheme. Quantum. Electron. 2004, 40, 703-710.

[92] Don, H.; Sun, H.; Wang, Q.; Dutta, N. K.; Jaques, J. 80 Gb/s All-optical logic AND operation using Mach-Zehnder interferometer with differential scheme. Microwave and Opt. Technol. Lett. 2004, 40, 173-177.

[93] Ji, W.; Zhang, M.; Ye, P. Simulation of an all-optical XOR gate with a semiconductor optical amplifier Mach-Zehnder interferometer sped up by a continuous-wave assistant Light. Opt. Network. 2005, 4, 524-530.

[94] Kim, J. Y.; Kang, J. M.; Kim, T. Y.; Han, S. K. All-Optical Multiple Logic Gates With XOR, NOR, OR, and NAND Functions Using Parallel SOA-MZI Structures: Theory and Experiment. IEEE J. Lightwave Technol. 2006, 24, 3392-3399.

[95] Castrejon, R. G. 160 Gb/s XOR Gate Using Bulk SOA Turbo-Switched Mach-Zehnder Interferometer. Presented at 4th Int. Conf. on Electrical and Electron. Eng., Mexico City, Sept. 5-7, 2007.

[96] Teimoor, H.; Apostolopoulos, D.; Vlachos, K. G.; Ware, C.; Petrantonakis, D.; Stampoulidis, L.; Avramopoulos, H.; Erasme, D. Optical Logic Gate Aided Packet Switching in Transparent Optical Networks. IEEE J. Lightwave Technol. 2008, 26, 2848-2856.

[97] Kang, L.; Rasras, M.; Dinu, M.; Cobot, S.; Cappuzzo, M.; Gomez, L. T.; Chen, Y. F.; Patel, S. S.; Dutta, N.; Piccirilli,

A.; Jaques, J.; Giles, C. R. All-optical XOR and XNOR operations at 86.4 Gb/s using a pair of semiconductor optical amplifier Mach-Zehnder interferometers. Opt. Express. 2009, 17, 19062-19066.

[98] Smith, B. J.; Kundys, D.; Peter, N. T.; Smith, P. G. R.; Walmsley, I. A. Phase-controlled integrated photonic quantum circuits. Opt. Express, 2009, 17, 13516-13525.

[99] Suzuki, M.; Uenohara, H. Investigation of all-optical error detection circuit using SOA-MZI-based XOR gates at 10 Gbit / s. Electron. Lett. 2009, 45, 224-225.

[100] Ma, S.; Chen, Z.; Dutta, N. K. All-optical logic gates based on two-photon absorption in semiconductor optical amplifiers. Opt. Commun. 2009, 282, 4508-4512.

[101] Ueno, Y.; Sakaguchi, J.; Nakamoto, R.; Nishida, T. Ultrafast, low-energy-consumption, semiconductor-based, all-optical devices. Presented at Asia-Pacific Conf. on Microwave photonics, Beijing, China, April 22-24, 2009.

[102] Al-Zayed, A. S.; Cherri, A.K. Improved all-optical modified signed-digit adders using semiconductor optical amplifier and Mach–Zehnder interferometer. Opt. Lasers & Technol. 2010, 42, 810-818.

[103] Taraphadar, C.; Chattopadhyay, T.; Roy, J. N. Mach–Zehnder interferometer-based all-optical reversible logic gate. Opt. Lasers & Technol. 2010, 42, 249-259.

[104] Chattopadhyay, T.; Roy, J. N. Design of SOA-MZI based all-optical programmable logic device (PLD). Opt. Commun. 2010, 283, 2506-2517.

[105] Takahashi, R.; Choi, W.Y.; Kawamura, Y.; Iwamura, H. Femtosecond All-optical AND gates based on low-temperature-grown be-doped strained InGaAs/InAlAs multiple quantum wells. Presented at 8th Annual Meeting on Lasers and Electro-Optics, San franncisco, Canada, Oct. 30-31, 1995.

[106] Dorren, H. J. S.; Yang, X.; Mishra, A. K.; Li, Z.; Ju, H.; de Waardt, H.; Khoe, G. D. All-Optical Logic Based on Ultrafast Gain and Index Dynamics in a Semiconductor Optical Amplifier. Select. Topics Quantum electron. 2004, 10, 1079-1092.

[107] Li, X.; Steel, D.; Gammon, D.; Sham, L. J. Quantum Information Processing Based on Optically Driven Semiconductor Quantum Dot. Optics and Photonics News. 2004, 70, 38-43.

[108] Naruse, M.; Yoshida, H.; Miyazaki, T.; Kubota, F.; Ishikawa, H. Ultrafast All-optical NOR gate based on intersubband and interband transitions. Photon. Technol. Lett. 2005, 17, 1701-1703.

[109] Sun, H.; Wang, Q.; Dong, H.; Dutta, N. K. XOR performance of a quantum dot semiconductor optical amplifier based Mach-Zehnder interferometer. Opt. Express. 2005, 13, 1892-1899.

[110] Ezra, Y. B.; Mahlab, U.; Haridim, M.; Lembrikov, B. I. Applications of all-optical signal processing in modern optical communications. Presented at Int. Conf. on Transparent Optical Networks, Rome, July 1-5, 2007.

[111] Ezra, Y. B.; Lembrikov, B. I.; Haridim, M. Ultrafast All-Optical Processor Based on Quantum-Dot Semiconductor Optical Amplifiers. Quantum. Electron. 2009, 45, 34-41.

[112] Manning, R. J.; Ibrahim, S. K.; Webb, R. P.; An, Y.; Poustie, A. J.; Maxwel, G. D.; Lardenois, S.; Harmon, R. A. 42.6 Gbit/s fully integrated all-optical XOR gate. Electron. Lett. 2009, 45, 1047-1049.

[113] Qureshi, M. S.; Sen, P.; Andrews, J. T.; Sen, P. K. All Optical Quantum CNOT Gate in Semiconductor Quantum Dots. Quantum Electron. 2009, 45, 59-65.

[114] Rostami, A.; Asghari nejad, H. B.; Qartavol, R. M.; Saghai, H. R. Tb/s optical logic gates based on Quantum-Dot semiconductor optical amplifiers. Quantum Electron. 2010, 46, 354-360.

[115] Soto, F. C.; Martinez, A.; Blasco, J.; Marti, J. Numerical analysis of the performance of Mach-Zehnder interferometric logic gates enhanced with coupled nonlinear ring-resonators. Opt. Express. 2007, 15, 2323-2335.

[116] Sanchis, P.; Soto, F. C.; Blasco, J.; García, J.; Martínez, A.; Marti, J.; Riboli F.; Paves, L. All-optical MZI XOR logic gate based on Si slot waveguides filled by Si-nc embedded in SiO_2. Presented at IEEE 3rd Int. Conf. on Group IV Photonics, Ottawa, Canada, Oct. 9, 2006.

[117] Zoiros, K. E.; Papadopoulos, G.; Houbavlis, T.; Kanellos, G. T. Theoretical analysis and performance investigation of ultrafast all-optical Boolean XOR gate with semiconductor optical amplifier-assisted Sagnac interferometer. Opt. Commun. 2006, 258, 114-134.

[118] Zhou, Y.; Wu, J.; Lin, J. Novel Ultrafast All-Optical XOR Scheme Based on Sagnac Interferometric Structure. Quantum. Electron. 2005, 41, 823-827.

[119] Huang, X.; Zhang, M.; Wang, L.; Ye, P. Novel scheme of 40 Gb/s all-optical NOT gate based on SOA-assisted Sagnac interferometer. Presented at Int. Conf. on Commun. Circuit, and Systems, Chengdu, China, June 27-29, 2004.

[120] Zoiros, K.; Houbavlis, T.; Machos, K.; Avramopoulos, H.; Girardin, F.; Guekos, G.; Hansemann, S.; Burkhard, H. 10 GHz boolean XOR with semiconductor optical ampllfier fiber Sagnac gate. Presented at the Conf. on lasers and Electro-Optics, Baltimore, MD, USA, May 23-28, 1999.

[121] Bintjas, C.; Kalyvas, M.; Theophilopoulos, G.; Stathopoulos, T.; Avramopoulos, H.; Occhi, L.; Schares, L.; Guekos, G.; Hansmann, S.; Dall'Ara, R. 20 Gb/s all-optical XOR with UNI gate. Photon. Technol. Lett. 2000, 12, 834-836.

[122] Theophilopoulos, G.; Yiannopoulos, K.; Kalyvas, M.; Bintjas, C.; Kalogerakis, G.; Avramopoulos, H. 40 GHz all-optical XOR with UN1 gate. Presented at Conf. and Exhibit on Opt. Fiber, Anaheim, California, March 17-22, 2001.

[123] Kehayas, E.; Tsiokos, D.; Vyrsokinos, K.; Stampoulidis, L.; Kanellos, G. T.; Bintjas, C.; Guekos, G.; Avramopoulos, H. All-optical half adder using two cascaded UNI gates. Presented at 16th IEEE Annual Meeting on Lasers and Elecrto-Optics, Sheraton El Conquistador Tucson, AZ, Oct 27-28, 2003.

[124] Tsiokos, D.; Kehayas, E.; Vyrsokinos, K.; Houbavlis, T.; Stampoulidis, L.; Kanellos, G. T.; Pleros, N.; Guekos, G.; Avramopoulos, H. 10-Gb/s All-optical half-adder with interferometric SOA gates. Photon. Technol. Lett. 2004, 16, 248-286.

[125] R. P. Webb, X. Yang, R. J. Manning, and R. Giller, "All-optical 40 Gb/s logic XOR gate with dual ultrafast nonlinear interfermetes, "31st Europ. Conf. on Opt. Commun., Vol. 2, pp. 225-226, 2005.

[126] Houbavlis, T.; Zoiros, K. E.; Kalyvas, M.; Theophilopoulos, G.; Bintjas, C.; Yiannopoulos, K.; Pleros, N.; Vlachos, K.; Avramopoulos, H.; Schares, L.; Occhi, L.; Guekos, G.; Taylor, J. R.; Hansmann, S.; Miller, W. All-optical signal processing and applications within the esprit project DO_ALL. IEEE J. Lightwave Technol. 2005, 23, 781-801.

[127] Siarkos, T.; Zoiros, K. E.; Nastou, D. On the feasibility of full pattern-operated all-optical XOR gate with single semiconductor optical amplifier-based ultrafast nonlinear interferometer. Opt. Commun. 2009, 282, 2729-2740.

[128] Glesk, I. Approaches to ultrafast all-optical signal processing. Presented at Asian Conf. on Commun. and Photon., Shanghai, China, Nov. 2-6, 2009.

[129] Taraphdar, C.; Chattopadhyay, T.; Roy, J. N. Polarization Encoded All-optical Ternary Max Gate. Presented at 4th Int. Conf. on Computers and Devices for Commun., Kolkata, Dec. 14-16, 2009.

[130] Yang, X.; Manning, R. J.; Hu, W. Simple 40 Gbit /s all-optical XOR gate. Electron. Lett. 2010, 46, pp. 222-223.

[131] Fjelde, T.; Wolfson, D.; Kloch, A.; Janz, C.; Coquelin, A.; Guillemot, I.; Gaborit, F.; Poingt, F.; Dagens, B.; Renaud, M. 10Gbit/s all-optical logic OR in monolithically integrated interferometric wavelength converter. Electron. Lett. 2000, 36, 813-815.

[132] Ibrahim, T. A.; Grover, R.; Kuo, L. C.; Kanakaraju, S.; Calhoun, L. C.; Ho, P. T. Photonic AND/NAND Logic Gates Using Semiconductor Microresonators. Presented at IEEE 16th Ann. Meet. On Laser and Electro-Optics Society (LEOS), Sheraton El Conquistador Tucson, AZ, Oct 26-30, 2003.

[133] Ibrahim, T. A.; Grover, R.; Kuo, L. C.; Kanakaraju, S.; Calhoun, L. C.; Ho, P. T. All-Optical AND/NAND Logic Gates Using Semiconductor Microresonators. IEEE Photon. Technol. Lett. 2003, 15, 1422-1424.

[134] Xu, Q.; Lipson, M. All-optical logic based on silicon micro-ring resonators. Opt. Express, 2007, 15, 924-929.

[135] Kuo, L. C.; Van, V.; Amarnath, K.; Ding, T. N.; Astar, W.; Carter G. M.; Ho, P. T Cascaded integrated photonic AND gates based on GaAs ring resonators. Presented at IEEE Conf. on Lasers and Electro-Optics, Long Beach, CA, May 21-26, 2006.

[136] Pereira, S.; Chak, P.; Sipe, J. E. All-optical AND gate by use of a Kerr nonlinear microresonator structure. Opt. Lett. 2003, 28, 444-446.

[137] Ibrahim, T. A.; Kuo, L. C.; Amamath, K.; Grover, R.; Van, V.; Ho, P. T. Photonic logic NOR gate using two symmetric microring resonators. Opt. Lett. 2004, 29, 2779-2781.

[138] Mikroulis, S.; Simos, H.; Roditi, E.; Syvridis, D. Ultrafast all-optical AND logic operation based on four wave mixing in a passive InGaAsP-InP microring resonator. Photon. Technol. Lett. 2005, 17, 1878-1880.

[139] Mikroulis, S.; Simos, H.; Roditi, E.; Chipouras, A.; Syvridis, D. 40-Gb/s NRZ and RZ operation of an All-optical AND logic gate based on passive InGaAsP/InP microring resonator. IEEE J. Lightwave Technol. 2006, 24, 1159-1164.

[140] Cahill, L. W.; Le, T. T. MMI Devices for Photonic Signal Processing. Presented at 9th Int. Conf. on Transparent Optical Networks, Rome, July 1-5, 2007.

[141] Caulfield, H. J.; Soref, R. A.; Vikram, C. S. Universal reconfigurable optical logic with silicon-on-insulator resonant structures. Photon. And Nanostructures: Fundamen. And Appl. 2007, 5, 14-20.

[142] Bhairavabhatla, V.; Talabattula, S. A Unique Filter-Preserver Device for Digital Photonic Circuits. Hyderabad, Nov. 19-21, 2008.

[143] Threepak, T.; Mitatha, S.; Yupapin, P. P. Novel All-Optical Logic Gate Using an Add-Drop Filter and Intensity Switch. Presented at 3rd Int. Conf. on Nanoelectronics, Hong Kong, Jan. 3-8, 2010.

[144] Mingaleev, S.; Kishvar, Y. Nonlinear photonic crystals toward all-optical technology. Opts. Photon. News, 2002, 4, 49-52.

[145] Sajacic, M.; Joannopoulos, J. D. Enhancement of nonlinear effects using photonic crystal. Nature Mat. 2004, 3, 211-219.

[146] Ibrahim, T. A.; Amarnath, K.; Kuo, L. C.; Grover, R.; Van, V.; Ho, P. T. Photonic logic NOR gate based on two symmetric microring resonators. Opt. Lett. 2004, 29, 2779-2781.

[147] Zaghloul, Y. A.; Zaghloul, A. R. M. Complete all-optical processing polarization- based binary logic gates and optical processors. Opt. Express, 2006, 14, 9879-9895.

[148] Soljacic, M. Photonic Crystal Enhancement of optical nonlinearities. Nature Mat. 36-43, 2006.

[149] Zhu, Z. H.; Ye, W. M.; Ji, J. R.; Yuan, X.; Zen, C. High-contrast light-by-light switching and AND gate based on nonlinear photonic crystals. Opt. Express. 2006, 14, 1783-1788.

[150] Angelakis, D. G.; Santos, M. F.; Yannopapas, V.; Ekert, A. A proposal for the implementation of quantum gates with photonic-crystal waveguides. Phys. Lett. A, 2007, 362, 377-380.

[151] Andalib, P.; Granpayeh, N. All-Optical Ultra-Compact Photonic Crystal Controllable Logic Gate Based on Nonlinear Ring Resonator. Presented at 5th IEEE Int. Conf. on Group IV Photonics, Cardiff, Sept. 17-19, 2008.

[152] Liu, Q.; Ouyang, Z.; Wu, C. J.; Liu, C. P.; Wang, J. C. All-optical half adder based on cross structures in two-dimensional photonic crystals. Opt. Express. 2008, 16, 18992-19000.

[153] Spano, R.; Cazzanelli, M.; Daldosso, N.; Tartara, L.; Yu, J.; Degiorgio,V.; Hernandez, S.; Lebour, Y.; Pelle-grino, P.; Garrido, B.; Jordana, E.; Fedeli, J. M.; Pavesi, L. Non linear optical properties of Silicon nanocrystals for applications in photonic logic gates devices. Presented at IEEE/LEOS Winter Topical Meeting Series, Sorrento, Jan. 14-16, 2008.

[154] Memarzadeh Isfahani, B.; Ahmadi Tameh, T.; Granpayeh, N.; Maleki Javan, A. R. All-optical NOR gate based on nonlinear photonic crystal microring resonators. J. Opt. Soc. Am. B. 2009, 26, 1097-1102.

[155] Kabilan, A. P.; Christina, X. S.; Caroline, P. E. Design of Optical Logic Gates Using Photonic Crystal. Presented at First Asian Himalayas Int. Conf. on Internet, Kathmandu, Nov. 3-5, 2009.

[156] Andalib, P.; Granpayeh, N.; All-optical ultra-compact photonic crystal AND gate based on nonlinear ring resonators. J. Opt. Soc. Am. B. 2009, 26, 10-16.

[157] Andalib, P.; Granpayeh, N.; All-optical ultra-compact photonic crystal NOR gate based on nonlinear ring resonators. Opt. A: Pure Appl. Opt. 2009, 11, 1-7.

[158] Jung, Y. J.; Yu, S.; Ku, S.; Yu, H.; Han, S.; Park, N.; Kim, J. H.; Jhon, Y. M.; Lee, S. Reconfigurable all-optical logic AND, NAND, OR, NOR, XOR and XNOR gates implemented by photonic crystal nonlinear cavities. Presented at the 8th Pacific Rim Conf. on Lasers and Electro-Optics, Shanghai, Aug. 30-3, 2009.

[159] Spano, R.; Cazzaneli, M.; Daldosso, N.; Tartara, L.; Yu, J.; Degiorgio, V.; Hernandez, S.; Lebour, Y.; Pellegrino, P.; Garrido, B.; Jordana, E.; Fedeli, J. M.; Pavesi, L. Non linear optical properties of Silicon nanocrystals for applications in photonic logic gates devices. Presented at IEEE Winter Topical Meeting, Sorrento, Jan. 14-16, 2008.

[160] Zeng, S.; Zhang, Y.; Li, B.; Pun, E. Y. B. Ultrasmal optical logic gates based on silicon periodic dielectric waveguides. Photon. and Nanostruct.: Fundam. and Appl. 2010, 8, 32-37.

[161] Benner, A. F. Digital optical logic using optically switched directional couplers. Electron. Lett. 1990, 26, 1037-1038.

[162] Wang, Y.; Liu, J. All-Fiber Logical Devices Based on the Nonlinear Directional Coupler. Photon. Technol. Lett. 1999, 11, 72-74.

[163] Fraga, W. B.; J. Menezes, W. M.; da Silvia, M. G.; Sobrinho, C. S.; Sombra, A. S. B. All optical logic gates based on an asymmetr ic nonlinear directional coupler. Opt. Commun. 2006, 262, 32-37.

[164] Wu, Y. D. All-optical logic gates by using multibranch waveguide structure with localized optical nonlinearity. Selected Topics in Quantum Electron. 2005, 11, 307-312.

[165] Sobrinho, C.S.; Ferreira, A.C.; Menezes, J.W.M.; Guimaraes, G. F.; Fraga, W. B.; Filho, A. F. G. F.; Rocha, H. H. B.; Marciano, S. P.; Saboia, K. D. A.; Sombra, A. S. Analysis of an optical logic gate using a symmetric coupler operating with pulse position modulation (PPM). Opt. Commun. 2008, 281, 1056-1064.

[166] Nakatsuhara, K.; Jeong, S. H.; Tsukishima, Y.; Mizumoto, T. Demonstration of all-optical AND gate operation in a GaInAsP waveguide. Presented at the Pacific Rim Conf. on Lasers and Electro-Optics, Seoul, South Korea, Aug.-Sept. 30-3, 1999.

[167] Vukovid, N. T.; MilovanoviL, B. Realization of Full Set of Logic Gates for All-Optical Ultrafast Switching. Presented at 5th Int. Conf. on Telecommun. in Modern Satellite, Nis, Sept. 21-21, 2001.

[168] Cahill, L. W.; Le, T. T. MMI Devices for Photonic Signal Processing. Presented at int. Conf. on Transparent Optical Networks, Rome, July 1-5, 2007.

[169] Day, I. E.; Snow, P. A.; Jiang, Z.; Penty, R. V.; White, I. H.; Davies, D. A. O.; Fisher, M. A.; Adams, M. J. Low power all-optical polarisation gate switch in a passive InGaAsP MQW waveguide at 1.53 um. Electron. Lett. 1994, 30, 1050-1051.

[170] Gerlovin, I. Y.; Ovsyankin, V. V.; Stroganov, B. V.; Zapasskii, V. S. Nonlinear optical dynamics of semiconductor nanostructures: feasibility of the photonic quantum gate. Luminescence, 2000, 87-89, 421-422.

[171] Cones, T.; Riccof, F.; Armenisef, M. N.; Verbe, C. M.; Kenad, R. P. Design of all-optical logic gates in polydiacetylene PTS-clad waveguides. Presented at Fundamental and Appl. Topical Meeting on Nonlinear Opt. Materials, Kauai, HI, Aug. 10-14, 1998.

[172] Liang, T. K.; Nunes, L. R.; Tsuchiy, M.; Abedin, K. S.; Miyazak, T.; Van Thourhout, D.; Baets, P. D. R.; Tsan, H. K. All-Optical high speed NOR gate based on Two Photon Absorption in Silicon Wire Waveguide. Presented at Conf. on Optical Fiber Commun., Anaheim, CA, March 5-10, 2006.

[173] T. K. Liang, L.R. Nunes, M. Tsuchiya, K.S. Abedin, T. Miyazaki, D. Van Thourhout, W. Bogaerts, P. Dumon, R.

Beats, and H. K. Tsang. High speed logic gate using two-photon absorption in silicon waveguides. Opt. Commun. 2006, 256, 171-174.

[174] Khorasaninejad, M.; and Saini, S. S. All-optical logic gates using nonlinear effects in silicon-on- insulator waveguides. Appl. Opt. 2009, 48, F31-F36.

[175] Parameswaran, K. R.; Fujimura, M.; Chou, M. H.; Fejer, M. M. Low-Power All-optical gate based on sum frequency mixing in APE waveguides in PPLN. Photon. Technol. Lett. 2000, 12, 654-656.

[176] Lee, Y. L.; Yu, B. A.; Eom, T. J.; Shin, W.; Noh, Y. C.; Ko, D. K.; Lee, J.; Oh, K. All-optical AND/NAND Logic Gates Based on Ti:PPLN Waveguide by Cascaded Nonlinear Optical Processes. Presented at Conf. on Lasers and Electro-Optics, Long Beach, CA, May 21-26, 2006.

[177] Kumar, S.; Gurkao, D.; Willner, A. E. All-optical half adder using a PPLN waveguide and an SOA. Presented at Conf. on Optical Fiber Commun., Los Angeles, California, Feb. 23-27, 2004.

[178] McGeehan, J. E.; Giltrelli, M.; WiIlner, A. E. All-optical digital 3-input AND gate using Sum- and Difference-frequency generation in a PPLN waveguide. Electron. Lett. 2007, 43, 409-410.

[179] Lin, S. C.; Sunand, N. H.; Chiang, J.-S. All-optical NOT gate using periodical poled Lithium Niobate waveguide. Presented at Pacific Rim Conf. on Lasers and Electro-Optics, Seoul, Aug. 26-31, 2007.

[180] McGeehan, J. E.; Giltrelli, M.; Willner, A. E. All-optical digital 3-input AND gate using sum- and difference-frequency generation in PPLN waveguide. Electron. Lett. 2007, 43, 409-410.

[181] Wang, J.; Sun, J.; Sun, Q.; Wang, D.; Zhou, M.; Zhang, X. Dual-channel-output all-optical logic AND gate at 20 Gbit/s based on cascaded second-order nonlinearity in PPLN waveguide. Electron. Lett. 2007, 43, 940-941.

[182] Wang, J.; Sun, J.; Zhang, X.; Huang, D.; Fejer, M. M. PPLN-based all-optical three-input 20/40 Gb/s AND gate for NRZ/RZ Signals and XOR Gate for NRZ-DPSK/RZ-DPSK Signals. Presented at Conf. on Optical Fiber Commun., San Diego, CA, Feb. 24-28, 2008.

[183] Wang, J.; Sun, J.; Sun, Q. Single-PPLN-based simultaneous half-adder, half-subtracter, and OR logic gate: proposal and simulation. Opt. Express. 2007, 15, 1690-1699.

[184] Wang, J.; Sun, J.; Sun, Q.; Wang, D.; Zhang, X.; Huang, D.; Fejer, M. M. PPLN-based flexible optical logic AND gate. Photon. Technol. Lett. 2008, 20, 211-213.

[185] Wang, J.; Sun, J.; Zhang, X.; Huang, D. PPLN-based all-optical 40 Gbit /s three-input logic AND gate for both NRZ and RZ signals. Electron. Lett. 2008, 44, 413-414.

[186] Wang, J.; Sun, Q.; Sun, J. Tunable dual-channel multicasting all-optical 40 Gbit /s logic AND operation and format conversion for CSRZ signals. Electron. Lett. 2009, 45, 420-421.

[187] Wang, J.; Sun, J.; Sun, Q. Experimental observation of a 1.5 m band wavelength conversion and logic NOT gate at 40 Gbit / s based on sum-frequency generation. Opt. Lett. 2009, 31, 1711-1713.

[188] Soccolich, C. E.; Chbat, M. W.; Islam, M. N.; Prucnal, P. R. Cascade of ultrafast soliton-dragging and trapping logic gates. Photon. Technol. Lett. 1992, 4, 1043-1046.

[189] Broderick, N. G. R.; Taverner, D.; Richardson, D. J.; Ibsen, M.; Laming, R. I. Nonlinear switching using bragg gratings. Presented at IEE Colloquium on Optoelectronic Integration and switching, Glasgow, UK, Nov. 13-13, 1997.

[190] Ross, W.; Drobizhev, M.; Sigel, C.; Rebane, A. Demonstration of an ultrafast logic gate by interface of coherent transients. Lasers Phys. 1999, 9, 1102-1108.

[191] Jeong, Y.; Baek, S. and Lee, B. All-optical signal gating in cascaded long-period. Photon. Technol. Lett. 2000, 12, 1216-1218.

[192] Brzozowski, L.; Sargent, E. H. Optical signal processing using nonlinear distributed feedback structures. Photon. Technol. Lett. 2000, 36, 550-555.

[193] Nefedov, I.; Morozov, Y.; Gusyatnikov, V.; Zheltikov, A. Optically controlling photonic band gap logic elements. Presented at 2nd Int. Conf. on Transparent Optical Networks, Gdansk, Poland, June 5-8, 2000.

[194] Nakatsuhara, K.; Jeong, S. H.; Tsukishirna, Y.; Mizumoto, T.; Mat, B. J.; Nakanot, Y. Demonstration of all-optical threshold operation in GaInAsP distribnted feedback waveguides and its application to AND gate. Presented at Forth Optoelectronic and Commun. Conf. on Communication, Beijing, China, Oct. 18-22, 1999.

[195] Glushko, E. Ya.; Zakh, A. A. Theory of the nonlinear all-optical logical gates based on PBG structures. Presented at Second Int. Conf. on Advanced Optoelectronics and Lasers, Crimea, Ukraine, Sept. 12-17, 2005.

[196] Samra, A. S. All-optical logic gates using diffraction grating fabricated by ion-exchange technique. Presented at IEEE Int. Conf. on Semiconductor Electron., Johor Bahru, Nov. 25-27, 2008.

[197] Warren, M. E.; Koch, S. W.; Gibbs, H. M. Optical bistability, logic gating, and waveguide operation in semiconductor Etalons. Comput. 1987, 20, 68-86.

[198] Suzuki, Y.; Shimada, J. High speed optical logic gate for optical computers. Electron. Lett. 1985, 21, 161-162.

[199] Inoue, K. High-speed all-optical gate switching experiment in a Fabry-Perot semiconductor laser amplifier. Electron. Lett. 1987, 23, 921-922.

[200] Zhou, Ping; Cheng, J.; Schaus, C. F.; Sun, S. Z.; Hains, C.; Myers, D. R.; Vawter, G. A. Versatile bistable optical, switches, and latching optical logic using integrated phototrystors and surface emitting lasers. Presented at int. Conf. on Electron Devices, Dec. 8-11, Washington, DC, USA, 1991.

[201] Cheng, J.; Zhou, P.; Sun, S. Z.; Hersee, S.; Myers, D. R.; Zolper, J.; Vawter, G. A. Surface-emitting laser based smart pixels for two dimensional optical logic and reconfigurable optical interconnections. Quantum Electron. 1993, 29, 741-756.

[202] Lo, B.; Zhou, P.; Lu, Y. C.; Cheng, J.; Leibenguth, R. E.; Adams, A. C.; Zilko, J. L.; Lear, K. L.; Zolper, J. C.; Chalmers, S. A.; Vawter, G. A. Binary optical switch and programmable optical logic gate based on the integration of GaAs/AlGaAs surface emitting lasers and hetrojunction phototransistors. Photon. Technol. Lett. 1994, 6, 398-401.

[203] Lo, B.; Lu, Y. C.; Cheng, J.; Hafich, M. J.; Klem, J.; Zolper, J. C. High speed, Cascaded optical logic operations using programmable optical logic gate arrays. Photon Technol. Lett. 1996, 8, 166-168.

[204] Kao, Y. H.; Goltser, I. V.; Islam, M. N., Raybon, G. Ultrafast optical logic gate using a semiconductor laser amplifier operating at transparency in a loop mirror. Presented at Conf. on Lasers and Elecro-Optics, Baltimore, May 18-23, 1997.

[205] Sharaiha, A.; Li, H. W.; Marchese, F.; Bihan, J. L. All-optical logic NOR gate using a semiconductor laser amplifier. Electron. Lett. 1997, 33, 323-325.

[206] Quareshi, K. K.; Chung, W. H.; Tam, H. Y. An all optical NOT gate with variable threshold using dual wavelength lnjection Locking. Presented at European Conf. on Laser and Electro-Optics, Munich, Germany, June 22-27, 2003.

[207] Hurtado, A.; A. Marcos, G.; Pereda, J. A. M. All-optical logic gates with 1550nm Fabry-Perot and distributed feedback semiconductor laser amplifiers. Presented at Spanish Conf. on Electron Devices, Tarragona, Feb. 2-4, 2005.

[208] Uddin, M. R.; Cho, J. S.; Won, Y. H. All-optical NOR and NOT gates at 10 Gb/s based on gain modulation in Fabry-Perot laser diode. Presented at 7th Int. Conf. on Optical Internet, Tokyo, Oct. 14-16, 2008.

[209] Liu, B.; Cai, H.; Zhang, XM.; Tamil, J.; Zhang Q. X.; Liut, A. Q. MEMS optical logic NOR gate using intergrated tunable lasers. Presented at IEEE 22nd Int. Conf. on Micro Electro Mechanical systems (MEMS), Sorrento, Jan. 25-29, 2009.

[210] Uddin, M. R.; Lim, J. S.; Jeong, Y. D.; Won, Y. H. All-optical digital logic gates using single mode Fabry–Pérot laser diode. Photon. Technol. Lett. 2009, 21, 1468-1470.

[211] Li, B.; Memon, M. I.; Mezosi, G.; Wang, Z.; Sorel, M.; Yu, S. All-optical digital logic gates using bistable semiconductor ring lasers. Opt. Commun. 2009, 30, 190-194.

[212] Li, B.; Memon, M. I.; Lu, D.; Mezosi, G.; Wang, Z.; Sorei, M.; Yu, S. Cavity enhanced four wave mixing in an integrated semiconductor ring laser for all optical digital logic operations. Presented at Int. Conf. on Photonics in switching, Pisa, Sept. 15-19, 2009.

[213] Belotti, M.; Galli, M.; Gerace, D.; Andeani, L. C.; Zain, M. R. M.; Johnson, N. P.; Sorel, M.; De La Rue, R. M. All-optical Logical operation in photonic wire nanocavities. Presented at European Conf. on lasers and Electro-Optics, Munich, June 14-19, 2009.

[214] Uddin, M. R.; Lim, J. S.; Jeong, Y. D.; Won, Y. H. Optical logic gate by the modulation of self-locking of a single mode FP-LD. Presented at Int. Conf. Photonics in switching, Pisa, Sept. 15-19, 2009.

[215] Hulin, D.; Antonetti, A.; Joffre, M.; Migus, A.; Mysyrowiz, A.; Peyghambarian, N.; Gibbs, H. M. Subpicosecond all optical Logic gate: an application of the optical stark effect. Appl. Phys. 1987, 22, 1269-1271.

[216] Murdocca, M. Layout methods for digital optical computing. Presented at IEEE Int. Conf. on Computer aided Design, Santa Clara, CA, USA, Nov. 5-9, 1989.

[217] Richardson, D.; Gibbs, H. M.; Koch, S. W. Computer simulations of fully cascadable picosecond all optical logic using nonlinear semiconductor Etalons. Quantum Electron. 1991, 27, 804-808.

[218] Hirano, A.; Tsuda, H.; Hagimoto, K.; Takahashi, R.; Kawamura, Y.; Iwamura, H. l0 ps pulse all-optical discrimination using a high-speed saturable absorber optical gate. Electron. Lett. 1995, 31, 736-737.

[219] Hirano, A.; Kobayashi, H.; Tsuda, H.; Takahashi, R.; Sato, K.; Hagimoto, K. 10 Gbit/s all optical pulse discriminator using a high speed saturable absorber optical gate. Presented 11th Int. Conf. on Integrated Optics and Optical Fiber Commun., Edinburgh , UK, Sept. 22-25, 1997.

[220] Hirano, A.; Kobayashi, H.; Tsuda, H.; Takahashi, R.; Asobe, M.; Sato, K.; Hagimoto, K. 10 Gbit/s RZ all-optical discrimination using refined saturable absorber optical logic. Electron. Lett. 1998, 34, 198-199.

[221] Ogura, I.; Hashimoto, Y.; Kurita, H.; Shimizu, T.; Yokoyama, H. Picosecond All-Optical Gate Using a Saturable Absorber in Mode-Locked Laser Diodes. Photon. Technol. Lett. 1998, 10, 603-605.

[222] Cho, P. S.; Mahgereftech, D.; Goldhar, J. All-optical 2R regeneration and wavelength conversion at 20 Gb/s using an electro-absorption modulator. IEEE Photon. Technol. Lett. 1999, 11, 1662-1664.

[223] Awad, E. S.; Cho, P.; Goldhar, J. High-speed All-optical AND gate using nonlinear transmission of electro-absorption modulator. IEEE. Photon. Technol. Lett. 2001, 13, 472-474.

[224] Yoo, H.; Lee, H. J.; Jeong, Y. D.; Won, Y. H. All-optical logic gates using absorption modulation of an Injection-locked Fabry-Perot laser diode. Presented at Int. Conf. on Photonics in switching, Heraklion, Crete, Oct. 16-18, 2006.

[225] Porzi, C.; Guina, M.; Bogoni, A.; Pot, L. All-optical NAND/NOR logic gates with passive nonlinear Etalon exploiting absorption saturation in semiconductor MQWs. Presented at IEEE Conf. on Photonics in switching, San Francisco, CA, Aug. 19-22, 2007.

[226] Porzi, C.; Guina, M.; Bogoni, A.; Pot, L. Photonic logic operations with nonlinear semiconductor Etalons exploiting saturable absorption in multiple quantum wells. Presented at 20th IEEE Annual meeting on Lasers and Electro-Optics, Lake Buena Vista, FL, Oct. 21-25, 2007.

[227] Porzi, C.; Guina, M.; Bogoni, A.; Pot, L. All-optical NAND/NOR logic gates based on semiconductor saturable absorber Etalons. Selected Topics in Quantum Electron. 2008, 14, 927-937.

[228] Kimura, Y.; Kitayama, K. I.; Shibata, N.; Seikai, S. All-fiber optic logic AND gate. Electron. Lett. 1986, 22, 277-278.

[229] Niiyama, A.; Koshiba, M. Three-Dimensional Beam Propagation Analysis of Nonlinear Optical Fibers and Optical Logic Gates. Light Technol. 1998, 16, 162-168.

[230] Yu, C.; Luo, L. T.; Wang, Y.; Pan, Z.; Yan, L. S.; Willner, A. E. All-Optical XOR Gate Using Polarization Rotation in Single Highly Nonlinear Fiber. Photon. Technol. Lett. 2005, 17, 1232-1234.

[231] Lee, J. H.; Nagashima, T.; Hasegawa, T.; Ohara, S.; Sugimoto, N.; Kikuchi, K. 40 Gbit/s XOR and AND gates using polarisation switching within 1 m-long bismuth oxide-based nonlinear fibre. Electron. Lett. 2005, 41, 1074-1075.

[232] White, H.; Penty, R. V. Demonestration of the optical Kerr effect in an all-fiber Mach-Zehnder interferometer at laser diode power. Electron. Lett. 1988, 24, 340-341.

[233] Betts, R. A.; Lear, J. W.; Dang, N. T.; Shaw, R. D.; Atherton, P. S. Transmission of Near-Transform-Limited Optical Pulses Generated Using an All-Optical Gate Over More Than 2400 km in a Recirculating Fiber Loop. Photon. Technol. Lett. 1992, 4, pp. 1290-1299.

[234] Olsson, B.; Andrekson, P. A. Polarization-independent all-optical AND-gate using randomly birefringent fiber in a nonlinear optical loop mirror. Presented at Conf. on optical fiber comun. San Jose, CA, USA, Feb. 22-27, 1998.

[235] Houbavlis, T.; Zoiros, K.; Vlachos, K.; Papakyriakopoulos, T.; Avramopoulos, H.; Girardin, F.; Guekos, G.; Dall'Ara, R.; Hansmann, S.; Burkhard, H. 10Gbit/s all-optical Boolean XOR with SOA fibre Sagnac gate. Electron. Lett. 1999, 35, 1650-1652.

[236] Houbavlis, T.; Zoiros, K.; Vlachos, K.; Papakyriakopoulos, T.; Avramopoulos, H.; Girardin, F.; Guekos, G.; Dall'Ara, R.; Hansmann, S.; Burkhard, H. All-Optical XOR in a Semiconductor Optical Amplifier-Assisted Fiber Sagnac Gate. Photon. Technol. Lett. 1999, 11, 334-336.

[237] Bogoni, A.; Poti L.; ti, R . P.; Meloni, G.; Ponzini, F.; Ghelfi, P. Regenerative and reconfigurable all-optical logic gates for ultra-fast applications. Electron. Lett. 2005, 41, 435-436.

[238] Miyoshi, Y.; Ikeda, K.; Tobioka, H.; Inoue, T.; Namiki, S.; Kitayama, K. I. Versatile all-optical logic gate using nonlinear optical loop mirror based muliperiodic transfer function. 32nd European Conf. on Opt. Commun. Cannes, France, Sept. 24-28, 2006.

[239] Miyoshi, Y.; Ikeda, K.; Tobioka, H.; Inoue, T.; Namiki, S.; Kitayama, K. I. Ultrafast all-optical logic gate using a nonlinear optical loop mirror based multi-periodic transfer function. Opt. Express. 2008, 16, 2570-2577.

[240] Jeong, J. M.; Marhic, M. E. All-optical logic gates based on cross-phased modulation in nonlinear fiber interferometer. Opt. Commun. 1991, 85, 430-436.

[241] Robinson, B. S.; Hamilton, S. A.; Savage, S. J. 40 Gb/s all-optical XOR using a fiber based folded ultrafast nonlinear interferometer. Presented at Conf. on Optical Fiber Commun. 2002, 561-563.

[242] Penty, R. V.; Davison, A. S.; White, L. H. Optically induced Kerr phased shifting in optical fiber gate at diode laser pump powers. Presented at IEE Colloquium on Non-linear optical waveguide, London, June 2-2, 1988.

[243] Yul, C.; Christen, L.; Luo, T.; Wang, Y.; Panz, Z.; Yan, L. A.; Willner, A. E. All-Optical XOR Gate Based on Kerr Effect in Single Highly-Nonlinear Fiber. Presented at IEEE Conf. on Lasers and Electro-Optics, San Francisco, California, May 16-21, 2004.

[244] Bogris, A.; Velanas, P.; Syvridis, D. Numerical Investigation of a 160-Gb/s Reconfigurable Photonic Logic Gate Based on Cross-Phase Modulation in Fibers. IEEE Photon. Technol. Lett. 2007, 19, 402-404.

[245] Huo, L.; Lin, C.; Chan, C. K.; Chen, L. K. A reconfigurable all-optical AND/OR logic gate using Multilevel Modulation and Self-Phase Modulation. Presented at Conf. on Optical fiber commun. and National fiber Opt. Eng. Conf., Anaheim, CA, March 25-29, 2007.

[246] Clark, A. S.; Fulconis, J.; Rarity, J. G.; Wadsworth, W. J.; O'Brien, J. L. An all optical fibre quantum controlled-NOT gate. Phys. Rev. 2008, 79, 1-4.

[247] Fok, M. P.; Shu, C. Exclusive-OR gate for Rz-DPSK signals using four wave mixing in a highly nonlinear Bismuth-Oxide fiber. Presented at European Conf. on Lasers and electro-Optics, Munich, June 17-22, 2007.

[248] Lai, D. M. F.; Kwok, C. H.; Yuk, T. I.; Wong, K. K. Y. Picosecond All-Optical Logic Gates (XOR, OR, NOT, and AND) in a Fiber Optical Parametric Amplifier. Presented at

Conf. on Optical Fiber Commun. San Diego, California, Feb. 24-28, 2008.

[249] Rowland, D. R. All-optical devices using nonlinear fiber couplers. IEEE J. Lightwave Technol. 1991, 9, 1074-1082.

[250] Islam M. N.; Sauer, J. R. GEO Modules as a Natural Basis for All-Optical Fiber Logic Systems. Quantum Electron. 1991, 27, 843-848.

[251] Koshiba, M.; Kojima, T.; Tsuji, Y.; Tsuji, M. Reduction in Higher Order Effects on Logic Functions of Asymmetric Nonlinear Optical Fiber Couplers by Bandwidth Limited Amplification. IEEE J. Lightwave Technol. 1997, 15, 279-287.

[252] Niiyama, A.; Koshiba, M. Three-dimensional beam propagation analysis of nonlinear optical fibers and optical logic gates. IEEE J. Lightwave Technol. 1998, 16, 162-168.

[253] Maeda, Y. All-optical NAND logic device operating at 1.51-1.55pm in Er-doped aluminosilicate glass. Electron. Lett. 1999, 35, 582-584.

[254] Bovino, F. A.; Larciprete, M. C.; Giardina, M.; Belardibi, A.; Sibillia, C.; Bertolotti, M.; Passaseo, A.; Tasco, V. Optical polarization based logic functions (XOR or XNOR) with nonlinear Gallium nitride nanoslab. Opt. Express, 2009, 17, 19334-19337.

[255] Lu, B.; Zhou, P.; Lu, Y.; Cheng, J.; Leibenguth, R. E.; Adams, A.C.; Zilko, J. L.; Lear, K. L.; Zolper, J. C.; Chalmers, S. A.; Vawter, G. A. Binary optical switch and programmable optical logic gate based on the integration of GaAs/AlGaAs surface-emitting lasers and heterojunction phototransistors. IEEE Photon. Technol. 1994, 6, 398-401.

[256] Zhou, P.; Cheng, J.; Schaus, C. F.; Sun, S. Z.; Hains, C.; Armour, E.; Myers, D. R.; Vawter, G. A. Inverting and latching optical logic gates based on the integration of vertical-cavity surface-emitting lasers and photothyristors. IEEE Photon. Technol. 1992, 4, 157-159.

[257] Choi, W. K.; Kim, D. G.; Choi, Y. W. Optical AND/OR gates based on monolithically integrated vertical cavity laser with depleted optical thyristor structure. Opt. Express. 2006, 14, 11833-11838.

[258] Choi, W. K.; Choi,Y. W. Differential switching operation of vertical cavity laser with depleted optical thyristor for optical logic gates. Electron. Lett. 2007, 43, 683-685.

[259] Kuznetz, O.; Speiser, S. Luminescence-based molecular scale logic circuits. Lumin. 2009, 19, 1415-1418.

[260] Singh, C. P.; Roy, S. All-optical logic gates with bacteriorhodopsin. Appl. Phys. 2003, 3, 163-169.

[261] Birge, R. R. protein based computers. Sci. Am. 1995, 272, 90-95.

[262] Rao, D. V. G. L. N.; Aranda, F. J.; Rao, D. N.; chen, Z.; Akkara, J. A.; Kaplan, D. L.; Nakashima, M. All-optical logic gates with bacteriorhodopsin films. Opt. Commun. 1996, 127, 193-197.

[263] Gu, L. Q.; Zhang, C. P.; Niu, A. F.; Li, J.; Zhang, G. Y.; Wang, Y. M.; Tong, M. R.; Pan, J. L.; Song, Q. W.; Parson, B.; Birge, R. R. Bacteriorhodopsin based photonic logic gate and its applications to grey level image subtraction. 1996, 131, 25-30.

[264] Zhang, T.; Zhang, C.; Fu, G.; Li, Y.; Gu, L.; Zhang, G.; Song, Q. W.; Parsons, B.; Bringe, R. R. All-optical logic gates using bacteriorhodopsin films. Opt. Eng. 2000, 39, 527-534.

[265] Hung, Y.; Wu, S. T.; Zhao, Y. All-optical switching characteristics in bacteriorhodopsin and its applications in integrated optics. Opti. Express. 2004, 12, 895-906.

[266] Ying, C. G.; Ping, Z. C.; Xia, G. Z.; Guo, T. G.; Yin, Z. G.; Wang, S. Q. All-optical logic gates based on bacteriorhodopsin film. Chin. Phys. 2005, 14, 774-778.

[267] Mershin, A.; Kolomenski, A. A.; Schuessler, H. A.; Nanopoulos, D. V.; Tubulin dipole moment, dielectric constant and Quantum behavior: computer simulations, experimental results and suggestions. Biosystems. 2004, 77, 73-85.

[268] Silivi, S.; Edvin, E. C.; Housecroft, C. E.; Beves, J. E.; Beves, E. L.; Tomasulo, M.; Raymo, F. M.; Credi, A. All-optical integrated logic operations based on chemical communication between molecular switches. Chem. Eur. 2009, 15, 178-185.

[269] Mitsuishi, M.; Matsui, J.; Miyashita, T. Photofunctional thin film devices composed of polymer nanosheet assemblies. Mater. Chem. 2009, 19, 325- 329.

[270] Mitsuishi, M.; Matsui, J.; Miyashita, T. Functional organized molecular assemblies based on polymer nano-sheets. Polymer. 2006, 38, 877-896.

[271] Fujihira, M. Photoelectric Conversion by Monolayer Assemblies. Mol. Cryst. Liq. Cryst. 1990, 183, 59-69.

[272] Miyashita, T.; Aoki, A.; Abe, Y. Fabrication of Photoresponsive Nano-Organized Polymer Assemblies. Mol. Cryst. Liq. Cryst. 1999, 327, 77-82.

[273] Chen, J.; Mitsuishi, M.; Aoki, A.; Miyashita, T. Photocurrent amplification by an energy/electron transfer cascade in polymer Langmuir-Blodgett films. Chem. Commun. 2002, 282, 2856-2857.

[274] Miyashita, T.; Aoki, A.; Abe, Y. Fabrication of Photoresponsive Nano-Organized Polymer Assemblies. Mol. Cryst. Liq. Cryst 1999, 327, 77-82.

[275] Matsui, J.; Mitsuishi, M.; Aoki, A.; Miyashita, T. Optical Logic Operation Based on Polymer Langmuir-Blodgett-Film Assembly. Angew. Chem. Int. Ed. 2003, 42, 2272-2275.

[276] Matsui, J.; M. Mitsuishi, Atsushi, and T. Miyashita, "Molecular Optical Gating Devices Based on Polymer Nanosheets Assemblies," J. Am. Chem. Soc., 2004, 126, pp. 3708-3709.

[277] Li, Y.; Zheng, H.; Li, Y.; Wang, S.; Wu, Z.; Liu, P.; Gao, Z.; Liu, H.; Zhu, D. Photonic logic gates based on control of free by a solvatochromic perylene bisimide. Organ. Chem. 2007, 72, 2878-2885.

[278] Zhang, D.; Su, J.; Ma, X.; Tian, H. An efficient multiple mode molecular logic system for pH, solvent, polarity, and Hg^{+2} ions. Tetrahedrom, 2008, 64, 8515-8521.

[279] Gunnlaugsson, T.; Dónail, D. A. M.; Parker, D. Luminescent molecular logic gates: the two-input inhibit (INH) function. Chem. Commun. 2000, 93-94.

[280] Balzani, V.; Credi, A.; F. Scandola, Light and information: molecular machines, molecular electronics, molecular logic. Chim. Ind. 1997, 79, 751-759.

[281] Ballardini, P. R. R.; Balzani, V.; Lopez, M. G.; Lawrence, S. E.; Diaz, M. V. M.; Montalti, Piersanti, M. A.; Prodi, L.; Stoddart, J. F.; Williams, D. J. Hydrogen bonded adducts of aromatic crown ethers with (9-anthracenyl) ammonium derivatives. Supramolecular photochemistry and photophysics. PH controllable supramolecular switching. Am. Chem. Soc. 1997, 119, 10641.

[282] G. Zong, and G. Lu, "An Anthracene-Based Chemosensor for Multiple Logic Operations at the Molecular Level. Phys. Chem. C, 2007, 113, 2541-2546.

[283] Toma, H. E. Supermolecular nanotechnology: from molecules to devices. Current Science. 2008, 95, 1202-1225.

[284] Kuznetz, O.; Speiser, S. Luminescence-based molecular scale logic circuits. Lumin. 2009, 129, 1-4.

[285] Szacilowski, K.; Macyk, W. Working prototype of an optoelectronic XOR/OR/YES reconfigurable logic device based on nanocrystalline semiconductors. Solid-State Electron. 2006, 50, 1649-1655.

[286] Rao, D. N.; Aranda, F. J.; Chen, Z.; Akkara, J. A.; Kaplan, D. L.; Nakashima, M. All-optical logic gates with Bacteriorhodopsin films. Opt. Commun. 1996, 127, 193.

[287] Kiyohiko, K.; Tetsuro, M. Integration of optical logic gates on molecular scale. Photochemistry. 1999, 30, 142-143.

[288] Sharma, P.; Sukhdev, Roy All-optical light modulation in pharaonis phoborhodopsin and its application to parallel logic gates. Appl. Phys. 2004, 96, 1687-1695.

[289] Sharma, P.; Roy, S. All-Optical Biomolecular Parallel Logic Gates with Bacteriorhodopsin. Transactions on Nanobioscience. 2004, 3, 129-136.

[290] Chen, Q. W.; Zhang, G.; Guo, C.; Wang, Z.; Tian, X.; Song, J. Time-dependent all-optical logic gates based on two coupled waves in bacteriorhodopsin film. Appl. Phys. 2005, 98, 044504-044505.

[291] Ying, G. C.; Ping, Z. C.; Xia, G. Z.; Guo, T. J.; Yin, Z. G.; Wang, Q. S., All-optical logic gates based bacteriorhodopsin film. Chin. Phys. 2005, 14, 774-778.

[292] Serak, S. V.; Tabiryan, N. V.; Peccianti, M.; Assanto, G. Spatial Soliton All-Optical Logic Gates. Photon. Technol. Lett. 2006, 18, 1287-1289.

[293] Yan, H. L.; He, W.; Huan, J.; Li, G. Y.; Yi, Z. H. All-Optical AND Logic Gate without Additional Input Beam by Utilizing Cross Polarization Modulation Effect. Chin. Phys. Lett. 2008, 25, 3901-3904.

[294] Williams, V. S.; Ho, Z. Z.; Peyghambarian, N..; Gibbons, W. M.; Grasso, R. P.; OBrien, M. K.; Shannon, P. J.; Sun, S. T. Picosecond all-optical logic gate in a nonlinear organic etalon. IEEE Appl. Phys. Lett. 2009, 57, 2399-2401.

[295] Roy, S.; Kulshrestha, K.; Prasad, M. Switching light with light in Chlorophyll-A molecules based on excited-State absorption. IEEE Trans. on Nanobioscience. 2009, 8, 83-91.

[296] R. Paschotta, Thermal Lens Effect, 2007. http://www.rp-photonics.com/ thermal_lensing. html

[297] Ian, A. M.; Nan, K. K. P. U. I.; Lees., T. M.; ORI, V. P. N. N.; AN, C. P. G. V. Realization of Optical Logic Gates Using the Thermal Lens Effect. Laser Chemistry, 2002, 20, 81-87.

[298] G. Eason, B. Noble, and I. N. Sneddon, “On certain integrals of Lipschitz-Hankel type involving products of Bessel functions,” Phil. Trans. Roy. Soc. London, vol. A247, pp. 529–551, April 1955.

[299] J. Clerk Maxwell, A Treatise on Electricity and Magnetism, 3rd ed., vol. 2. Oxford: Clarendon, 1892, pp.68–73.

[300] I. S. Jacobs and C. P. Bean, “Fine particles, thin films and exchange anisotropy,” in Magnetism, vol. III, G. T. Rado and H. Suhl, Eds. New York: Academic, 1963, pp. 271–350.

Fatemeh Davoodi was born in Tehran, Iran on January 09, 1986. She received her B.Sc. degree in Electronics in Electrical Engineering from Isfahan University, Isfahan, Iran, in 2008, and M.Sc. degree in Communications Engineering (Fields and Waves) from K. N. Toosi University of Technology, Tehran, Iran, in 2011. She has worked as a lecturer at department of Electrical Engineering of Azad University and as test manager on Gigabit Passive Optical Network (GPON) in ITRC for one year. She is also a specialist in SDH and WDM Laboratory of ITRC. Her research fields of interest include all-optical logic gates, plasmonic circuits, optical nonlinear effects, and GPON tests.

Nosrat Granpayeh has received his B.Sc., M.Sc. and Ph.D. degrees in Telecom. Eng. from Telecom. College of Iran, Radio and Television College, Tehran, Iran and University of NSW, Sydney Australia, in 1975, 1980, and 1996, respectively.

In 1975, as an honor graduate of the Faculty of Electrical & Computer Engineering of K. N. Toosi University of Technology, Tehran, Iran, he was employed as an instructor there, where he was later promoted to lecturer, assistant and associate professor in 1980, 1996, and 2007 respectively. His research interests are in optical devices, equipments and materials, optical fibers, and optical fiber nonlinear effects. He is the author or co-author of 40 journal- and 60 conference- papers. He is a member of OPSI, IEEE, IEEE Photonics Society, IAEEE, and OSA.